ACS OMEGA

http://pubs.acs.org/journal/acsodf

Review

Recent Advances in Deep Eutectic Solvents as Shale Swelling Inhibitors: A Comprehensive Review

Kakon Sultana, Md Tauhidur Rahman,* Khairul Habib,* and Likhan Das

Cite This: *ACS Omega* 2022, 7, 28723−28755

Read Online

ACCESS | Metrics & More | Article Recommendations

ABSTRACT: Inhibitors have evolved from their primary function of controlling swelling during hydraulic fracturing processes in shale reservoirs. This study provides a comprehensive review of recent deep eutectic solvent (DES) advancements as inhibitors in swelling inhibition techniques. The swelling inhibitory potentials and mechanisms of DESs have been studied analytically and compared to existing conventional inhibitors. The functional effects of concentration, temperature, and types of DES are explored. Data on the effect of DES on rheology, swelling, zeta potential, shale cutting recovery, surface tension, particle size distribution, XRD, and FTIR analyses are presented. Along with preparation procedures, environmental concerns and applications of DESs in several fields are discussed. This study suggests that DESs are preferable swelling inhibitors due to their inhibitory performance, cost-effectiveness, and environmental friendliness. Moreover, this review includes guidelines and recommendations for selecting and designing DES to inhibit swelling more effectively.

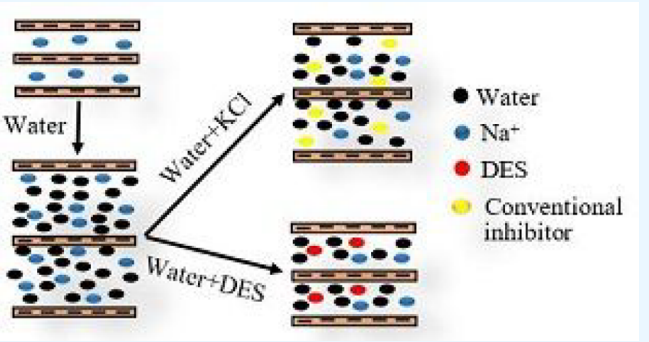

1. INTRODUCTION

Increased energy consumption and the depletion of conventional energy reserves have sparked a lot of interest in utilizing unconventional sources.[1] If natural gas is found in a rock formation with a permeability of fewer than 1 millidarcy, it is classified as unconventional gas in the largest context.[2,3] In addition to this, an unconventional source or reservoir refers to any formation with high organic content and low porosity.[4−7] Coal bed methane, oil sands, tight oil and gas, gas hydrates, and shale oil and gas are examples of unconventional reservoirs.[5,8,9] Shale gas is the most discussed unconventional reservoir because of its vast reserve, which accounts for about half of the total unconventional reserves.[10] However, due to the unique composition of shale formations, only a small percentage of this massive reserve is technically attainable. The condition of shale gas is determined by the size of the pores: liberated gas is stored in big holes or fractures, whereas adsorbed gas is held in small pores.[11]

Shales are one type of sedimentary rock made up mostly of clay minerals (smectite, illite, kaolinite, chlorite, and vermiculite), as well as quartz, calcite, feldspar, and other minerals.[12] Because of the presence of organic sediments, shale formation has ultralow permeability, small pore throats, and low porosity.[13] These negative properties make shale oil and gas production challenging utilizing conventional production methods. As a result, advanced technologies are required to discover these vast sources, which can serve the world's increasing energy demand. It is possible to extract a large amount of hydrocarbon from shale formations using advanced technology such as horizontal drilling and hydraulic fracturing and so on.[14−16] Prior to hydraulic fracturing, horizontal drilling is typically utilized to enhance the contact surface area. Hydraulic fracturing is applied to expand the connectivity of the pores in the shale formation. The success of fracturing processes is determined by the quality of induced fracture networks as well as the after effects.[17] The success and after effects of horizontal drilling and hydraulic fracturing are mostly influenced by the drilling and fracturing fluids. The drilling or fracturing fluids can be of different types such as oil-based fluids and water-based fluids.

Oil-based fracturing or drilling fluids were formerly employed and had outstanding inhibitory property. However, environmental disposal challenges, high initial costs, and safety concerns limited their use, paving the way for water-based fracturing and drilling fluids. When water-based fluids come into contact with the clay minerals in the shale formation, they cause problems like hydration and swelling. When water comes into contact with clay minerals, the negative layers attract water

Received: May 14, 2022
Accepted: July 28, 2022
Published: August 9, 2022

https://doi.org/10.1021/acsomega.2c03008
ACS Omega 2022, 7, 28723−28755

molecules and allow water to adsorb on the interlayer gap.[18−20] Swelling of clay can obstruct shale gas production by causing a slew of issues such as particle buildup in the mud, hole collapse, tight holes, drill pipe sticking, pore plugging, reduced permeability, and so on.[21−28] Swelling may also lower the diameter of fractures, decreasing the reservoir's ultimate permeability.[29] Many additives, such as inorganic salts, organic salts, surfactants, amine derivatives, polymers, and others, were added to water-based fluids to prevent these problems. The insertion of salts such as ammonium chloride, potassium chloride, and divalent brines with a high concentration was the most extensively utilized and early method. Although these salts can slow the hydration and swelling of clay, their use at high concentrations is harmful to biological and chemical environments. Furthermore, these salts are inflexible and unsuitable for mud compositions.[30] KCl is sometimes combined with polymers to achieve stronger inhibition than either the KCl or the polymer alone. However, these polymers have several drawbacks, such as heat breakdown and increased viscosity at high temperatures.[31,32] Ammonium compounds and derivatives have been utilized for a long time; however, they have significant drawbacks, such as ammonium salts being incompatible with anionic additives.[33] Ionic liquids (ILs) have recently been employed as fracturing fluid additives to inhibit clay swelling.[34] Several studies have been done to explain the inhibition performance, mechanisms, and effects of different moieties of ILs as clay swelling processes.[35] However, a recent study has shown that ILs based on imidazolium are costly, hazardous, nondecomposable, and needed complicated processes and apparatuses to prepare.[36]

In recent years, research has focused on environmentally safe, cost-effective, easy-to-prepare, and high-performance inhibitors. DESs are fourth-generation ILs that are marketed as a more environmentally benign and cost-effective alternative to conventional inhibitors. DES is made up of large asymmetrical ions with low lattice energy, giving it a low melting point.[37] This solvent is a connotation of quaternary ammonium salt and metal salt, also known as a hydrogen bond donor (HBD). The final mixture has a minor melting point compared to any of the discrete components.[38] At room temperature, most of them remain in the liquid phase. Some of their appealing qualities (for example, low vapor pressure, nonflammability, and so on) have made them very attractive in the field of modern research. One of the desired aspects of using this particular solution is a specific type of chemistry attributable to its adaptable nature.[39] Due to the considerable flexibility in adopting individual components and their composition, there are no limits to the number of DESs that can be generated. These qualities have sparked burgeoning attention from the scientific community in using DESs rather than ILs as solvents in a wide range of sectors.[40−43] As a result, there has been plenty of potential for the improvement of fundamental research in the subject of DES.[44]

The most critical concern associated with shale gas production, as aforementioned, is shale hydration, which induces swelling. As a result, this issue has a direct negative influence on shale gas extraction. Studies have been conducted on this issue for decades in order to explore an appropriate inhibitor. Inorganic salts, nanosilica, polyamines, polyglycerols, surfactants, silicates, and nanocomposites have all been described as swelling inhibitors in the literature.[45−49] Several reviews on shale inhibitors evaluated the influence of recently tested inhibitors, such as ILs, polymers, surfactants, and amine-based chemicals, and outlined their general inhibitory processes.[50−57] Rahman et al. reviewed 23 ILs and presented the effects of chain length and cationic and anionic parts on swelling inhibition.[1] Quainoo et al. presented a comprehensive review of several bioinhibitors, including their economic aspects, performance, and environmental friendliness.[58] Abbas et al. provided a critical parametric review of polymeric inhibitors as well as their inhibition performance.[59] A review on the application of surfactants and nanomaterials as shale inhibitors for water-based drilling fluid was discussed by Muhammed et al.[60] Sivabalan et al. did a minireview where they addressed DES as the new norm for the oil and gas industry.[61] However, they presented the use of DES in gas hydrate inhibition processes instead of shale swelling. Also, a minireview on the synthesis method, properties, and applications of DES was highlighted by Mr et al.[62]

So far, there is no other substantial review on the impact of DESs on shale swelling inhibition. The important contributions of DESs in shale inhibitory mechanisms, on the other hand, have not been rigorously studied or completely described in the open literature. Furthermore, the mechanism of swelling inhibition in the presence of DES demands a deeper investigation. Additionally, other notable qualities such as environmental friendliness and biodegradability may be important in understanding their potential industrial application. Therefore, a state-of-the-art evaluation that discusses the aforementioned concerns and makes significant recommendations on the design and application of DES in shale formation is indispensable. The ease of manufacturing of DESs led to their extensive implementation in a variety of disciplines via the trial-and-error approach.[63] This research could eventually replace the hazardous chemicals used in the oil and gas industry to minimize shale swelling.

2. FUNDAMENTALS OF SWELLING

2.1. Shale. Shales are the most abundant sedimentary rock (approximately 60% of all sedimentary rocks) and are found in a wide range of geologic eras from the Paleozoic to the Cenozoic.[64] Extrusion, dehydration, recrystallization, and cementation of weak clay constitute the most common sedimentary rock, which can be found in sedimentary basins all over the world. Muds, silts, and other sediments are transported to different environments such as the Midcontinental Shelf, lake (away from shore), delta, lagoon, Tidal Flat, Deep Marine, basins of shallow seas, river floodplains, and playas through currents and deposited there. They are compacted and formed shale rocks.

Permeability is an essential aspect to consider when exploring these unconventional sources of natural gas.[67−69] The presence of natural fractures or cracks in the rock determines permeability, which allows fluid to move within the rock.[70] Permeability and porosity in shale rocks are highly reliant on the mineral composition, distribution, quantity, and thermal maturity of organic matter.[71] Shale rocks exhibit micro- and nanosized pores with varying degrees of water and residual organic matter.[72,73] Furthermore, due to the nanometer-scale pore diameters, shale permeability is extremely low, often in the nano- to microdarcies.[74−77] Table 1 represents some of the petrophysical and geomechanical properties of shales.

Shale is a term used to describe rocks that include fine-grained particles (typically less than 4 μm in diameter). Yet they also hold silt-sized particles having a diameter of up to 62

https://doi.org/10.1021/acsomega.2c03008
ACS Omega 2022, 7, 28723−28755

Table 1. Some Petrophysical and Geomechanical Properties of Shales[65,66]

property	average value/range
bulk density (mg/m^3)	2.30
porosity (%)	15 (7−30)
permeability (m/s)	1×10^{-9} (1×10^{-6}−10^{-12})
UCS (MPa)	20 (3−30)
Young's modulus (GPa)	5.0
Poisson's ratio	0.22
resistivity (Ohm-m)	0.5−15

μm. Any shale rock is classified as silty shale or clay shale according to the dominated constituents of the rock. Shale rock maintains a laminated structure with a tendency to scatter into thin layers of sharp edges, and these layers are usually parallel to the bedding-plane surface. Shale rock is mainly composed of silt and clay-sized mineral particles that are frequently referred to as "mud". So, shale is referred to as "mudstone". Shales are classed as carbonaceous or bituminous depending on their organic matter composition. Shale is defined as carbonaceous if the organic content in plant fragments and the depositional environment are continental or transitional. Bituminous shale is formed by organic materials from animal bits. Both types of shales have the potential to be used to produce petroleum oil and gas.[78]

The shale's mineral content is a major determinant of whether the solid bitumen-hosted porosity is sustained or disrupted. When compared to a clay-rich mature shale of similar maturity, a quartz-rich mature shale retains more solid bitumen-hosted (meso and macro) porosity. As a result, a quartz-rich shale's gas holding capacity must be greater than that of a clay-rich shale of equal maturity, organic matter type, and TOC level.[79]

Clay minerals are the vital components of any shale and similar types of rock. Shale formations, in particular, can have up to 70% clay content.[80] In addition to clay minerals, they also contain other minerals such as quartz, feldspar, other constituents, etc. Other constituents include organic matter, iron, sulfide or carbonate minerals, and heavy minerals. Depending on the predominance of the quartz, feldspar or mica shale may be classified as quartz, feldspathic, or micaceous.[81] The average chemical composition of shales is displayed in Table 2.

Clays are minerals that form naturally as igneous rocks deteriorate and disintegrate.[83] Clay minerals can be found in almost 90% of all hydrocarbon-producing reservoirs, not just in shale reservoirs.[84,85] Clay minerals belong to the phyllosilicate family and are tiny hydrous layer silicates. With tiny particles less than 2 μm in diameter, they have a platy or flaky texture. Tetrahedral and octahedral sheets are formed by atom planes in the layered silicate.[86,87] The tetrahedral sheets are composed of tetrahedra linked with adjacent tetrahedra by sharing oxygen ions at three corners, and the shared oxygen (basal oxygens) forms a hexagonal pattern. The fourth tetrahedral oxygen (apical oxygen) of all tetrahedra is perpendicular to the sheet and forms part of the adjacent octahedral sheet. Si and Al are the most common tetrahedral cations, with Fe^{3+} being unusual. The octahedral sheet is made up of cations (Al, Fe, and Mg) that are octahedrally coordinated by shared apical oxygens and unshared OH groups in the hexagonal hole created by the basal oxygens.[88,89] Three octahedra comprise the smallest structural unit. A 1:1 layer is made up of one tetrahedral sheet and one octahedral sheet merged. OH anions constitute the unshared plane of anions in the octahedral sheet. An octahedral sheet is sandwiched between two tetrahedral sheets in a 2:l layer.[83] Clay minerals based on bentonite can have thixotropic gel formation with water, high water absorption, and high cation exchange capacity in general (CEC). CEC is defined as the amount of positive charge that can be exchanged. So, the higher the value of CEC, the higher the rate of swelling in shale particles. Clay minerals' CEC is governed by crystal size, pH, and the type of cation that can be exchanged.[90] Clay minerals present in the soil environment include layer and chain silicates, sesquioxides, and other inorganic minerals.[91] Clay is classified according to how the tetrahedral and octahedral sheets are arranged into layers. Types of clay mineral include allophone, kaolinite, halloysite, smectite, illite, chlorite, vermiculite, attapulgite−palygorskite−sepiolite, and mixed-layer minerals.[92] Figure 1 represents the basic structure of a clay particle.

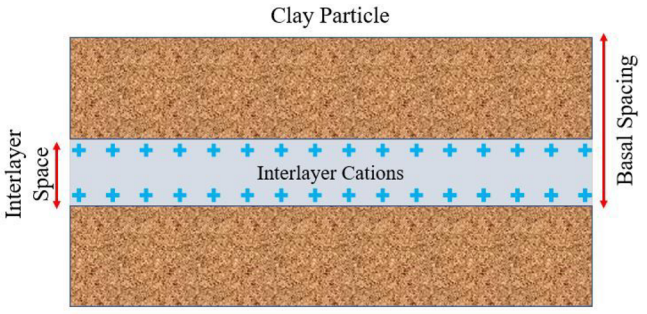

Figure 1. Basic structure of a clay particle. Reprinted with permission from ref 93. Copyright 2013 RSC Advances.

The kaoline group is a 1:1 layered mineral comprised of one tetrahedral and one octahedral sheet. Kaolinite, which is the most common mineral in this group, is dioctahedral, exhibiting Al^{3+} octahedral and Si^{4+} tetrahedral coordination with an effective surface area range from 10 to 30 m^2/g. The sheets are bound together by van der Waals bonds between the tetrahedral sheet's basal oxygens and the octahedral sheet's hydroxyls.[94] Hydrogen bonding holds layers together securely, restricting expansion and limiting the reactive area to exterior surfaces with limited cation exchange capacity. So, isomorphic substitution for Si^{4+} and Al^{3+} in this mineral is insignificant. There seems to be little, whether any, isomorphous substitution in the kaolinite group due to its lack of structural charge.[95] Kaolinite has a limited potential to adsorb ions owing to its poor surface area and lack of isomorphous substitution.[96] As a result, soils dominated by the 1:1 mineral have poor cation adsorption and are low in fertility. Lower CEC also indicates a lower tendency of hydration when it comes into contact with water molecules and thus a lower rate of swelling.

Table 2. Average Chemical Composition of Shales[82]

composition	SiO_2	Al_2O_3	Fe_2O_3	TiO_2	MnO	MgO	CaO	Na_2O	K_2O	P_2O_5
percentage	60.9	18.5	7.2	0.9	0.1	2.9	2.4	1.8	4.0	0.2

https://doi.org/10.1021/acsomega.2c03008
ACS Omega 2022, 7, 28723−28755

Among all the groups of clay minerals, the smectite group is considered an expansible group of clays. Montmorillonite [(0.5Ca, Na) (Al, Mg, Fe)$_4$(Si, Al)$_8$O$_{20}$(OH)$_4$·nH$_2$O] is the most well-known member of this family. The term "smectite" has come to refer to the entire family of clays that incorporates montmorillonite.[97] Smectite (montmorillonite) is a flake-like clay mineral with an expanding lattice. Each layer is made up of two tetrahedral (silica) sheets sandwiched between an octahedral sheet.[98] Due to the isomorphic substitution, aluminum (Al^{3+}) or iron (Fe^{2+}) ions can substitute Si^{4+} in tetrahedral sheets. Magnesium (Mg^{2+}) or iron (Fe^{2+}) ions can replace the aluminum ions in the octahedral sheets. A negative charge layer forms on the mineral's surface as a result of this substitution. Negative charges have a repulsive tendency, and they cause repulsive forces between two layers. The repulsion of two layers might cause the sandwiched silicate layers to detach, causing swelling.[99] Oxygen atoms in one unit's bottom tetrahedral sheet and another unit's top tetrahedral sheet have a small affinity. This generates a changeable gap between layers, which is populated by swappable cations and water. Water and exchangeable cations can freely enter the interlayer region as a result, leading to layer growth of 9.6−20 Å. They also differ due to the occurrence of isomorphous substitution in the octahedral or tetrahedral layer. The cation exchange capacity (CEC) is the number of cations required to balance the charge shortfall caused by these replacements. The thermal stability of montmorillonite clays is weak. High cation exchange capacity, swelling, and shrinking capacity are all features of these minerals. As a result, they are classified as reactive clays.[100] Montmorillonite has a CEC of 80−100 mequiv per 100 g.[101]

Bentonite is an inaccurate type of aluminum phyllosilicate clay made up of 98% montmorillonite that is formed in the presence of water by in situ devitrification of volcanic ash or mechanical and chemical weathering of the parent rock. The presence of the hydroxide group on the platelet's edge causes this type of clay to be thixotropic.[102]

The major component of shales is illite clay. It has a layered structure of 2:1. Weathering of K- and Al-rich rocks under high pH conditions produces illite-type clays. Members of the illite group do not commonly accept water. Because their structures allow for partial replacement of Al onto the tetrahedral site, the surplus negative charge can be accommodated by introducing potassium (K), calcium (Ca), or magnesium (Mg) into the interlayer site. These interlayer cations of K, Ca, or Mg prohibit H_2O from entering the structure. As a result, illite clays do not expand.[103] Illite also has the lowest CEC, indicating that it has a lower tendency to swell when exposed to water.

Vermiculites are chemically sophisticated clay minerals that emerge when biotite and other initially ferromagnet minerals interact.[97] Vermiculite is a phyllosilicate clay mineral with a 2:1 ratio. Al, Mg, and Fe are octahedral ions. It has the biggest expandable surface area of all the clay minerals and has a high cation exchange capacity. In fact, the minerals with the highest CEC in the mineral part of soils are vermiculites (Table 3); nevertheless, the presence of hydroxy−Al interlayers can significantly diminish the effective CEC.[104] So, it does not expand as much as smectites despite having a higher CEC value. It has two layers of water within interlayers and exchangeable cations like Ca^{2+} and Mg^{2+}. Some K^+ ions are removed during weathering. In interlayer gaps, hydrated cations have taken their place.

Table 3. General Properties of the Four Major Clay Mineral Groups[105,97,101,106]

group name	layer type	basal spacing	CEC (mEq/100 g)
kaoline	1:1	7.2 Å	3−15
smectite	2:1	up to 19 Å	80−130
illite	2:1	10 Å	10−40
vermiculites	2:1	up to 14 Å	100−150

2.2. Swelling. Water is introduced to the interlayer space of dried clay minerals when they are exposed to absorbed water in a controlled environment, allowing the interlayer space to swell or expand. Clay minerals' interlayer space swells due to hydration energy forces related to particle interaction.[107] Any water molecule that makes contact with a clay particle enters the dry clay's interlayer region. Following that, anions and cations exchange electrostatic ions. The formation of repulsive van der Waals forces results from this phenomenon, which causes hydrated clay particles to expand.[108]

Water molecules move into the shale layers through osmosis and inflow into the interlayer voids whenever the concentration of interfacial cations is more than the adjacent water, as shale acts as a semipermeable stratum.[109] The interlayer space is enlarged as a result of the migrating water molecules, inducing osmotic swelling.[1] The volumetric expansion of shales is caused by another sort of swelling referred to as crystalline swelling. The hydrational force generated between the absorbed water molecules and exchangeable cations generates crystalline swelling. This force gradually weakens electrostatic forces between exchangeable cations and surface negative charges.[110,111]

During the drilling and hydraulic fracturing processes in petroleum reservoirs, the presence of certain types of clay minerals, such as reactive clays, induces hydration, swelling, and other destabilization complications.[10] Water content variations in swelling clays can have significant volume repercussions. The layer charge density of clay minerals as well as the type of interlayer ions (monovalent or divalent) all influence the swelling capacity of clay minerals. The percent of ions present in the surrounding solution with clay minerals, the amount of water present in the clay mineral interlayer, and the quantity and types of minerals is the clay mineral composition.[96] Shale swelling can cause wellbore fragility, which is among the most expensive and complicated problems to deal with during drilling operations. Moreover, the presence of water diminishes shale's Young's modulus (also known as brittleness).[112,113]

Montmorillonite, the predominant clay from the smectite group, shows more swelling behavior than any other clay mineral where the inner crystalline swelling takes place as formerly mentioned. Chemically, this type of clay consists of isomorphic substitutions in the tetrahedral sheet of Si^{4+} by Al^{3+} and Al^{3+} by Mg^{2+} in the octahedral ones. As a result of this collaboration, the negative residual charge of montmorillonite is balanced by cations in the interlayer space. Other phenomena such as the high difference in ion concentrations, mainly in cation concentration at the surface of the clay layers and pore water, also lead to the swelling behavior of clays, which is referred to as osmotic swelling.[114] It has a high base exchange capacity (90−150 mequiv/100 g) and will rapidly absorb Na^+ and other cations, leading to swelling and dispersion.[115] Figure 2 is the representation of montmorillonite clay's structure.

https://doi.org/10.1021/acsomega.2c03008
ACS Omega 2022, 7, 28723−28755

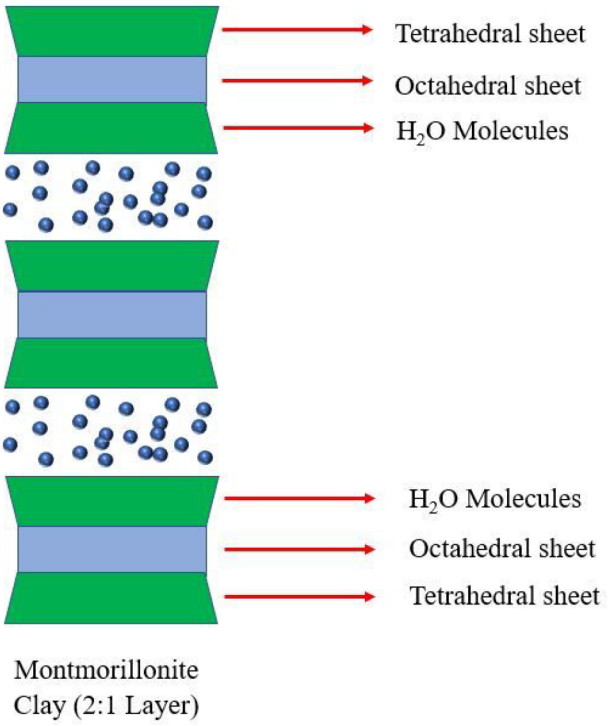

Figure 2. Structure of montmorillonite clay. Reprinted with permission from ref 116. Copyright 1987 Cambridge University Press.

3. DES: A PROGRESSIVE SOLVENT

Due to the adaptability, DESs are now regarded as viable alternatives to traditional organic solvents.[37] DESs are chemical compounds of two or three compounds with a lower melting temperature than the individual elements.[117,118] The first DES was a combination of cholinium chloride and urea with a melting point of 12 °C, which was dramatically less than the melting temperatures of the starting components, which were 302 and 133 °C, correspondingly.[117] Figure 3 represents the preparation of DESs as a combination of choline chloride and urea.

The fall in the melting point of the solution related to the melting point of each component is attributable to charge dissociation through the hydrogen bonding between the halide ion and the hydrogen donor molecule.[120,121] As previously stated, DESs are produced by combining two or more economical and environmentally sustainable components, which are made when a hydrogen bond is formed between a HBD and a HBA. Choline chloride, quaternary ammonium salt, and phosphate salt are some of the most regularly utilized HBAs. Choline chloride (ChCl), which is identical with vitamin B, is the most common. It is a salt that is both nontoxic and biodegradable. With more readily available and profitable mixes of organic salts and a complexing agent, science has revolutionized the manufacture of DESs.[117] The salt acts as a hydrogen bond acceptor in this mixture, while other agents act as hydrogen bond donors. Figure 4 represents a list of typical HBDs and halide salts as HBAs.

The DES combination is typically processed using one of two strategies. The heating process is one of them (frequently used in the literature). This procedure includes continuously combining and stirring two components at a temperature of about 100 °C until a uniform liquid is generated.[117] The grinding process is another strategy. The compounds must be added at room temperature and smashed in a mortar for this approach to work. This process comes to an end after acquiring a liquid solution.[63] Other methods of preparing DESs include the freeze-drying of aqueous solutions of the components of DESs, an evaporation method consisting of dissolving the components of DES in water, followed by evaporation at 50 °C. The resulting liquid is then placed in a desiccator in the presence of silica gel and an ultrasound-assisted synthesis of natural DES.[122−124]

3.1. Comparison between DESs and ILs. Though the physical properties of DESs and ILs are similar in general, the molecular level interactions and structural organization in these solvents are observed to be substantially different. The combination of ionic and molecular species in DESs results in a more structurally complicated liquid, including contributions from hydrogen bonding and electrostatic forces.[125] The following attributes established ILs and deep eutectic solvents apart from each other.

- DESs differ from ILs in two distinct ways. Their chemical formation process is one of them, and their source of basic components is another. A complexation between a halide salt or a hydrogen bond acceptor and a hydrogen bond donor results in DESs. The majority of DESs is derived from nonionic substances such as salts and molecular components. ILs, on the other hand, are mainly composed of ionic components that are bonded together by ionic bonds.[38]
- In contrast to ILs, which are generated from solutions composed predominantly of one type of discrete anion and cation, DESs are formed from a eutectic mixture of Lewis or Bronsted acids and bases that can contain a variety of anionic and/or cationic species.[37]
- Compared to DESs, ILs have a narrower range of surface tension. For instance, the surface tension of ChCl/urea (molar ratio: 1:2) was measured at room temperature (25 °C) as 52 mN m^{-1}, while that of ChCl/ethylene glycol (molar ratio: 1:2) was 49 mN m^{-1}. The surface

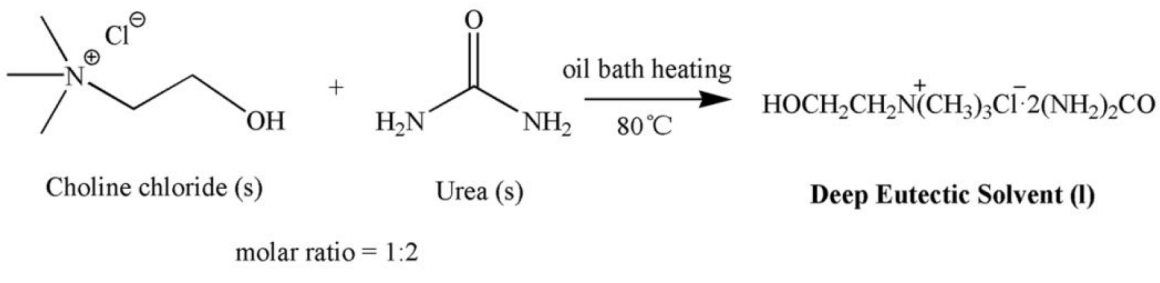

Figure 3. Deep eutectic solvent preparation. Reprinted with permission from ref 119. Copyright 2014 RSC Advances.

https://doi.org/10.1021/acsomega.2c03008
ACS Omega 2022, 7, 28723−28755

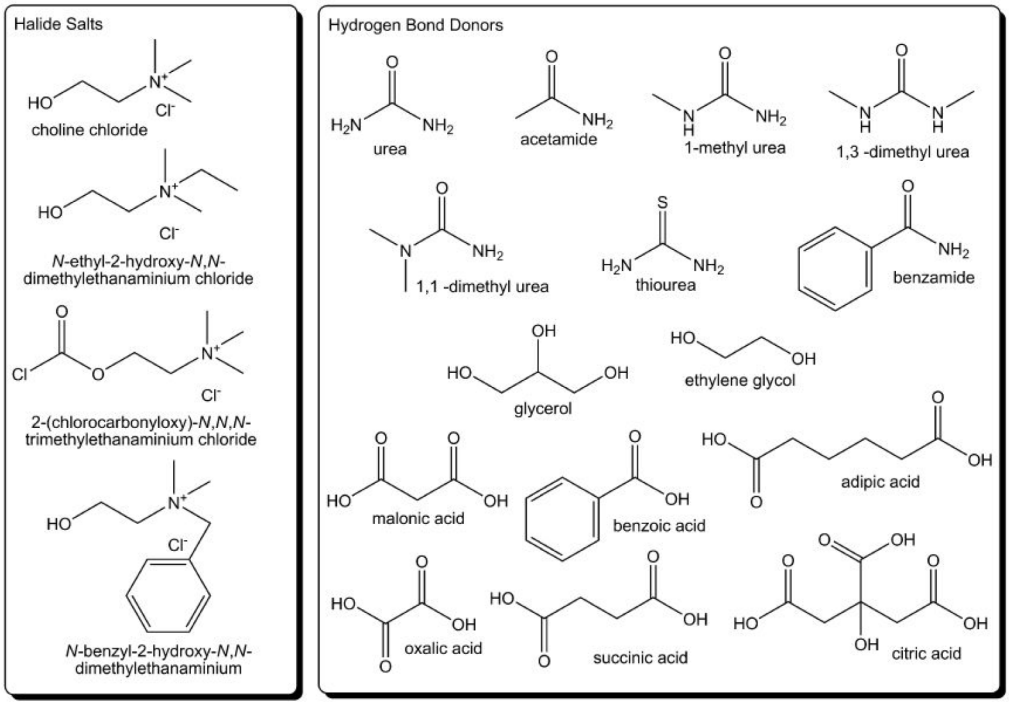

Figure 4. Common types of HBDs and halide salts as HBAs. Reprinted with permission from ref 37. Copyright 2014 ACS Publications.

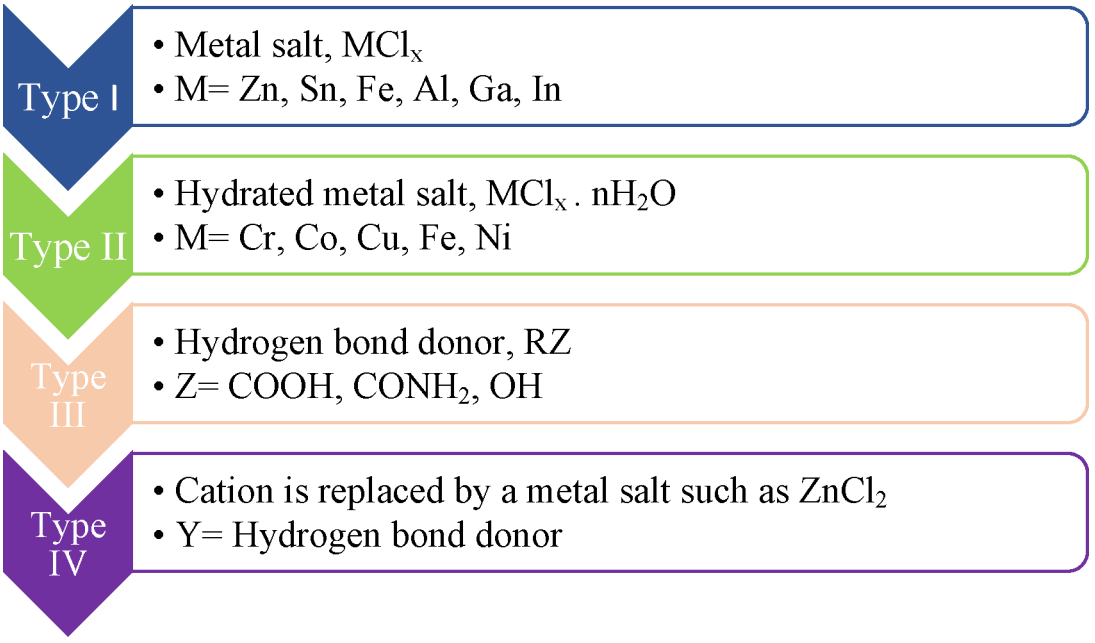

Figure 5. Four types of DESs based on the general formula Cat^+X^-zY, where Cat^+ (cation) is generally ammonium, phosphonium, or sulfonium; X is a Lewis base, usually a halide anion; Y represents a Lewis or Bronsted acid; and *z* is the number of Y molecules. Reprinted with permission from ref 37. Copyright 2014 ACS Publications.

tension was determined to be 46.6 mN m^{-1} for C_4mimBF_4 and 37.5 mN m^{-1} for 1-butyl-3-methylimidazolium tetrafluoroborate $C_4mim\ (CF_3CO_2)_2N$. When it comes to conductivity, DESs have a narrower range. The conductivity of ChCl/urea, for example, is 0.75 mS cm^{-1}. The conductivity of C_4mimBF_4 and $C_4mim\ (CF_3CO_2)_2N$, on the other hand, was measured to be around 3.5 mS cm^{-1} and 3.9 mS cm^{-1}, respectively.[117,126−128] The enormous size of the ions and comparatively free volume in the ionic systems are thought to be the cause of this disparity.[37]

- DESs have several advantages over typical ILs, including ease of synthesis and availability of reasonably inexpensive components (the components are toxicologically well-characterized, allowing for easy transportation for large-scale processing); nevertheless, they are less chemically inert in general.[37,129] The simple mixing of the two components, usually with mild heating, is all that is required to make DESs. This

https://doi.org/10.1021/acsomega.2c03008
ACS Omega 2022, 7, 28723−28755

allows for large-scale applicability while retaining a lower cost of production than typical ILs (such as imidazolium-based liquids).

- DESs also outperformed ILs in terms of environmental issues. If biodegradability is taken into account, DESs surpassed ILs. DES and IL biodegradation rates have been studied in a variety of ways. According to the findings, DESs are more biodegradable than standard ILs. For example, the Sturm and closed-bottle test procedures were used to investigate the degradation potential of several imidazolium cations in the presence of [Br], [BF_4], [PF_6], [$N(CN)_2$], [$(CF_3SO_2)_2N$], and octyl sulfate as the counterions. Nonetheless, with the exception of the ILs containing octyl sulfate, no molecule demonstrated considerable biodegradation.[130−133] A number of DESs were tested for biodegradability. All of the tested DESs showed a biodegradation rate of more than 69.3% after 28 days, indicating that they can all be regarded as biodegradable green solvents.[134]
- In terms of conductivity, DESs are highly conductive, and ILs can be addressed as a moderate to highly conductive solution.[135]

3.2. Classification of Deep Eutectic Solvents. The researcher initially categorized DES as a liquid compound with a melting point lower than 100 °C when compared to its pure ingredients.[136] The classification of DESs is illustrated in Figure 5.

Metal salts or metal salt hydrates are associated with organic salts or other neutral compounds in types I, II, and IV DESs, whereas the type III DES has one organic salt, often an ammonium halide with a structure comparable to that of ILs, and a hydrogen bond donor. The capability to solvate a broad range of transition metal particles, including chlorides and oxides, has stimulated interest in type III eutectics, which are mainly composed of choline chloride and hydrogen bond donors.[137,138]

Table 4 shows the general formula that is used to categorized four types of DESs according to their HBD and HBA.

Table 4. General Formula for the Classification of DESs[37]

type	general formula	terms
type I	$Cat^+X^-zMCl_x$	M = Zn,[1,5,6] Sn,[7] Fe, Al,[8] Ga,[9] In[10]
type II	$Cat^+X^-zMCl_x{\cdot}yH_2O$	M = Cr[11] Co, Cu, Ni, Fe
type III	Cat^+X^-zRZ	Z = CONH,[12] COOH,[13] OH[14]
type IV	$MCl_x + RZ = MCl_{x-1} + {\bullet}RZ + MCl_{x+1}^-$	M = Al, Zn and Z = $CONH_2$, OH

3.3. Physicochemical Properties of Deep Eutectic Solvents. In recent years, researchers have given extensive attention to DESs. The principal reason behind this interest is the physicochemical properties of DESs. DESs are chemically tailorable, in addition to having properties such as nonflammability, lower rate of volatility, low vapor pressure, and chemical and thermal stability. So, they can be formulated for particular applications. Major physicochemical properties of DESs such as density, viscosity, ionic conductivity, thermal stability, polarity, phase behavior, and interfacial tension are discussed in this study.

Only combinations with a melting point underneath the ideal eutectic temperature are addressed under DESs. It would not be called a "deep" solvent otherwise, as it would be indistinguishable from any other solution.[139] Choline chloride and urea, for example, constitute a DES with a molar ratio of 1:2 and a melting temperature of 285.15 K. However, purified choline chloride and urea melt at 575.15 and 407.15 K, respectively.[136] As previously stated, DESs are mainly composed of a HBD and a HBA. This solvent is a mixture of two or more pure chemicals, rather than a single pure molecule. We show a binary solution of A and B compounds in Figure 6, showing the equivalence points.

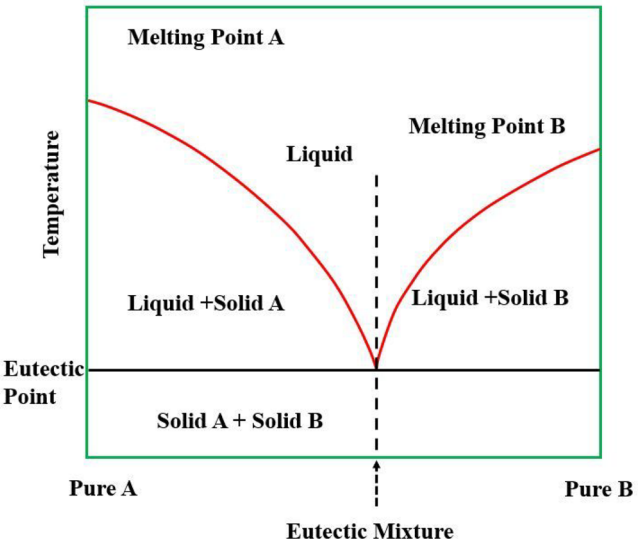

Figure 6. On a binary diagram, a schematic illustration of a eutectic point. Reprinted with permission from ref 140. Copyright 2016 Wiley Online Library.

The ratio of hydrogen bond donors and acceptors can affect the solvent's melting point reduction. The coupling of hydrogen bonds with anionic groups diminishes as the attraction of hydrogen bonds to cationic groups rises. The melting point is dropped due to this precise interaction (also referred to as low lattice energy) between the cationic and anionic groups. Most DESs have freezing values in the range between 69 and 149 °C, and yet none of the individual compounds have a freezing point lower than 150 °C.[38]

The density of a substance is an important physical attribute, as it has an impact on the design and functioning of a process. The percent of DESs that has been reported exhibits densities that seem to be higher than that of water. For example, metal-salt-based DESs have densities of 1.3−1.6 $g{\cdot}cm^{-3}$.[141] Hydrophobic DESs, on the other hand, have densities that are lower than that of water.[142] The temperature and composition have an impact on the density of the DES.[143] According to some research, this solvent has a temperature-dependent density profile. The molecular degree of motion increases as the temperature increases, expanding volume and reducing the density of the sample. Also, solvent densities are also affected by the mole fraction of individual components.[143] For instance, the densities of the DES of $ZnCl_2$/acetamide (1:4) as well as the DES of $ZnCl_2$/urea (1:3.5) are 1.36 and 1.63 $g{\cdot}cm^{-3}$, correspondingly. This difference in the densities is due to their different molecular compositions.[144] The density of the DESs

https://doi.org/10.1021/acsomega.2c03008
ACS Omega 2022, 7, 28723−28755

is between that of the associated salt and the density of the HBD utilized in their synthesis.[145] The ammonium-salt-based DESs exhibit relatively low density as a result of obvious steric hindrance from alkyl chains. Densities of choline chloride-based DESs and *N*,*N*-diethyl ethanol ammonium chloride-based DESs increased when the mole percentage of glycerol increased as the HBD.[143]

The thermal stability of any solvent indicates how well it can endure a temperature range. Acquiring this information is vital for quality control. The melting and decomposition temperatures of DESs, which are extremely effective for their utilization for alternative solvents, are one of their most prominent qualities. These qualities govern the range of temperature through which a DES can maintain a liquid state and consequently its application range.[63] Thus, according to researchers, the variety of HBDs used has a considerable impact on the thermal properties of any DES. The thermal stability of DESs is greatly influenced by the nature of the HBD. For example, DESs comprising a HBD and having greater viscosity have a higher degradation temperature, and DESs become more stable as the extent of the alkyl chain in any HBD extends. Urea, glycerol, and glucomore have a higher boiling point temperature and thus thermally stable yield DESs such as ChCl:Glyce, ChCl:Urea, and ChCl:Gluc which are more thermostable.[146]

Ionic conductivity is electrical conductivity due to the motion of ionic charge. The fundamental controller of conductivity is known to be viscosity; most DESs have low ionic conductivities (κ < 2 mS cm^{-1} at ambient temperature). Conductivity increases remarkably as viscosity decreases due to ionic species' free mobility as the hole mobility increases.[38] For example, ammonium-based salt DESs are greater in value than phosphonium-based salt DESs in ionic conductivity. According to several studies, the conductivity of DESs typically exhibits considerable non-Arrhenius behavior, which is defined as an increase in the measured rate coefficient with an elevation in reverse temperature.[147−149]

For any fluid, viscosity is one of the crucial properties. It controls the fluid flow properties and conductivity, thereby influencing their suitability for particular applications. In general, DESs are considered to have the highest viscosity of any other molecular solvents and ILs.[37] DES possesses lower mobility of free spaces because of the presence of an immense hydrogen-bonding network between the compounds which results in a higher viscosity value. van der Waals and electrostatic interactivity also may contribute to the high viscosity of DESs.[38] However, hydrophobic DESs based on DL-menthol had extremely low viscosities (7.61 mPa.s at 25 °C for a 1:3 DL-menthol/octanoic acid ratio) according to a previous study.[150] Ammonium-based salt DESs have substantially lower viscosities than phosphonium-based salt DESs, according to studies. Within the ammonium group, the viscosities of the different DESs increased as their molecular weights increased. The viscosity of phosphonium-based salt DESs, on the other hand, was unaffected by their molecular weight.[151] The viscosity of polyethylene-glycol-based DESs is often lower than regular DESs. At 25 °C, the viscosity of ChCl/urea (1:2 molar ratio) was determined to be around 800 mPa s.[152] Depending on the nature of polyethylene glycol, its viscosity when mixed with urea is only 134.08 mPa at 25 °C.[153] DESs have a linear but inverse relationship with temperature. Their viscosities decrease as temperature increases.

One of the most important physical properties of DESs is surface tension, which provides a lot of information about the molecular influence on the degree of interactions in a solution.[39] Surface tension arises from the strong interactions between water molecules, called hydrogen bonding. Surface tension arises when intermolecular interactions in a liquid induce cohesive tension, which helps to minimize the surface area of the liquid's interface with other phases in contact with the liquid. This can alternatively be expressed as the amount of energy necessary to raise the surface area of a liquid by one unit of area. Compared to other physicochemical properties, the studies correlated to the surface tension of DESs are quite narrow. The surface tension of DESs is significantly greater than that of most common solvents. The surface tension of DESs exhibited a linear relationship with temperature, with the surface tension falling as the temperature is increased, similar to the tendency for viscosity.[154] Surface tensions of DESs have been found to range somewhere around 35−75 mN m^{-1} at 25 °C.[155] The excessive addition of ChCl to glycerol is thought to impair the strength of intermolecular interactions, such as the glycerol hydrogen bonding network.[38] For example, choline chloride/D-fructose has a substantial value of surface tension, which reflects their extensive hydrogen-bond network.[156]

Polarity is a key indicator of solvent strength, as it reflects the overall solvation capability of a solvent. This feature is frequently assessed using solvatochromic parameters, which examine the hypsochromic (blue) shift or bathochromic (red) shift of UV−vis bands for negatively solvatochromic dyes (e.g., Reichardt's betaine dye) and positively solvatochromic dyes (e.g., Nile red) as a function of the solvent's charge, accordingly.[157] The polarity of DESs is said to be governed by the hydrogen bond donor in their molecular structure.[158] When water is added to DESs, conversely, the hydrogen-bond-accepting basicity decreases, and the polarizability/polarity improves.[159]

Solvents with low vapor pressure have less possibility of losses due to evaporation during the reaction process, purification, and other operations. DES is considered to have a lower vapor pressure than any other conventional solvents.[160] For DESs, the type of salt and HBD determines the range of vapor pressures. For example, urea (HBD) based DESs are found to have a lower vapor pressure than the glycol-based DESs.[161] The formation of a hydrogen bond between the HBD and HBA greatly affects the vapor pressure during the synthesis of DESs. When treating solvents or utilizing them in mass and heat transfer procedures, vapor pressure data of DES solutions are very crucial.[162]

The hydrophilic DES's practical application is limited to just polar molecules, which is a significant disadvantage of the solvent. HDESs, or hydrophobic DESs, are a new form of extractive media capable of extracting nonpolar organic and inorganic compounds from aquatic media.[163] The development of hydrophobic DES using a variety of long-chain quaternary ammonium salts and acids for the enhancement and extraction of a variety of chemicals has been explored.[164,165] One of the distinctions between hydrophilic and hydrophobic DESs is that the former often induces a substantial depression in the melting point, while the latter can produce both enormous and moderate depressions. This difference in melting point depression behavior is due to the influence of charged and polar moieties in hydrophilic DESs, resulting in extensive hydrogen bond interactions, whereas in hydrophobic (D)ESs, a large depression is only obtained when

https://doi.org/10.1021/acsomega.2c03008
ACS Omega 2022, 7, 28723−28755

Figure 7. Application of DESs in several fields.

salts are present. Some applications demand this type of hydrophobic DES.[142]

DESs have been used in the field of electroanalytical synthesis technology over the years. As a consequence, DESs must have the potential to degrade precursors during the reaction time and under synthesis circumstances. According to the majority of studies, increasing the temperature and decreasing the mole fraction can improve the solubility of any DES.[44,117] It was also reported that the solubility of the DES is governed by the DES's own chemical structure.[166]

3.4. Application of Deep Eutectic Solvents in Different Fields of Interest. Negligible vapor pressure, noninflammability, chemical tolerability, solubility potential for a wide variety of substances, and water nonreactivity are some of the physicochemical characteristics that make DES a fascinating solvent. Additionally, they are simple to make utilizing low-toxicity, usually available, and low-cost substances. DESs have gained popularity as green solvents in a variety of fields, including chemistry, material engineering, and biology, due to these advantages. Figure 7 represents the application of DESs in different fields.

The physical properties of DESs are similar to other ILs, and their chemical properties suggest application areas that are significantly different.

1. An advanced type of water-immiscible extractant (for example, hydrophobic DES as an extractant for volatile fatty acid).[167]
2. In the latest days, much emphasis has been placed on replacing traditional extraction processes with "green" extraction techniques. Many researchers have found that deep eutectic mixtures hold some fascinating physicochemical properties that make them an exceptional solvent in the field of extraction. DES is used as an alternative to ILs in the metal extraction process, and it is also used as an extractant for organic compounds.[138,168]
3. Due to some other benefits such as lower cost, easier synthesis than ILs, and having an environmentally friendly profile, the use of DESs in analytical microextraction techniques is on the surge.[169]
4. DESs have a very strong ability to solubilize different types of chemicals with nonidentical properties. Thus, they can be used as extraction media for anthocyanins, flavones, xantonoides, and many other compounds.[170]
5. In the case of the fuel desulfurization process, it can lessen the sulfur content of fuels below the environmental regulations, which is about 10 ppm. Different types of DESs based on polyethylene glycol (PEG) could successfully remove thiophene and dibenzothiophene from fuel with extraction efficiencies ranging from 6% to 85%.[171]
6. Some DESs perform as an excellent solvent for the elemental mercury extraction process.[172]
7. Global warming is now one of the most alarming topics in today's world. Our environment is now on the verge

https://doi.org/10.1021/acsomega.2c03008
ACS Omega 2022, 7, 28723−28755

Table 5. Biodegradability of Different Types of DESs[134]

no.	DES and reference substance	biodegradability (%)			
		7 days	14 days	21 days	28 days
1	ChCl/urea (1:2)	39.7 ± 0.6	81.2 ± 0.7	90.3 ± 0.6	97.1 ± 0.7
2	ChCl/acetamide (1:2)	25.8 ± 0.5	62.5 ± 0.1	81.1 ± 0.6	89.5 ± 0.6
3	ChCl/ethylene glycol (1:2)	24.1 ± 0.5	58.2 ± 0.5	77.3 ± 0.5	81.9 ± 0.6
4	ChCl/glycerol (1:2)	46.3 ± 1.5	83.2 ± 0.6	90.9 ± 0.6	95.9 ± 0.7
5	ChCl/1,4-butanediol (1:4)	29.4 ± 0.8	51.6 ± 1.1	62.0 ± 0.1	73.6 ± 0.9
6	ChCl/triethylene glycol (1:4)	10.7 ± 1.5	29.7 ± 0.5	51.4 ± 0.3	69.3 ± 0.5
7	ChCl/xylitol (1:1)	31.6 ± 2.4	66.0 ± 0.6	77.6 ± 0.8	84.3 ± 0.6
8	ChCl/D-sorbitol (1:1)	37.4 ± 1.5	63.4 ± 0.4	80.1 ± 0.6	86.2 ± 0.5
9	ChCl/p-toluenesulfonic acid (1:1)	32.3 ± 1.4	72.8 ± 0.4	76.3 ± 2.1	80.4 ± 0.3
10	ChCl/oxalic acid (1:1)	40.6 ± 0.4	61.4 ± 0.5	65.0 ± 0.4	73.4 ± 1.5
11	ChCl/levulinic acid (1:2)	33.9 ± 0.8	49.4 ± 1.0	67.2 ± 0.5	74.2 ± 2.2
12	ChCl/malonic acid (1:1)	34.6 ± 1.3	50.2 ± 0.6	60.8 ± 1.6	76.3 ± 1.3
13	ChCl/malic acid (1:1)	37.9 ± 0.9	62.9 ± 0.7	73.3 ± 0.6	79.4 ± 1.0
14	ChCl/citric acid (1:1)	39.5 ± 1.3	65.3 ± 1.6	75.0 ± 0.8	81.6 ± 0.7
15	ChCl/tartaric acid (2:1)	54.2 ± 1.4	76.4 ± 0.6	81.3 ± 1.0	84.6 ± 0.3
16	ChCl/xylose/water (1:1:1)	50.8 ± 1.3	70.6 ± 0.3	82.0 ± 1.1	89.7 ± 0.7
17	ChCl/sucrose/water (5:2:5)	55.6 ± 0.4	68.0 ± 1.9	87.4 ± 1.8	91.6 ± 0.3
18	ChCl/fructose/water (5:2:5)	48.4 ± 0.5	73.6 ± 1.3	88.2 ± 1.6	93.7 ± 1.3
19	ChCl/glucose/water (5:2:5)	58.6 ± 1.2	77.4 ± 1.0	89.4 ± 1.0	92.0 ± 0.4
20	ChCl/maltose/water (5:2:5)	53.0 ± 0.8	73.7 ± 2.0	84.6 ± 1.2	90.0 ± 0.5
21	sodium benzoate	57.9 ± 1.0	62.8 ± 1.1	79.0 ± 0.2	81.5 ± 0.7

of destruction due to this problem. It is affecting our world's atmosphere, and as a result, all living beings are suffering. We all know that excess CO_2 emission is the main cause of this phenomenon. One step to reduce this vast amount of CO_2 to slow down the global warming process to save our environment is to adsorb and sequestrate CO_2. The significance of DESs in this domain can be influential because of their high efficiency and sustainability in the CO_2 adsorption process.[173,174]

8. Extraction of subquality natural gas usually leads to relatively high amounts of impurities, such as CO_2, which have to be removed before usage. DES has the potential to capture and remove CO_2 from natural gas. Thus, it is used as a low-cost and biodegradable gas sweetener in the gas industry.[175]
9. The high thermal stability of DESs improves their ability to be used as a chemical additive or preflooding agent in the thermal enhanced oil recovery process. It improves the pure steam recovery by 12%. Produced oil has higher API gravity, lower sulfur, and more saturated hydrocarbons.[176]
10. In the gas industry, hydrate formation is a major flow assurance obstacle. DESs have a unique ability to form a hydrogen bond with the water molecule. This makes them a novel hydrate inhibitor.[177]
11. DES is used for the solubilization of water-insoluble drugs, transdermal drug delivery, inorganic nanoparticle synthesis, and designing polymeric and self-assembled drug carriers.[178]
12. DESs are implemented as functional additives for starch-based plastics.[179]
13. The production of cellulose derivatives involves the usage of DESs.[180]
14. For the synthesis of biodiesel fuel from low-grade palm oil, DESs have been employed as catalysts.[181]
15. In electrochemical operations, it is employed as an electrolyte in electroplating and electroless plating of metals, for example.[182]
16. For enzyme-catalyzed epoxide hydrolysis, DESs are feasible cosolvents.[183]
17. It is utilized to execute the biodiesel extraction machine.[184]

3.5. Environmental Aspects of DESs. Nowadays, DESs are considered to be the alternative to ILs. Compared to conventional ILs, DESs are relatively inexpensive, easy to synthesize, renewable, and good biocompatible organic solvents. DESs are generally touted as "green" simply because the components involved in their preparation are usually environmentally friendly.[117] Also, they have been attracting scientific and technological attention due to their unique physical and chemical properties. This surging interest in DESs is attributed to their potential to be environmentally benign because of their nontoxic and biodegradable characteristics. The microbial breakdown of chemical substances is known as biodegradation. When opposed to chemical disintegration, biodegradation appears to be more environmentally safe.

A substance is called biodegradable if it is capable of being decomposed by bacteria or other living organisms, which helps them avoid pollution. A chemical should be biodegradable to be environmentally friendly. Understanding the ecological consequences and outcome of DESs requires a clear understanding of their biodegradability. Although few studies have been done on the safety of DES solvents, their nontoxic properties make them a more enticing solvent than classic ILs.[185]

Researchers tested the biodegradability of a variety of DESs. The closed bottle test was used by Zhao et al. to determine the biodegradability of 20 choline chloride-based DESs. After 28 days, all of the tested DESs had a biodegradation rate of >69.3%, indicating that they may all be termed biodegradable green solvents. The ability of the chemicals to cross the cell wall helps to understand their biodegradable potential. The

https://doi.org/10.1021/acsomega.2c03008
ACS Omega 2022, 7, 28723−28755

rate of degradability for all of these DESs is considered to be attributable to the individual components used in DES synthesis of biodegradable substances such as choline chloride, urea, and glycerol.[134] Table 5 depicts the biodegradability rate of different DESs examined by the Closed Bottle test.

The biodegradability of DESs appeared to be influenced by the HBD used: The order of amine-based DESs, sugar-based DESs, alcohol-based DESs, and acid-based DESs varied.[134] Also, according to prior research, DESs made from ethylene and glycol are more biodegradable than DESs formed from glycerol as hydrogen bond donors.[186,187] Choline chloride-based salts have lower toxicity than ethylene ammonium chloride-based salts.[188]

DESs were shown to be more carcinogenic than their constituents in several trials. Charge delocalization is considered to be the cause of this abnormality. Charge decolonization proceeds between the HBD and HBA during the development of a hydrogen bond between the DESs' components. Delocalized charge compounds are generally more hazardous than localized charge chemicals.[189−191]

3.6. Prospects and Challenges of DESs. The purpose of DESs is to reduce the use and generation of hazardous substances, primarily through the promotion of innovative research on the creation of sustainable technologies. This is due to adaptability, low vapor pressure, good recyclability, low cost, chemical and thermal stability, and ease of preparation.[117,192−195] DESs have hit the mainstream over the last two decades. There has been more research done to further investigate the field of numerous applications and the potential of DESs, which will serve the globe as a new and alternative solvent to the conventional one.[196−199] DESs have been used in processes including greenhouse gas capture, alternate media for catalyzed reactions, analytical chemistry microextraction, stationary phase separation, therapeutic applications, and so on.[200−205] Most of these solvents are nonflammable, biodegradable, and less toxic, making them environmentally beneficial.[38,155,206,207] Most of these solvents have been proven to be practically eco-friendly.[190,208,209] As a result, they are gaining some traction as a viable alternative to toxic solvents. DESs have been identified as low-cost IL replacements. Another concern is that ILs are expensive, yet they are only required in extremely low concentrations. Despite this, current research has revealed that the use of ILs has negative environmental consequences.[210,211] On the contrary, recent studies have shown that cholinium-based liquids are less hazardous and more sustainable chemicals.[212] In that case, cholinium-based DESs may be a feasible alternative to ILs.

One of the greatest impediments to the widespread usage of ionic liquids in the industry is the high expense of manufacturing them. This is mostly due to the high cost of raw ingredients as well as the time-consuming preparation and purification processes. Since with widely obtainable components producing DESs on a large scale is simpler, DESs have been found as low-cost substitutes for ILs.[145] Conventional inorganic salts are inexpensive, but they must be used in high concentrations to obtain optimal inhibitory results. Based on prior research on shale swelling inhibitors, it is obvious that when compared to conventional shale swelling inhibitors including KCl, PDA, and others the amount of DESs required to suppress the rate of shale swelling is quite low.[213−215] As a result, when compared to typical inhibitors, the quantity of DESs required is reduced. This lowers the cost of inhibitors. It is also less expensive than conventional ionic liquids.[117] Studies showed that the swelling rate was reduced by 43.02% using traditional KCl, which had a concentration of roughly 5 wt %. With similar concentrations, DESs such as urea-DES, gly-DES, oxa-Des, and cit-DES reduced the swelling rate of the Na-bent sample by 29.38%, 21.57%, 37.31%, and 39.66%, respectively.[216]

Here are some of the challenges regarding this burgeoning field of interest, which are associated with today's greatest considerations. The formulation of structure−property correlations for these DESs is becoming progressively vital to understanding their possibilities in transdisciplinary disciplines. DESs are, nonetheless, progressing steadily in the sphere of a fundamental understanding.[125] The chemical composition of the different components determines the properties of DESs, which can be tuned by changing the constituent entities. Because of this, DESs are often referred to as task-specific solvents.[206] The high densities and viscosities of DESs compared to conventional solvents, which could be a barrier on a large scale or in continuous-flow operations, are a significant drawback acknowledged by some studies.[194] The behavior of DES mixtures and how this influences DES characteristics, specifically viscosity, which is still a major limitation of hydrophilic DES, should be studied in detail.[217]

The hygroscopic properties of the major DESs require more investigation since they may have an impact on the ability to stabilize and store these solvents. Studies showed that due to the hygroscopic nature of DESs stringent humidity control is required during storage and handling in order to obtain reliable data and products.[218] According to studies, the inclusion of water in DESs significantly reduces the viscosity and alters the polarity, conductivity, density, and solvation qualities.[219−221] So, to regulate and get the intended qualities, it will be necessary to operate DESs in a controlled environment and clearly define the target product profiles (TPPs) and related critical quality attributes (CQAs).[222]

4. DES AS A SWELLING INHIBITOR

Researchers have already invented numerous compounds after many years of investigation, which were introduced as fracturing fluids to alleviate the challenging issues associated with shale swelling, including amine derivatives, surfactants, polymers, and other organic and inorganic salts. They can prevent water from combining with clay minerals, but their use is constrained by a variety of factors, including inadequate inhibitive efficacy, cost, and environmental considerations.[51,52,54] A typical shale swelling inhibitor comprising more than 2% KCl will have a chloride content of more than 9500 ppm. On the contrary, surface discharge of salt brines comprising more than 3000 ppm chloride on lease or 1000 ppm chloride off lease is generally prohibited by most regulatory legislation.[223] Considerations regarding managing and mixing huge amounts of salts, as well as the environmental implications of discarding unused saltwater and producing fracturing water, have encouraged researchers to look into novel clay stabilizing compounds.[85] Researchers have already investigated several types of DESs as swelling inhibitors. Studies show that the inhibition ability of any type of DES is measured by determining the rheological properties, linear swelling test, XRD diffraction analysis, hot-rolling recovery test, zeta potential test, particle size distribution, surface tension measurement, and so on.[214,216,224] Hence, most of the test experiments were done using a shale sample of Na-bentonite. Table 6 recapitulates all the standings and conditions under

https://doi.org/10.1021/acsomega.2c03008
ACS Omega 2022, 7, 28723−28755

Table 6. Performance Evaluation of DESs as Potential Swelling Inhibitor

no.	author	inhibitor	abbreviated name	shale sample used	conc. (wt %)/pres. (MPa)/temp. (°C)	swelling reduction (%)	recovery rate (%)	yield point (Pa)	apparent viscosity (mPa.s)	zeta potential (mV)	XRD (Å)	surface tension (mN/m)	particle size distribution (μm)
01	Ma et al. (2021)	urea-choline chloride	urea-DES	Na-bent	1−5/5/90−150	43.33	NA	NA	5−22	−8.7	1.3−1.4	64.64	6−69.24
02	Ma et al. (2021)	glycerol- choline chloride	gly-Des	Na-bent	1−5/5/90−150	58.84	NA	NA	4−124	−1.73	1.42−1.43	54.51	9−111.70
03	Ma et al. (2021)	oxalic-choline chloride	oxa-DES	Na-bent	1−5/5/90−150	28	NA	NA	0.7−6	−4.12	1.39−1.44	61.38	6−287
04	Ma et al. (2021)	citric-choline chloride	cit-DES	Na-bent	1−5/5/90−150	23.34	NA	NA	1−8	−1.96	1.41−1.43	64.90	7−97.58
05	Jia et al. (2019a)	urea-choline chloride	CU-DES	Na-bent	(0.05−2) w/v%/10/25−160	69.54	75−82	9−49	10−67	−32 to −16	14.36−18.46	NA	1−105.58
06	Jia et al. (2019a)	urea-choline chloride	CU-DES	shale powder	(0.05−2) w/v%/10/25−160	72.64	NA	NA	NA	NA	NA	NA	NA
07	Jia et al. (2019b)	choline chloride-propanedioic acid	CM-DES	Na-bent	0.05−2/10/70−160	50−60	74−86.95	10−88	10−102	−21.20	13.28−15.25	68−72.19	4−172
08	Jia et al. (2019b)	choline chloride-3-phenylpropionic acid	CP-DES	Na-bent	0.05−2/10/70−160	36−71	89−90.94	9−54	9−61	−15.20	13.70−14.71	40.91−61.56	6−179
09	Jia et al. (2019b)	choline chloride-itaconic acid and 3-mercaptopropionic acid	CIM-DES	Na-bent	0.05−2/10/70−160	53−62	84−89.27	8−66	10−77	−18.90	13.95−15.09	64−71.13	8−225
10	Beg et al. (2021)	tetrabutyl ammonium bromide- diethanolamine	DES-I	Na-bent	NA	NA	NA	33−66	29.78−59.47	NA	NA	NA	NA
11	Beg et al. (2021)	tetrabutyl ammonium bromide- diethylene glycole	DES-II	Na-bent	0.05−1/68.95/25−105	NA	NA	39.80−72.98	33.45−62.12	NA	NA	NA	NA

https://doi.org/10.1021/acsomega.2c03008
ACS Omega 2022, 7, 28723−28755

Table 7. Yield Point (YP) and Apparent Viscosity (AV) Values of Several Inhibitors (DESs)

author	testing medium	temp (°C)	inhibitor conc.	clay conc.	YP (Pa)	AV (mPa.s)
Ma et al. (2021)	water	90	NA	5 wt %	NA	3.05
Ma et al. (2021)	water	90	NA	10 wt %	NA	11.45
Ma et al. (2021)	water	90	NA	15 wt %	NA	82.44
Ma et al. (2021)	KCl	90	5 wt %	5 wt %	NA	4.58
Ma et al. (2021)	KCl	90	5 wt %	10 wt %	NA	4.96
Ma et al. (2021)	KCl	90	5 wt %	15 wt %	NA	6.30
Ma et al. (2021)	KCl	90	5 wt %	20 wt %	NA	7.63
Ma et al. (2021)	KCl	90	5 wt %	25 wt %	NA	16.03
Ma et al. (2021)	KCl	90	5 wt %	30 wt %	NA	35.69
Ma et al. (2021)	KCl	90	5 wt %	35 wt %	NA	70.23
Ma et al. (2021)	polyether amino	90	5 wt %	5 wt %	NA	4.58
Ma et al. (2021)	polyether amino	90	5 wt %	10 wt %	NA	4.77
Ma et al. (2021)	polyether amino	90	5 wt %	15 wt %	NA	4.96
Ma et al. (2021)	polyether amino	90	5 wt %	20 wt %	NA	6.11
Ma et al. (2021)	polyether amino	90	5 wt %	25 wt %	NA	9.16
Ma et al. (2021)	polyether amino	90	5 wt %	30 wt %	NA	13.36
Ma et al. (2021)	polyether amino	90	5 wt %	35 wt %	NA	19.47
Ma et al. (2021)	polyether amino	90	5 wt %	40 wt %	NA	26.91
Ma et al. (2021)	urea-DES	90	5 wt %	5 wt %	NA	7.63
Ma et al. (2021)	urea-DES	90	5 wt %	10 wt %	NA	5.92
Ma et al. (2021)	urea-DES	90	5 wt %	15 wt %	NA	7.82
Ma et al. (2021)	urea-DES	90	5 wt %	20 wt %	NA	8.40
Ma et al. (2021)	urea-DES	90	5 wt %	25 wt %	NA	8.40
Ma et al. (2021)	urea-DES	90	5 wt %	30 wt %	NA	8.97
Ma et al. (2021)	urea-DES	90	5 wt %	35 wt %	NA	11.64
Ma et al. (2021)	urea-DES	90	5 wt %	40 wt %	NA	22.14
Ma et al. (2021)	gly-DES	90	5 wt %	5 wt %	NA	4.01
Ma et al. (2021)	gly-DES	90	5 wt %	10 wt %	NA	3.82
Ma et al. (2021)	gly-DES	90	5 wt %	15 wt %	NA	4.96
Ma et al. (2021)	gly-DES	90	5 wt %	20 wt %	NA	5.92
Ma et al. (2021)	gly-DES	90	5 wt %	25 wt %	NA	6.30
Ma et al. (2021)	gly-DES	90	5 wt %	30 wt %	NA	7.44
Ma et al. (2021)	gly-DES	90	5 wt %	35 wt %	NA	8.97
Ma et al. (2021)	gly-DES	90	5 wt %	40 wt %	NA	12.40
Ma et al. (2021)	oxa-DES	90	5 wt %	5 wt %	NA	0.76
Ma et al. (2021)	oxa-DES	90	5 wt %	10 wt %	NA	1.15
Ma et al. (2021)	oxa-DES	90	5 wt %	15 wt %	NA	2.10
Ma et al. (2021)	oxa-DES	90	5 wt %	20 wt %	NA	2.29
Ma et al. (2021)	oxa-DES	90	5 wt %	25 wt %	NA	2.86
Ma et al. (2021)	oxa-DES	90	5 wt %	30 wt %	NA	3.82
Ma et al. (2021)	oxa-DES	90	5 wt %	35 wt %	NA	5.34
Ma et al. (2021)	oxa-DES	90	5 wt %	40 wt %	NA	6.30
Ma et al. (2021)	cit-DES	90	5 wt %	5 wt %	NA	1.34
Ma et al. (2021)	cit-DES	90	5 wt %	10 wt %	NA	0.76
Ma et al. (2021)	cit-DES	90	5 wt %	15 wt %	NA	1.91
Ma et al. (2021)	cit-DES	90	5 wt %	20 wt %	NA	2.29
Ma et al. (2021)	cit-DES	90	5 wt %	25 wt %	NA	3.44
Ma et al. (2021)	cit-DES	90	5 wt %	30 wt %	NA	4.39
Ma et al. (2021)	cit-DES	90	5 wt %	35 wt %	NA	5.92
Ma et al. (2021)	cit-DES	90	5 wt %	40 wt %	NA	8.40
Ma et al. (2021)	water	150	5 wt %	5 wt %	NA	4.30
Ma et al. (2021)	water	150	5 wt %	10 wt %	NA	11.67
Ma et al. (2021)	water	150	5 wt %	15 wt %	NA	48.52
Ma et al. (2021)	water	150	5 wt %	20 wt %	NA	139.42
Ma et al. (2021)	KCl	150	5 wt %	5 wt %	NA	4.30
Ma et al. (2021)	KCl	150	5 wt %	10 wt %	NA	3.07
Ma et al. (2021)	KCl	150	5 wt %	15 wt %	NA	13.21
Ma et al. (2021)	KCl	150	5 wt %	20 wt %	NA	14.74
Ma et al. (2021)	KCl	150	5 wt %	25 wt %	NA	22.11
Ma et al. (2021)	KCl	150	5 wt %	30 wt %	NA	60.50
Ma et al. (2021)	polyether amino	150	5 wt %	5 wt %	NA	3.38

https://doi.org/10.1021/acsomega.2c03008
ACS Omega 2022, 7, 28723−28755

Table 7. continued

author	testing medium	temp (°C)	inhibitor conc.	clay conc.	YP (Pa)	AV (mPa.s)
Ma et al. (2021)	polyether amino	150	5 wt %	10 wt %	NA	5.83
Ma et al. (2021)	polyether amino	150	5 wt %	15 wt %	NA	7.98
Ma et al. (2021)	polyether amino	150	5 wt %	20 wt %	NA	9.21
Ma et al. (2021)	polyether amino	150	5 wt %	25 wt %	NA	12.28
Ma et al. (2021)	polyether amino	150	5 wt %	30 wt %	NA	17.81
Ma et al. (2021)	polyether amino	150	5 wt %	35 wt %	NA	35.01
Ma et al. (2021)	polyether amino	150	5 wt %	40 wt %	NA	57.12
Ma et al. (2021)	urea-DES	150	5 wt %	5 wt %	NA	7.98
Ma et al. (2021)	urea-DES	150	5 wt %	10 wt %	NA	5.53
Ma et al. (2021)	urea-DES	150	5 wt %	15 wt %	NA	4.61
Ma et al. (2021)	urea-DES	150	5 wt %	20 wt %	NA	4.91
Ma et al. (2021)	urea-DES	150	5 wt %	25 wt %	NA	5.53
Ma et al. (2021)	urea-DES	150	5 wt %	30 wt %	NA	6.45
Ma et al. (2021)	urea-DES	150	5 wt %	35 wt %	NA	10.13
Ma et al. (2021)	urea-DES	150	5 wt %	40 wt %	NA	17.20
Ma et al. (2021)	gly-DES	150	5 wt %	5 wt %	NA	4.30
Ma et al. (2021)	gly-DES	150	5 wt %	10 wt %	NA	3.99
Ma et al. (2021)	gly-DES	150	5 wt %	15 wt %	NA	4.30
Ma et al. (2021)	gly-DES	150	5 wt %	20 wt %	NA	4.61
Ma et al. (2021)	gly-DES	150	5 wt %	25 wt %	NA	4.91
Ma et al. (2021)	gly-DES	150	5 wt %	30 wt %	NA	4.61
Ma et al. (2021)	gly-DES	150	5 wt %	35 wt %	NA	8.91
Ma et al. (2021)	gly-DES	150	5 wt %	40 wt %	NA	14.13
Ma et al. (2021)	oxa-DES	150	5 wt %	5 wt %	NA	1.84
Ma et al. (2021)	oxa-DES	150	5 wt %	10 wt %	NA	3.69
Ma et al. (2021)	oxa-DES	150	5 wt %	15 wt %	NA	3.69
Ma et al. (2021)	oxa-DES	150	5 wt %	20 wt %	NA	3.38
Ma et al. (2021)	oxa-DES	150	5 wt %	25 wt %	NA	4.30
Ma et al. (2021)	oxa-DES	150	5 wt %	30 wt %	NA	5.22
Ma et al. (2021)	oxa-DES	150	5 wt %	35 wt %	NA	7.98
Ma et al. (2021)	oxa-DES	150	5 wt %	40 wt %	NA	13.21
Ma et al. (2021)	cit-DES	150	5 wt %	5 wt %	NA	3.99
Ma et al. (2021)	cit-DES	150	5 wt %	10 wt %	NA	4.61
Ma et al. (2021)	cit-DES	150	5 wt %	15 wt %	NA	3.99
Ma et al. (2021)	cit-DES	150	5 wt %	20 wt %	NA	3.38
Ma et al. (2021)	cit-DES	150	5 wt %	25 wt %	NA	4.30
Ma et al. (2021)	cit-DES	150	5 wt %	30 wt %	NA	5.53
Ma et al. (2021)	cit-DES	150	5 wt %	35 wt %	NA	7.98
Ma et al. (2021)	cit-DES	150	5 wt %	40 wt %	NA	14.74
Jia et al. (2019a)	DI water	25	NA	4%	11.81	15.78
Jia et al. (2019a)	DI water	25	NA	8%	24.54	35.14
Jia et al. (2019a)	DI water	25	NA	12%	55.61	78.88
Jia et al. (2019a)	DI water	25	NA	16%	124.27	142.35
Jia et al. (2019a)	KCl	25	5 w/v %	4%	10.87	11.12
Jia et al. (2019a)	KCl	25	5 w/v %	8%	10.25	11.47
Jia et al. (2019a)	KCl	25	5 w/v %	12%	10.56	11.83
Jia et al. (2019a)	KCl	25	5 w/v %	16%	10.56	12.91
Jia et al. (2019a)	KCl	25	5 w/v %	20%	11.18	13.98
Jia et al. (2019a)	KCl	25	5 w/v %	24%	14.91	20.08
Jia et al. (2019a)	KCl	25	5 w/v %	28%	29.83	51.63
Jia et al. (2019a)	KCl	25	5 w/v %	32%	82.64	102.19
Jia et al. (2019a)	PDA	25	2 w/v %	4%	9.32	10.40
Jia et al. (2019a)	PDA	25	2 w/v %	8%	9.94	11.12
Jia et al. (2019a)	PDA	25	2 w/v %	12%	10.56	11.83
Jia et al. (2019a)	PDA	25	2 w/v %	16%	10.25	12.19
Jia et al. (2019a)	PDA	25	2 w/v %	20%	10.25	12.91
Jia et al. (2019a)	PDA	25	2 w/v %	24%	12.43	17.21
Jia et al. (2019a)	PDA	25	2 w/v %	28%	24.85	38.37
Jia et al. (2019a)	PDA	25	2 w/v %	32%	46.29	69.20
Jia et al. (2019a)	PDA	25	2 w/v %	36%	90.72	114.38
Jia et al. (2019a)	ChCl	25	1 w/v %	4%	10.87	10.76

https://doi.org/10.1021/acsomega.2c03008
ACS Omega 2022, 7, 28723−28755

Table 7. continued

author	testing medium	temp (°C)	inhibitor conc.	clay conc.	YP (Pa)	AV (mPa.s)
Jia et al. (2019a)	ChCl	25	1 w/v %	8%	10.25	10.76
Jia et al. (2019a)	ChCl	25	1 w/v %	12%	10.25	11.47
Jia et al. (2019a)	ChCl	25	1 w/v %	16%	10.25	12.91
Jia et al. (2019a)	ChCl	25	1 w/v %	20%	10.87	14.34
Jia et al. (2019a)	ChCl	25	1 w/v %	24%	11.50	17.21
Jia et al. (2019a)	ChCl	25	1 w/v %	28%	22.37	40.88
Jia et al. (2019a)	ChCl	25	1 w/v %	32%	42.25	67.77
Jia et al. (2019a)	ChCl	25	1 w/v %	36%	73.32	102.91
Jia et al. (2019a)	CU-DES	25	1 w/v %	4%	9.63	10.40
Jia et al. (2019a)	CU-DES	25	1 w/v %	8%	9.94	11.12
Jia et al. (2019a)	CU-DES	25	1 w/v %	12%	9.94	11.47
Jia et al. (2019a)	CU-DES	25	1 w/v %	16%	9.94	12.55
Jia et al. (2019a)	CU-DES	25	1 w/v %	20%	10.56	13.63
Jia et al. (2019a)	CU-DES	25	1 w/v %	24%	11.18	15.78
Jia et al. (2019a)	CU-DES	25	1 w/v %	28%	14.91	18.65
Jia et al. (2019a)	CU-DES	25	1 w/v %	32%	18.64	22.23
Jia et al. (2019a)	CU-DES	25	1 w/v %	36%	23.61	36.57
Jia et al. (2019a)	CU-DES	25	1 w/v %	40%	49.71	67.05
Jia et al. (2019b)	water	70	NA	5%	11.51	16.10
Jia et al. (2019b)	water	70	NA	10%	50.02	63.90
Jia et al. (2019b)	KCl	70	5 w/v %	5%	9.16	11.43
Jia et al. (2019b)	KCl	70	5 w/v %	10%	9.39	12.21
Jia et al. (2019b)	KCl	70	5 w/v %	15%	10.57	12.99
Jia et al. (2019b)	KCl	70	5 w/v %	20%	14.32	21.30
Jia et al. (2019b)	KCl	70	5 w/v %	25%	33.35	45.71
Jia et al. (2019b)	KCl	70	5 w/v %	30%	104.50	126.75
Jia et al. (2019b)	PDA	70	2 w/v %	5%	8.69	9.87
Jia et al. (2019b)	PDA	70	2 w/v %	10%	8.69	10.39
Jia et al. (2019b)	PDA	70	2 w/v %	15%	8.92	11.95
Jia et al. (2019b)	PDA	70	2 w/v %	20%	11.04	15.58
Jia et al. (2019b)	PDA	70	2 w/v %	25%	23.48	30.65
Jia et al. (2019b)	PDA	70	2 w/v %	30%	51.66	67.27
Jia et al. (2019b)	PDA	70	2 w/v %	35%	109.43	121.56
Jia et al. (2019b)	CM-DES	70	1 w/v %	5%	9.39	10.91
Jia et al. (2019b)	CM-DES	70	1 w/v %	10%	9.16	11.43
Jia et al. (2019b)	CM-DES	70	1 w/v %	15%	9.39	12.47
Jia et al. (2019b)	CM-DES	70	1 w/v %	20%	10.80	12.73
Jia et al. (2019b)	CM-DES	70	1 w/v %	25%	14.56	16.88
Jia et al. (2019b)	CM-DES	70	1 w/v %	30%	28.65	31.95
Jia et al. (2019b)	CM-DES	70	1 w/v %	35%	50.72	58.70
Jia et al. (2019b)	CM-DES	70	1 w/v %	40%	88.30	102.08
Jia et al. (2019b)	CP-DES	70	1 w/v %	5%	9.16	9.35
Jia et al. (2019b)	CP-DES	70	1 w/v %	10%	8.92	10.13
Jia et al. (2019b)	CP-DES	70	1 w/v %	15%	9.39	10.39
Jia et al. (2019b)	CP-DES	70	1 w/v %	20%	9.63	10.65
Jia et al. (2019b)	CP-DES	70	1 w/v %	25%	10.10	14.55
Jia et al. (2019b)	CP-DES	70	1 w/v %	30%	16.20	19.22
Jia et al. (2019b)	CP-DES	70	1 w/v %	35%	26.54	33.77
Jia et al. (2019b)	CP-DES	70	1 w/v %	40%	54.48	61.56
Jia et al. (2019b)	CIM-DES	70	1 w/v %	5%	8.69	10.91
Jia et al. (2019b)	CIM-DES	70	1 w/v %	10%	8.92	11.43
Jia et al. (2019b)	CIM-DES	70	1 w/v %	15%	9.63	11.43
Jia et al. (2019b)	CIM-DES	70	1 w/v %	20%	10.57	12.47
Jia et al. (2019b)	CIM-DES	70	1 w/v %	25%	16.20	18.70
Jia et al. (2019b)	CIM-DES	70	1 w/v %	30%	21.60	25.97
Jia et al. (2019b)	CIM-DES	70	1 w/v %	35%	41.33	45.97
Jia et al. (2019b)	CIM-DES	70	1 w/v %	40%	66.22	77.14
Beg et al. (2021)	DES-I	25	0.05 w/v %	NA	41.09	34.41
Beg et al. (2021)	DES-I	25	0.1 w/v %	NA	47.89	39.04
Beg et al. (2021)	DES-I	25	0.25 w/v %	NA	55.26	44.67
Beg et al. (2021)	DES-I	25	0.50 w/v %	NA	60.93	48.29

https://doi.org/10.1021/acsomega.2c03008
ACS Omega 2022, 7, 28723−28755

Table 7. continued

author	testing medium	temp (°C)	inhibitor conc.	clay conc.	YP (Pa)	AV (mPa.s)
Beg et al. (2021)	DES-I	25	0.75 w/v %	NA	65.75	52.92
Beg et al. (2021)	DES-I	25	1 w/v %	NA	67.73	55.81
Beg et al. (2021)	DES-I	100	0.05 w/v %	NA	33.87	29.78
Beg et al. (2021)	DES-I	100	0.1 w/v %	NA	37.13	32.39
Beg et al. (2021)	DES-I	100	0.25 w/v %	NA	43.93	37.88
Beg et al. (2021)	DES-I	100	0.50 w/v %	NA	57.96	44.82
Beg et al. (2021)	DES-I	100	0.75 w/v %	NA	63.77	50.75
Beg et al. (2021)	DES-I	100	1 w/v %	NA	66.60	54.65
Beg et al. (2021)	DES-II	25	0.05 w/v %	NA	43.10	36.50
Beg et al. (2021)	DES-II	25	0.1 w/v %	NA	51.92	41.95
Beg et al. (2021)	DES-II	25	0.25 w/v %	NA	60.90	49.51
Beg et al. (2021)	DES-II	25	0.50 w/v %	NA	66.94	54.42
Beg et al. (2021)	DES-II	25	0.75 w/v %	NA	72.82	59.47
Beg et al. (2021)	DES-II	25	1 w/v %	NA	72.00	61.86
Beg et al. (2021)	DES-II	100	0.05 w/v %	NA	39.18	33.45
Beg et al. (2021)	DES-II	100	0.1 w/v %	NA	48.16	38.89
Beg et al. (2021)	DES-II	100	0.25 w/v %	NA	52.73	44.47
Beg et al. (2021)	DES-II	100	0.50 w/v %	NA	65.80	52.96
Beg et al. (2021)	DES-II	100	0.75 w/v %	NA	72.98	58.54
Beg et al. (2021)	DES-II	100	1 w/v %	NA	71.84	62.12

which the inhibition performance assessments were done and testified information presented by the former studies using numerous types of DESs. As previously mentioned, bentonite clay is relatively more swellable than any other clay particles. So, Na-bent was intentionally taken into account to find out the best performance given by the DESs as a swelling inhibitor. The inhibitory function of DESs was attributed to its intense electrostatic interaction and hydrogen bonding with Na-bent. DESs are adsorbed on the surface and interlayers of Na-bent, compressing the diffuse electric double layer and restricting Na-bent dispersion, attributable to choline cations, OH, COOH, NH_2, and other functional groups.[214,216,224]

4.1. Rheological Parameter Analysis of Several DESs.

In general, the rheological parameters are measured to know the deformation and flow behavior of any fluid. Drilling and fracturing fluids' rheological qualities are examined on a regular basis in the petroleum industry. In addition, these properties are also used to analyze the antiswelling ability of chemicals. Clay particles absorb the water and rapidly swell once they are dispersed in water.[225] In a dispersion system, the plate-like clay particles can be compounded together in three different ways, such as face-to-face (FF), edge-to-face (EF), and edge-to-edge (EE).[226] The flat surface of these plate-like particles has negative charges, whereas the edges have positive charges. The dominating EF pair may build the spatial structure when the Na-bent is disseminated in water and hydrated. The constant structure of Na-bent in the dispersion system raises viscosity and therefore the yield stress value, which is accountable for considerably increasing the fluid's flow resistance. So, it can be included that increasing swelling in clay particles resulted in a higher value of viscosity, which eventually resists the fluid flow. The system's viscosity will increase with a higher Na-bent content in the dispersion.[213] So, lower apparent viscosity (AV) and yield point (YP) values indicate a more effective inhibitor. Inhibitors are used to reduce the swelling rate of shale formation during drilling and other operations. After adding inhibitors to Na-bent, rheological parameters including AV and YP may be determined, and the inhibitors' inhibitory ability can be easily assessed. Several studies showed that when Na-bent content reaches about 20 wt % the sample becomes too viscous to measure the AV and YP. According to research on swelling inhibitors, introducing inhibitors to shale reduces the rate of swelling. As a result, the viscosity and yield point are minimized.

Ma et al. (2021) analyzed the rheological properties of Na-bent suspension with and without adding inhibitors.[216] The experiment showed that the suspension of Na-bent with increasing concentration quickly became too viscous to measure the AV value without any inhibitor. However, after adding inhibitors, the value of AV increased sharply, indicating the degree of inhibition. At a temperature of 90 °C, the AV value of 5 wt % of Na-bent was 3.50 mPa.s, but with increasing concentration up to 15 wt % the AV value reached 82.44 mPa.s. A sharp increase in the AV value indicates that the Na-bent content greatly affects the AV value. Table 7 shows that the AV values of 15 wt % of Na-bent are 1.91 mPa.s, 2.10 mPa.s, 4.96 mPa.s, 7.82 mPa.s, 4.96 mPa.s, and 6.30 mPa.s for 5 wt % of cit-DES, oxa-DES, urea-DES, gly-DES, polyether amino, and KCl, respectively. So, these inhibitors effectively reduced the AV value. Due to the adsorption of inhibitors on the surface of clay Na-bent particles, the negative charges neutralized and eventually hindered the swelling of clay.[1] This action resulted in lowering the AV value. We know that at higher temperature the rate of swelling increased, so this experiment was conducted at higher temperature to assess the thermal stability of studied inhibitors. From Table 7 at 150 °C temperature, the AV value of 20 wt % of Na-bent suspension without any inhibitors is 139.42 mPa.s. The AV values were reduced to 14.74 mPa.s, 9.21 mPa.s, 4.91 mPa.s, 4.61 mPa.s, 3.38 mPa.s, and 3.38 mPa.s after the addition of 5 wt % of KCl, polyether amino, urea-DES, gly-DES, oxa-DES, and cit-DES, respectively. All the chemicals exhibited good inhibitory ability. Among these six different types of inhibitors, cit-DES presented the finest performance in reducing the AV value of dispersed Na-bent. It also holds a thermal stability during the experiment. Though the four DESs showed good antiswelling potentiality, urea-DES perform worse than other DESs.

https://doi.org/10.1021/acsomega.2c03008
ACS Omega 2022, 7, 28723−28755

Jia et al. (2019a) studied the inhibition property of a different type of chemical named CU-DES and compared it with two other traditional inhibitors mostly used in oil and gas drilling activities.[224] CU-DES was comprised of choline chloride and urea. In this study CU-DES is also compared with the single-component choline chloride. To see the dispersion inhibition capability of these inhibitors, rheological properties were analyzed. At 25 °C, the inhibitor-free suspension of 4 w/v % of Na-bent has a YP value of 11.81 Pa and AV value of 15.78 mPa.s. These values reached 124.27 Pa and 142.35 mPa.s for 16 w/v % of Na-bent suspension. In contrast, after adding 5 w/v % of KCl, the YP and AV values reduced to 10.56 Pa and 11.83 mPa.s, respectively. A lower YP value indicate a good antiswelling activity. An amount of 2 w/v % of PDA reduced the YP value to 10.25 Pa, and ChCl exhibited the same YP as 2 w/v % of PDA for 16 w/v % of Na-bent but at a lower concentration of about 1 w/v %. So, ChCl is better than KCl and PDA at a lower concentration. In the case of 1 w/v % of CU-DES, the YP value sharply reduced to 9.94 Pa.s, which is lower than the other three inhibitors.

In can be depicted from the Table 7 that even with higher Na-bent content CU-DES with lower concentration maintains a low YP value. For instance, YP of 32 w/v % of Na-bent is 82.64 Pa with 5 w/v % of KCl, but this higher value of YP reduced to about 18.64 Pa after the addition of CU-DES at same temperature. The intercalation of CU-DES into the interlayer of Na-bent clay particles and the electrostatic forces between the charges of DES and the clay surface is considered to be responsible for the high inhibitory ability.

Jia et al. (2019b) investigated the antiswelling property of recently invented inhibitors called DESs.[214] In this study, three different types of DESs are used. Several measurements are done to analyze the swelling inhibition potential of these inhibitors. Inhibitor-free Na-bent content gave a YP value as high as 50.02 Pa at 10 w/v %. After adding the conventional KCl (5 w/v %) the YP reduced to 9.39 Pa. Here a sharp decrease of YP is seen. An amount of 2 w/v % of PDA also resulted in a lower value of YP of about 8.69 Pa. So, at the same temperature PDA at lower concentration gave a better performance than KCl. CIM-DES, CM-DES, and CP-DES greatly cut down the YP values at lower concentration than the traditional inhibitors. Table 7 depicts that the same amount of Na-bent holds the YP values of 8.92, 9.16, and 8.92 Pa for 1 w/v % of CIM-DES, CM-DES, and CP-DES, respectively. These three DESs also exhibit the ability to maintain a lower YP, even with the increasing content of Na-bent suspension. Figure 8 represents the YP values of these three DESs with a higher concentration of Na-bent. At lower concentration of 1 w/v %, CIM-DES, CM-DES, amd CP-DES greatly reduce the YP values. This is due to the antiswelling property of these inhibitors. These DESs shrink the electric double layer by accessing on the interlayer gap of clay particles, which eventually reduced the repulsion forces between the clay particles.[214] This process also made it more difficult for water molecules to penetrate into the interlayer area, lowering the swelling rate of clays. YP values of Na-bent with three DESs clearly indicate the swelling inhibition phenomenon. Among the three DESs, the CP-DES performed well in reducing the YP value. From Figure 8, we see that with 40 w/v % of Na-bent CP-DES holds the value of YP at 54.48 Pa, which is lower than that for CM-DES and CIM-DES. This activity may be credited to the existence of a benzene ring in CP-DES. Benzene is hydrophobic, so it is possible that after the intercalation of CP-DES into the clay surface the benzene ring itself played a role to prevent the water molecules from entering into the clay's interlayer space, which resulted in lower hydration and eventually a lower YP of clays.

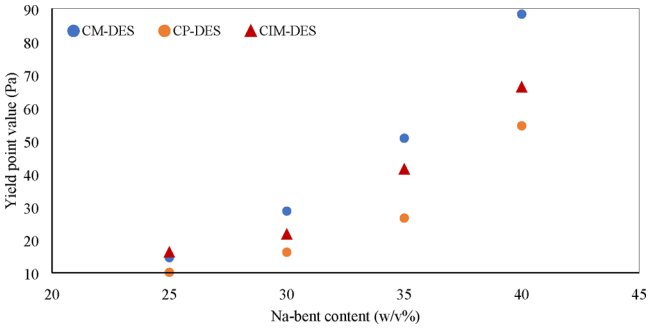

Figure 8. Yield point values of CIM-DES, CM-DES, and CP-DES at 70 °C.

Beg et al. (2021) assessed the rheological properties of two DESs named DES-I (tetrabutyl ammonium bromide-diethanolamine) and DES-II (tetrabutyl ammonium bromide-diethylene glycol).[215] In this study, these two DESs were added to a synthesized base mud. Table 7 demonstrates the yield point and apparent viscosity of these two DESs. At a lower temperature of about 25 °C, the YP and AV values of DES-I were amplified with increasing concentration, and this measurement at higher temperature also delivers a similar type of growing value of YP and AV. However, it is understood that the base mud with DESs maintained a lower YP and AV. A higher YP of a sample defines a higher swelling rate. In the case of DES-I and DES-II, they hold the same YP and AV throughout the whole measurement with different conditions. So, it can be inferred that the addition of DESs to the base mud increased the rheological characteristics. This helps to prevent swelling during the drilling operations.

4.2. Linear Swelling Test. The linear swelling test is conducted to assess the antiswelling efficiency of an inhibitor as a function of time. In this test, a Na-bent pellet is immersed in freshwater/deionized water without any inhibitor to measure the dispersion rate of the shale sample. Then, the sample is tested with different inhibitors. In both cases, the swelling height or swelling rate is measured. A high swelling rate/swelling height characterizes poor inhibition efficiency and vice versa. Because the frequency of swelling is affected by several parameters, including the quantity of the inhibitor, the presence of swelling clay minerals in the shale, cation exchange capacity, and shale purity, experimental conditions are important.[1] So, it is not practical to compare the performance of inhibitors tested in distinctive experimental conditions (pressure, temperature, PH, etc.). The efficacy of inhibitors was measured in comparison to water to overcome this constraint of diverse experimental settings. Generally, the authors reset swelling data using swelling height or swelling percentage. In this work, the inhibitor's efficiency is calculated by eq 1.

$$\mathrm{SIH} = \frac{\left(\frac{\mathrm{SH}}{\mathrm{SP}}\right)\text{ in water} - \left(\frac{\mathrm{SH}}{\mathrm{SP}}\right)\text{ in inhibitor}}{\left(\frac{\mathrm{SH}}{\mathrm{SP}}\right)\text{ in water}} \quad (1)$$

https://doi.org/10.1021/acsomega.2c03008
ACS Omega 2022, 7, 28723−28755

Here, SIE = swelling inhibition efficiency; $\left(\frac{SH}{SP}\right)$in water = swelling height/percentage in water; and $\left(\frac{SH}{SP}\right)$ in inhibitor = swelling height/percent inhibitor solution. This equation's effectiveness using swelling height is comparable to itself, but not to efficiencies derived using swelling percentages.[1] Table 4 shows the inhibition efficiency of several DESs with different concentrations and times.

Ma et al. (2021) conducted the linear swelling test for Na-bent shale samples with six different types of inhibitors with the same concentration of 5 wt %.[216] Among the six inhibitors, KCl and polyether amino are the conventional swelling inhibitors, but the other four are new types of chemicals having a good antiswelling ability. At the beginning of the linear swelling test, the sample was powdered and seized through the mesh. Then, the powdered samples were shaped into pellet form. The pellets were then immersed in inhibitor-free water solutions and inhibitor solutions. Na-bent immersed in inhibitor-free water solution swelled very rapidly after dispersion. This quick dispersion was proved through the increased swelling height of the immersed Na-bent pellet. The swelling rate was 51.8% after 16 h of testing in inhibitor-free water. All of the evaluated inhibitors exhibited a positive result in lowering the swelling height after being added. The traditional KCl reduced the swelling rate to 43.02%. Polyether amino showed a better result than KCl, reducing the rate of swelling to 38.68%. Table 4 shows that the swelling inhibition efficiency is 25.41% for KCl and 34.3% for polyether amino, respectively. In the interlayer space of the Na-bent sample, KCl exchanged K^+ ions for Na^+ ions, preventing water molecules from invading the interlayer gaps. So, the swelling started at the time of the ion exchange process and stopped after the intercalation of ions within the interlayer spaces. This described the change in the swelling trend of KCl as an inhibitor. This phenomenon is also responsible for the result of polyether amino as an inhibitor. Apart from the KCl and polyether amino, the new types of inhibitor mainly called DES also showed an effective result in reducing the Na-bent swelling. DESs, namely, urea-DES, gly-DES, oxa-DES, and cit-DES, reduced the swelling rate of the Na-bent sample up to 29.38%, 21.57%, 37.31%, and 39.66%, respectively. Among these four types of different DESs, urea-Des and gly-DES exhibited the best result in reducing the swelling rate, even more than the traditional inhibitors. Their swelling inhibition efficiency is more than 40%, which may indicate quality for being a good inhibitor.

Jia et al. (2019a) used shale powder pellets and Na-bent pellets individually to see the swelling rate in inhibitor-free water and inhibitor solutions.[224] It was found that after 24 h of the experiment the final swelling degree of Na-bent immersed in deionized water was as high as 155.07%, and for shale powder, the rate was about 68.24%. After adding four different inhibitors the swelling rate reduced dramatically for the Na-bent pellet. For every inhibitor, the swelling curve showed an identical change trend with the rate increasing at the beginning of the experiment and then decreasing moderately. The final rate of swelling reduced to 73.68% for 5 w/v % of KCl, 57.56% for 2 w/v % of PDA, 53.89% for 1 w/v % of choline chloride, and 47.29% for 1 w/v % of CU-DES. So, these four types of inhibitors showed their antiswelling capacity in the order of 5 w/v % KCl < 2 w/v % PDA < 1 w/v % ChCl < 1 w/v % CU-DESs. Experiments done on the shale pellets also resulted in a similar trend of antiswelling performance for every inhibitor. The rate of swelling was 31.35% for 5 w/v % of KCl, 24.79% for 2 w/v % of PDA, 21.11% for 1 w/v % of choline chloride, and 18.65% for 1 w/v % of CU-DES. Among these four inhibitors, CU-DES showed better performance in lowering the swelling rate for both Na-bent and shale powder. The intercalations between the negative charges of clay surfaces and CU-DES cations form an electrostatic force that repels the water molecules and thus hinders the swelling of clay. The antiswelling action of CU-DES is also due to hydrogen bonds formed between the functional groups of CU-DES and the charges of clay particles.

Jia et al. (2019b) studied three different kinds of inhibitors with varying concentrations and compared them with conventional inhibitors.[214] In DI water, a Na-bent particle inflated rapidly. After immersing for 24 h, the swelling height of the pellet reached 11.17 mm. From Table 8, it can be concluded that all types of inhibitors in this study played an effective role to reduce the swelling rate of shale samples. The swelling rate followed a traditional change trend of increasing at the very beginning of the experiment and then reducing slowly. The shale sample immersed in three different types of inhibitor solutions showed a positive change in the swelling rate, but it can be interpreted from Figure 9 that the swelling inhibition performance of CP-DES was the most attractive of any other inhibitors. Figure 9 depicts that at 0.5 w/v % CM-DES and CIM-DES showed better efficiency in reducing the swelling height. At 1 w/v %, these two inhibitors almost coincide, but with increasing concentration, their rate of inhibition efficiency does not improve that much. In the case of CP-DES at 1 w/v %, the swelling inhibition efficiency was almost double that at 0.5 w/v %, and at 2 w/v % its efficiency was more than the other two DESs. However, it can be said that at 1 w/v % CP-DES performs better.

Beg et al. (2021) used a base mud and three types of inhibitors. In this study, a linear swelling test was conducted for 2 h.[215] The sample expanded quickly in inhibitor-free water, according to the observations. After the final hour, the swelling rate was about 28.93%. After adding 5 w/v % of KCl as an inhibitor, the swelling rate reduced to about 24.41%. An amount of 0.2 w/v % of a BMIM mixture lowered this rate to 22.07%. Two DESs were used as an inhibitor for this study, named DES-I and DES-II, with concentrations of about 0.2 w/v %. Both of them showed incredible antiswelling activity. Their reduced rate of swelling for the sample mud was about 13.18% and 8.58%, respectively. However, one drawback of this study is that all of the samples were tested for linear swelling for just 2 h. The results are for only some limited time and concentration. So, we could not conclude which of the inhibitors was better because the results can fluctuate with time. Also, concentration is an important factor affecting the inhibition efficiency for any type of inhibitor.

4.3. Shale Cutting Hot-Rolling Recovery Test. The (hot-rolling) shale cutting dispersion test is a method of determining how drilling fluids interact with the shale formation. The hot-rolling dispersion test is designed to resemble the dispersion of shale cuttings in drilling settings.[224] This process assesses the quality of shale. As a result, a higher recovery rate indicates that the shale sample is tough and resistant to hydration and swelling. Some factors such as the moisture content of the shale, shale composition, viscosity of the test fluid, the rotation speed of the rollers, and test temperature greatly influence the test results. In addition, the

https://doi.org/10.1021/acsomega.2c03008
ACS Omega 2022, 7, 28723−28755

Table 8. Swelling Inhibition Efficiency of Several DESs

author	shale sample	inhibitor	inhibitor conc.	time	efficiency (%)
Ma et al. (2021)	Na-bent	KCl	5 wt %	16 h	16.98
Ma et al. (2021)	Na-bent	polyether amino	5 wt %	16 h	25.41
Ma et al. (2021)	Na-bent	urea-DES	5 wt %	16 h	43.33
Ma et al. (2021)	Na-bent	glycol-DES	5 wt %	16 h	58.84
Ma et al. (2021)	Na-bent	oxa-DES	5 wt %	16 h	28
Ma et al. (2021)	Na-bent	ct-DES	5 wt %	16 h	23.34
Jia et al. (2019a)	Na-bent	KCl	5 w/v %	24 h	52.49
Jia et al. (2019a)	Na-bent	polyether diamine	2 w/v %	24 h	62.88
Jia et al. (2019a)	Na-bent	choline chloride	1 w/v %	24 h	65.25
Jia et al. (2019a)	Na-bent	CU-DES	1 w/v %	24 h	69.54
Jia et al. (2019a)	shale powder	KCl	5 w/v %	24 h	54.06
Jia et al. (2019a)	shale powder	polyether diamine	2 w/v %	24 h	63.67
Jia et al. (2019a)	shale powder	choline chloride	1 w/v %	24 h	69.07
Jia et al. (2019a)	shale powder	CU-DES	1 w/v %	24 h	72.67
Jia et al. (2019b)	Na-bent	KCl	5 w/v %	24 h	0.09
Jia et al. (2019b)	Na-bent	polyether diamine	2 w/v %	24 h	53.72
Jia et al. (2019b)	Na-bent	CM-DES	0.5 w/v %	24 h	50.13
Jia et al. (2019b)	Na-bent	CM-DES	1 w/v %	24 h	58.12
Jia et al. (2019b)	Na-bent	CM-DES	2 w/v %	24 h	60.45
Jia et al. (2019b)	Na-bent	CP-DES	0.5 w/v %	24 h	36.14
Jia et al. (2019b)	Na-bent	CP-DES	1 w/v %	24 h	67.98
Jia et al. (2019b)	Na-bent	CP-DES	2 w/v %	24 h	71.66
Jia et al. (2019b)	Na-bent	CIM-DES	0.5 w/v %	24 h	53.99
Jia et al. (2019b)	Na-bent	CIM-DES	1 w/v %	24 h	58.48
Jia et al. (2019b)	Na-bent	CIM-DES	2 w/v %	24 h	62.87
Beg et al. (2021)	Na-bent	KCl	5 w/v %	2 h	15.62
Beg et al. (2021)	Na-bent	BMIM(cl)	0.2 w/v %	2 h	23.71
Beg et al. (2021)	Na-bent	DES-I	0.2 w/v %	2 h	54.44
Beg et al. (2021)	Na-bent	DES-II	0.2 w/v %	2 h	70.34

rheological behavior of the testing fluid also affects the test.[227] In the oil and gas industry, this test is very popular to investigate the potential of different types of inhibitors. The higher the recovery rate of shale cuttings after hot rolling, the better the inhibitory quality of the inhibitor supplied to the shale sample in this test technique.[224]

Jia et al. (2019a) compared the hot-rolling dispersion test between four types of inhibitor.[224] Amounts of 350 mL of DI water or inhibitor solutions were applied to a 50 g dry shale sample. The sample was then rolled for 16 h at 80 °C, 120 °C, and 160 °C in a roller oven. The remaining shale cuttings were filtered on a 40 mesh sieve and washed with DI water after cooling to room temperature. After 4 h of drying at 105 °C, the recovered shale cuttings were weighed. The following eq 2 was used to calculate the recovery rate of shale cuttings after hot rolling:

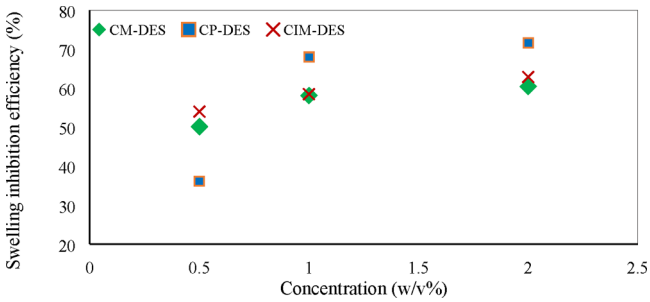

Figure 9. Swelling inhibition efficiency of three different types of DESs at different concentrations.

$$r\ (\%)\frac{m}{m_0} = 100\% \tag{2}$$

where r is the recovery rate, and m and m_o are the weights of shale cuttings after and before the hot-rolling. The sample of DI water obtains the lowest recovery of shale cuttings after hot-rolling at all temperatures. Data from Table 9 represent that at 80 °C DI water recovery is just 14.34%, and higher temperatures produce more severe dissolution. The recovery of shale cuttings in DI water is nearly nil when the temperature reaches 160 °C, showing that the shale cuttings are extremely easy to hydrate and disseminate. The use of inhibitors, on the other hand, significantly reduces the frequency of shale disintegration. After adding PDA of 2 w/v %, KCl of 5 w/v %, and ChCl of 1 w/v %, the recovery rate was raised to 33.90%, 40.57%, and 43.81%, respectively. The recovery of shale cuttings in solution with 1 w/v % of CU-DES is considerably more than those with 2 w/v % of PDA, 5 w/v % of KCl, and 1 w/v % of ChCl, which is about 82.67% at the same temperature. Though all the inhibitors have suppressed the dispersion rate, at higher temperatures their performances decline dramatically. As at higher temperatures the swelling rate increases, KCL, PDA, and ChCl could not maintain the inhibitive potentiality. However, CU-DES accelerates recovery to 75% at 160 °C, compared to 17.57%, 30.97%, and 35.32% for KCl, PDA, and ChCl systems, correspondingly. Here the CU-DES proved to have an excellent temperature tolerance. So, it can be concluded that CU-DES is a thermally stable inhibitor.

To study the thermally stable DESs, Jia et al. (2019b) compared the recovery percentage of the hot-rolling dispersion test between the conventional shale swelling inhibitors KCl and PDA and recently invented DESs named CIM-DES, CM-DES, and CP-DES.[214] Here the recovery rate of DI water was the lowest at all temperatures and tended to zero at temperatures of 160 °C. The recovery rate was improved by varying degrees after adding several types of inhibitors. Table 9 represents the recovery rate of this inhibitor at different temperatures. After hot-rolling for 16 h at 80 °C, the recovery rate for 5 w/v % of KCl, 2 w/v % of PDA, 1 w/v % of CM-DES, 1 w/v % of CP-DES, and 1 w/v % of CIM-DES was

https://doi.org/10.1021/acsomega.2c03008
ACS Omega 2022, 7, 28723−28755

Table 9. Shale Cutting Hot-Rolling Dispersion Tests

author	inhibitor/ experimental solution	inhibitor conc.	rolling temp and time	increment in recovery percentage
Jia et al. (2019a)	DI water	NA	80 °C; 16 h	14.34%
Jia et al. (2019a)	DI water	NA	120 °C; 16 h	10.09%
Jia et al. (2019a)	DI water	NA	160 °C; 16 h	2.67%
Jia et al. (2019a)	KCl	5 w/v %	80 °C; 16 h	33.90%
Jia et al. (2019a)	KCl	5 w/v %	120 °C; 16 h	24.76%
Jia et al. (2019a)	KCl	5 w/v %	160 °C; 16 h	17.57%
Jia et al. (2019a)	PDA	2 w/v %	80 °C; 16 h	40.57%
Jia et al. (2019a)	PDA	2 w/v %	120 °C; 16 h	37.71%
Jia et al. (2019a)	PDA	2 w/v %	160 °C; 16 h	30.97%
Jia et al. (2019a)	ChCl	1 w/v %	80 °C; 16 h	43.81%
Jia et al. (2019a)	ChCl	1 w/v %	120 °C; 16 h	40.76%
Jia et al. (2019a)	ChCl	1 w/v %	160 °C; 16 h	35.32%
Jia et al. (2019a)	CU-DES	1 w/v %	80 °C; 16 h	82.67%
Jia et al. (2019a)	CU-DES	1 w/v %	120 °C; 16 h	79.24%
Jia et al. (2019a)	CU-DES	1 w/v %	160 °C; 16 h	75%
Jia et al. (2019b)	DI water	NA	80 °C; 16 h	14.30%
Jia et al. (2019b)	DI water	NA	120 °C; 16 h	10.31%
Jia et al. (2019b)	DI water	NA	160 °C; 16 h	2.81%
Jia et al. (2019b)	KCl	5 w/v %	80 °C; 16 h	33.75%
Jia et al. (2019b)	KCl	5 w/v %	120 °C; 16 h	24.38%
Jia et al. (2019b)	KCl	5 w/v %	160 °C; 16 h	17.34%
Jia et al. (2019b)	PDA	2 w/v %	80 °C; 16 h	40.78%
Jia et al. (2019b)	PDA	2 w/v %	120 °C; 16 h	37.50%
Jia et al. (2019b)	PDA	2 w/v %	160 °C; 16 h	30.93%
Jia et al. (2019b)	CM-DES	1 w/v %	80 °C; 16 h	86.95%
Jia et al. (2019b)	CM-DES	1 w/v %	120 °C; 16 h	80.63%
Jia et al. (2019b)	CM-DES	1 w/v %	160 °C; 16 h	74.06%
Jia et al. (2019b)	CP-DES	1 w/v %	80 °C; 16 h	90.94%
Jia et al. (2019b)	CP-DES	1 w/v %	120 °C; 16 h	89.77%
Jia et al. (2019b)	CP-DES	1 w/v %	160 °C; 16 h	89.06%
Jia et al. (2019b)	CIM-DES	1 w/v %	80 °C; 16 h	89.27%
Jia et al. (2019b)	CIM-DES	1 w/v %	120 °C; 16 h	86.48%
Jia et al. (2019b)	CIM-DES	1 w/v %	160 °C; 16 h	84.38%
Beg et al. (2021)	base mud	NA	NA	84.30%
Beg et al. (2021)	base mud + KCl	5 w/v %	16 h	88.6%
Beg et al. (2021)	base mud + DES-I	0.1 w/v %	16 h	94.80%
Beg et al. (2021)	base mud + DES-I	0.5 w/v %	16 h	98.80%
Beg et al. (2021)	base mud + DES-II	0.1 w/v %	16 h	95.90%
Beg et al. (2021)	base mud + DES-II	0.5 w/v %	16 h	99.60%

33.75%, 4078%, 86.95%, 90.94%, and 89.27% respectively. So, at a lower concentration, all three DESs have shown better inhibition ability. These three inhibitors also showed excellent temperature tolerance. For instance, whenever the temperature was increased from 80 to 160 °C, the reduction rate of recovery in CM-DES, CP-DES, CIM-DES, KCl, and PDA was 14.88%, 2.41%, 5.34%, 48.24%, and 23.5%. This experiment also provided an investigation including a tertiary recovery. Any shale inhibitor's endurance was demonstrated by tertiary recovery. At tertiary recovery, the rate was almost zero for the case of DI water and KCl solution. Despite having a low recovery rate, PDA has shown stability in its third recovery. The reduction rate was only 29.01% from the first recovery. Except for CIM-DES, all DESs have exceptional durability as shown in Figure 10. The recovery rate reduced by 18.39% for CM-DES and 16.54% for CP-DES, but the shale reduction rate was almost 64% lower than the first recovery for CIM-DES. So, it can be said that at higher temperatures CP-DES performs best as an inhibitor. This may be attributed to the presence of a long alkyl chain, which makes it thermally stable.

Beg et al. (2021) used a modified base mud synthesized by mixing 4.0 w/v % of bentonite powder in tap water using a Hamilton Beach mixer for 15 min.[215] The dispersion was kept for 16 h to allow complete hydration of the clay unit layers for exfoliation of bentonite. The dispersion was further mixed with 0.25 w/v % of XG and PAC-RG using a Hamilton Beach mixer for 5 min for each polymeric additive. In this study, the hot-rolling method was applied with two types of DESs indicating DES-I (tetrabutylammonium bromide and diethanolamine) and DES-II (tetrabutylammonium bromide and diethylene glycol). The base mud recovery rate was good with DI water solution, as the mud was already rich in xanthan gum and regular grade polyanionic cellulose. After adding two types of DESs after 16 h of hot-rolling, the recovery rate increased up to 94.80% for 0.1 w/v % of DES-I and 95.90% for DES-II at the same concentration, as shown in Table 9. Increasing the concentration to 0.5 w/v %, the recovery rate also increased. So, it can be said that these two inhibitors work best at higher concentrations, but this experiment is done at only one temperature condition. The effects of temperature on the durability of these two DESs are still unknown. Generally, inhibitors become unstable with increasing temperature. So, this study does not provide enough information about the best use of these two swelling inhibitors.

4.4. Zeta Potential Measurement of Different DESs. Clay minerals have a flat surface that attracts cations into the

https://doi.org/10.1021/acsomega.2c03008
ACS Omega 2022, 7, 28723−28755

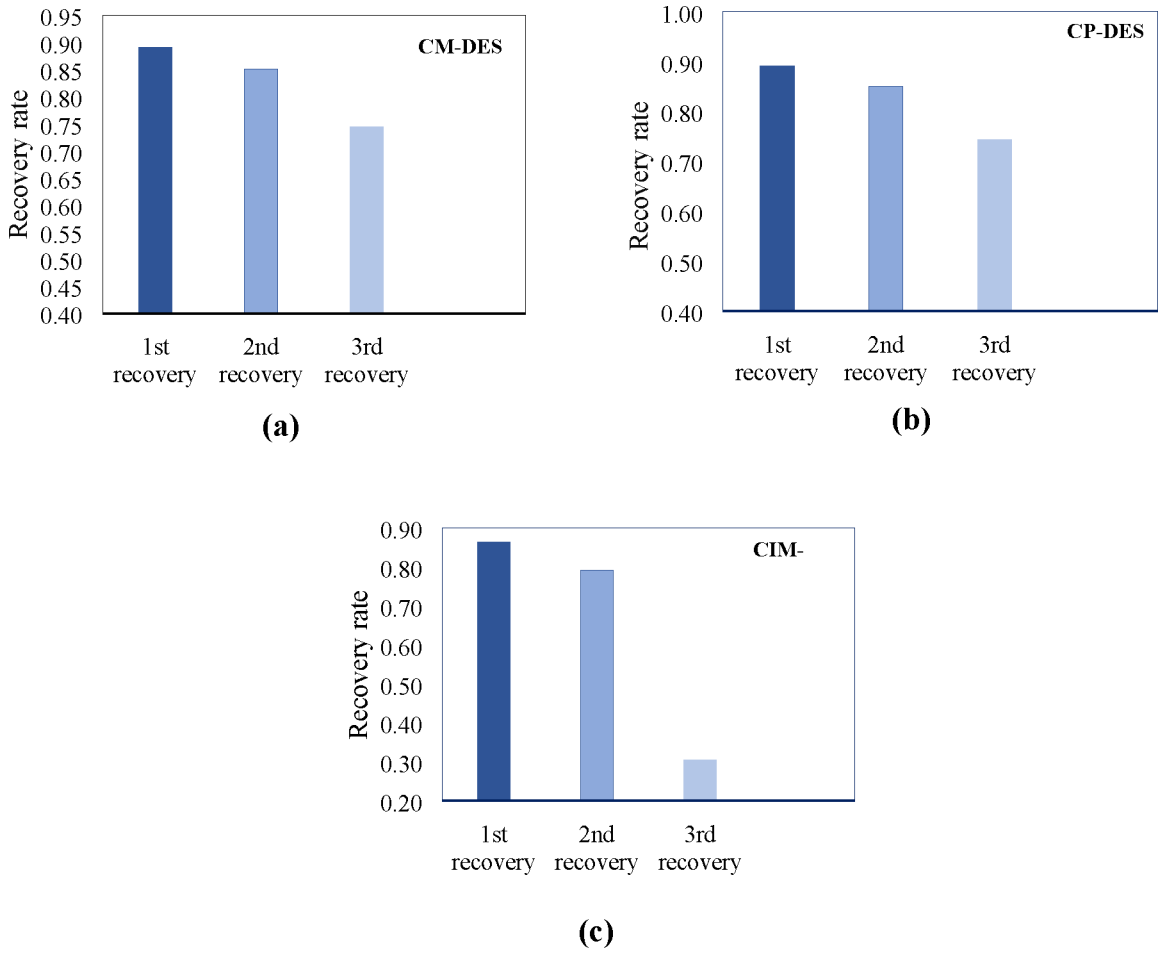

Figure 10. Tertiary recovery rate of shale cuttings in three different DES solutions at 120 °C: (a) 1 w/v % of CM-DES; (b) 1 w/v % of CP-DES; and (c) 1 w/v % of CIM-DES.

interlayer space due to isomorphous substitution in the crystal lattice. Diffused Na^+ ions produce an electrical double layer on the negatively charged surface of clay particles when Na-bent is scattered in water. Any inhibitor that penetrates the spaces between the layers of clay particles reduces the negative charges on the clay surface. The double electric layers are repressed as a result of the lowered surface negative charges. As a result, the amount of inlayer space is reduced.[1]

The zeta potential is a fundamental measure of colloidal dispersion stability. An electrically stabilized colloidal system has a higher absolute zeta potential (more than 30 mV). On the contrary, an inferior absolute value of zeta potential specifies the inhibition mechanism of dispersions in any colloidal system.[23,228] So, a lower zeta potential value either negative or positive is decent for the steadiness of clay minerals. According to a study, inhibitor which can decrease the value zeta potential of clay−water suspension 20% can be addressed as a good inhibitor.[23]

Table 10 represents the zeta potential value of a Na-bent sample after adding several DES solutions at different concentrations. Here, Na-bent dispersed in water with a 0 w/v % concentration of CU-DES has a value of zeta potential as high as −42.20 mV. By increasing the concentration of DES, the value of the zeta potential decreased effectively. The Na-bent sample with 0.05 w/v % of CU-DES has a value of zeta potential of about −32.15. At this concentration, the inhibitor shows efficiency of about 23.69%. By raising the concentration of CU-DES to 0.1 w/v %, the zeta potential value was reduced to −29.01 mV. Eventually the zeta potential value of that clay sample was reduced to −26.91 mV, −24.38 mV, −19.40 mV, and −16.78 mV with a concentration of about 0.3 w/v %, 0.5 w/v %, 1 w/v %, and 2 w/v %, respectively.[224] So, it can be said that with higher concentration the efficiency of CU-DES is reduced, showing that CU-DES performs better at a lower concentration.[224] In the case of CM-DES, CIM-DES, and CP-DES the zeta potential value is −21.20 mV, −18.90 mV, and −15.20 mV, respectively. CP-DES shows better performances among the three DESs at a similar concentration.[214] This is due to the presence of the benzene ring in CP-DES. Benzene is hydrophobic in nature. Longer alkyl chain length may also be responsible for reducing the zeta potential value at a higher rate. At a constant concentration of about 5 wt %, urea-DES, gly-DES, oxa-DES, and cit-DES also reduced the absolute value of zeta potential at a higher rate. They reduced the absolute value of zeta potential up to 96%, which represents a stable colloidal system. As an inhibitor, gly-DES lowered the value by 96.4%. So, it can be said that the lower zeta potential value is credited to the presence of three hydroxyl groups (−OH) in glycerol. The hydroxyl group enters into the interlayer space and forms a hydrogen bond and eventually reduced the electric double layer.

4.5. Surface Tension Measurements of Different DESs. The capillary force is important in any hydrophilic shale formation because it drives water into the shale

https://doi.org/10.1021/acsomega.2c03008
ACS Omega 2022, 7, 28723−28755

Table 10. Zeta Potential Values of Several DESs at Different Concentrations

author	shale sample	inhibitor	inhibitor conc.	zeta potential value (mV)
Jia et al. (2019a)	Na-bent	CU-DES	0 w/v %	−42.20
Jia et al. (2019a)	Na-bent	CU-DES	0.05 w/v %	−32.15
Jia et al. (2019a)	Na-bent	CU-DES	0.1 w/v %	−29.01
Jia et al. (2019a)	Na-bent	CU-DES	0.3 w/v %	−26.91
Jia et al. (2019a)	Na-bent	CU-DES	0.5 w/v %	−24.38
Jia et al. (2019a)	Na-bent	CU-DES	1 w/v %	−19.40
Jia et al. (2019a)	Na-bent	CU-DES	2 w/v %	−16.78
Jia et al. (2019b)	Na-bent	CM-DES	1 w/v %	−21.20
Jia et al. (2019b)	Na-bent	CIM-DES	1 w/v %	−18.90
Jia et al. (2019b)	Na-bent	CP-DES	1 w/v %	−15.2
Ma et al. (2021)	Na-bent	urea-DES	5 wt %	−8.7
Ma et al. (2021)	Na-bent	gly-DES	5 wt %	−1.73
Ma et al. (2021)	Na-bent	oxa-DES	5 wt %	−4.12
Ma et al. (2021)	Na-bent	cit-DES	5 wt %	−1.96

formation. As a result, the shale hydrates and loses some of its stability. Capillary force is proportional to surface tension, as given in eq 3.[216]

$$P_c = 2\sigma \cos\theta / r \quad (3)$$

where P_c is the capillary force (Pa); σ is the surface tension of the testing fluid (mN/m); θ is the contact angle (deg); and r is the pore-throat radius of the shale sample (mm). The capillary suction pressure drives the invasion of water into the shale, and a low surface tension would be beneficial for shale stability.[229]

Some studies have shown that adding DESs into the drilling fluid lowers the surface tension of that fluid, thus inhibiting the shale hydration. Table 11 represents the surface tension of seven different types of DESs with different concentrations.[214,216] At different concentrations the values for surface tension change at a different rate. For higher concentrations, the surface tension declined at a higher rate. At a concentration of 10 g/L, CM-DES and CIM-DES lower the surface tension to 68.1 and 64.2 mN/m, respectively. Among the three DESs with the same concentrations, CP-DES shows the best surface activity, thus reducing the surface tension to a higher degree. For 10 g/L of CP-DES, the surface tension is 40.91 mN/m.[214] In another study, four types of DESs represent their potential for reducing the surface tension to a higher degree. At a lower concentration of about 1 wt %, all four DESs, named urea-DES, gly-DES, oxa-DES, and cit-DES, lower the surface tension of water to 64.64 mN/m, 54.51 mN/m, 61.38 mN/m, and 64.90 mN/m, respectively.[216] The resultant surface tension values depict that all those DESs hold an antiswelling property and can be utilized as potential inhibitors for shale stabilization.

Figure 11 represents the percentage efficiency of different DESs at different concentrations. Figure 11(a) shows that the

Table 11. Surface Tension of Different DESs at Varying Concentrations

author	inhibitor	inhibitor conc.	surface tension (mN/m)
Jia et al. (2019b)	CM-DES	0 g/L	72.50
Jia et al. (2019b)	CM-DES	0.5 g/L	72.19
Jia et al. (2019b)	CM-DES	1 g/L	71.43
Jia et al. (2019b)	CM-DES	2 g/L	70.90
Jia et al. (2019b)	CM-DES	3 g/L	70.52
Jia et al. (2019b)	CM-DES	4 g/L	70.14
Jia et al. (2019b)	CM-DES	6 g/L	69.46
Jia et al. (2019b)	CM-DES	8 g/L	68.85
Jia et al. (2019b)	CM-DES	10 g/L	68.09
Jia et al. (2019b)	CIM-DES	0 g/L	72.50
Jia et al. (2019b)	CIM-DES	0.5 g/L	71.13
Jia et al. (2019b)	CIM-DES	1 g/L	69.91
Jia et al. (2019b)	CIM-DES	2 g/L	68.17
Jia et al. (2019b)	CIM-DES	3 g/L	67.26
Jia et al. (2019b)	CIM-DES	4 g/L	66.50
Jia et al. (2019b)	CIM-DES	6 g/L	65.21
Jia et al. (2019b)	CIM-DES	8 g/L	64.60
Jia et al. (2019b)	CIM-DES	10 g/L	64.30
Jia et al. (2019b)	CP-DES	0 g/L	72.50
Jia et al. (2019b)	CP-DES	0.5 g/L	61.56
Jia et al. (2019b)	CP-DES	1 g/L	56.25
Jia et al. (2019b)	CP-DES	2 g/L	51.16
Jia et al. (2019b)	CP-DES	3 g/L	47.29
Jia et al. (2019b)	CP-DES	4 g/L	43.95
Jia et al. (2019b)	CP-DES	6 g/L	42.51
Jia et al. (2019b)	CP-DES	8 g/L	41.82
Jia et al. (2019b)	CIM-DES	10 g/L	40.91
Ma et al. (2021)	urea-DES	1 wt %	64.64
Ma et al. (2021)	gly-DES	1 wt %	54.51
Ma et al. (2021)	oxa-DES	1 wt %	61.38
Ma et al. (2021)	cit-DES	1 wt %	64.90

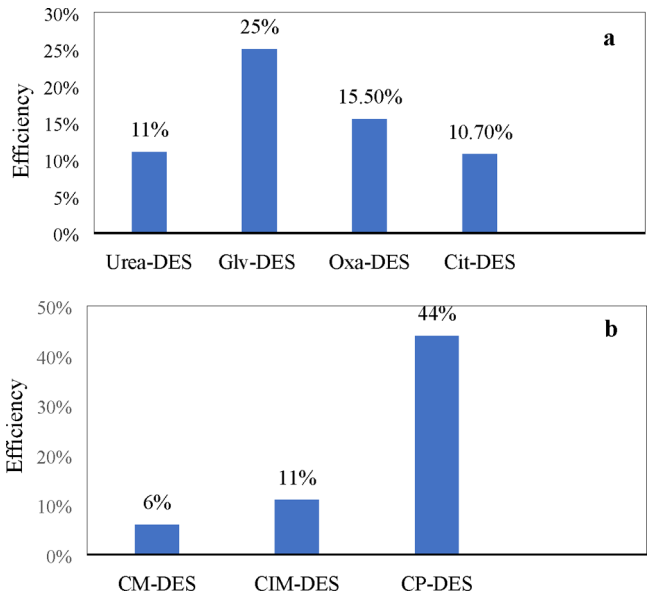

Figure 11. (a) Surface tension reduction efficiency of four types of DESs at 1 wt % of concentration. (b) Three types of DESs at 10 g/L of concentration.

gly-DES gave a better surface tension reduction of water among the other three DESs at the same concentration. As

https://doi.org/10.1021/acsomega.2c03008
ACS Omega 2022, 7, 28723−28755

mentioned earlier, the driving force of water infiltration into shale strata could be decreased by low surface tension. Adding gly-DES may reduce the shale hydration rate effectively. This is thought to be due to the stronger hydrogen bond formation among the glycerol and clay surfaces. The water molecules are repelled from entering the interlayer space by this strong connection. The presence of hydroxyl ions in glycerol may be responsible for the better performance of gly-DES as an antiswelling inhibitor. Figure 11(b) presents the efficiency of three types of DESs at a 10 g/L concentration. Among them, CP-DES shows the highest reduction of surface tension. The existence of the benzene ring in CP-DES, as well as the longer alkyl chain compared to the other two DESs, may explain the higher degree of surface tension reduction.

4.6. Particle Size Distribution Measurement of Different DESs. Through hydration, clay materials can disperse into tiny particles or maybe into a single unit of platelets. After sufficient hydration of the Na-bent sample, the hydration degree can be assumed by analyzing the particle size distributions. As the diffusion electric double layer was compressed, the Na-bent particles agglomerated which led to the increase of particle size.[216] The agglomeration of Na-bent particles by DESs is beneficial to weaken the hydration and dispersion of Na-bent. The additional inhibitors may be able to effectively restrain this process, so the larger particle size of the Na-bent reflects the better inhibitory effect of inhibitors.

Table 12 presents the particle size distribution of Na-bent dispersion with different concentrations of CU-DES, 5 wt % of urea-DES, gly-DES, oxa-DES, and cit-DES and 1 w/v % of CM-DES, CIM-DES, and CP-DES. According to the size of d_{50}, the inhibitor's inhibitory ability can be ranked: gly-DES > cit-DES > oxa-DES > urea-DES.[216] CU-DES at different concentrations gave different size distributions of Na-bent particles. The median size (d_{50}) of Na-bent particles in DI water is 3.57 μm. The particle size grows with the increasing CU-DES concentration. When the concentration of CU-DES reaches 2 w/v %, the d_{50} is 39.27 μm which is about 11 times larger than that in DI water.[224] The effect of CP-DES and CIM-DES was superior to that of CM-DES. For instance, d_{50} increased to as high as 42.12 μm depending on the species of inhibitors.[214]

Table 12. Particle Size Distributions of Different Types of DESs at Different Concentrations

			particle size distribution (μm)		
author	inhibitor	inhibitor concentration	d_{10}	d_{50}	d_{90}
Ma et al. (2021)	urea-DES	5 wt %	6.09	30.00	69.24
Ma et al. (2021)	gly-DES	5 wt %	9.42	49.76	111.70
Ma et al. (2021)	oxa-DES	5 wt %	6.88	39.31	281.70
Ma et al. (2021)	cit-DES	5 wt %	7.31	43.57	97.58
Jia et al. (2019b)	CM-DES	1 w/v %	4.37	27.72	172.61
Jia et al. (2019b)	CP-DES	1 w/v %	8.04	42.12	225.28
Jia et al. (2019b)	CIM-DES	1 w/v %	6.65	40.55	179.31
Jia et al. (2019a)	CU-DES	0.05 w/v %	1.18	9.61	74.31
Jia et al. (2019a)	CU-DES	0.1 w/v %	2.02	14.60	93.37
Jia et al. (2019a)	CU-DES	0.3 w/v %	2.74	18.35	100.75
Jia et al. (2019a)	CU-DES	0.5 w/v %	4.80	23.26	97.84
Jia et al. (2019a)	CU-DES	1 w/v %	15.04	32.75	65.94
Jia et al. (2019a)	CU-DES	2 w/v %	18.19	39.27	105.58

4.7. XRD Measurement of Different DESs. Whenever clay minerals come into contact with water, a water molecule enters the interlayer space between the clay particles. This phenomenon is considered as swelling of clay which eventually enlarges the interlayer spacing of clay minerals. The crystalline swelling can be attributed to interlayer spacing between 9 and 20 Å, and osmotic swelling can be linked to spacing between 20 and 130 Å.[1] X-ray diffraction (XRD) analysis measures the XRD forms and interlayer gap (d_{001}) of original Na-bent and Na-bent altered by diverse DESs. It provides a detailed understanding of the adsorption behavior/intercalation of different DESs into the interlayer space of clay particles. After XRD analysis of a dry sample and a wet sample, we discovered the interlayer spacing of both phases. The result of dry samples indicates the adsorption ability of the particular inhibitor, and the wet sample provides the data to understand the inhibition efficiency of that inhibitor, which indicates the ability of an inhibitor to lower the swelling rate of any shale formation. In this study, the inhibition efficiency of several different DESs with distinct concentrations is discussed.

Ma et al. (2021) used four different types of DESs as an inhibitor to test the shale swelling inhibition efficiency with the same concentration of 5 wt %.[216] An amount of 3 g of Na-bent was mixed with 100 mL of DI water and 5 wt % of inhibitor solutions for 12 h. This mixture was centrifuged for 15 min at 4000 rpm and rinsed three times with deionized water. After collecting the precipitate, a D8 advance diffractometer was utilized to conduct X-ray diffraction (XRD) investigations (Bruker, Germany). Before the XRD measurement, the other part of the precipitate was dried at 105 °C and ground to powder. From Table 13 we can see that four distinct types of inhibitors named urea-DES, gly-DES, oxa-DES, and cit-DES were used to carry out this experiment. The interlayer space of original Na-bent in the case of a dry sample is 12.11 Å, which increased to 18.95 Å in the case of the wet sample, which indicates that the Na-bent sample is fully hydrated and swelled. The interlayer spacing for the wet sample increased by about 56.48%. So, it can be said that when the water molecules enter the space between clay particles swelling occurred. After adding 5 wt % of urea-DES, gly-DES, oxa-DES, and cit-DES in the dry shale sample, the interlayer spacing reached 13.98 Å, 14.71 Å, 13.88 Å, and 14.08 Å, respectively. Among the four DESs, the interlayer spacing increased more for the dry sample with gly-DES. The increment is almost 2.6% more than the original sample. So, it can be interpreted that the gly-DES has more adsorption ability into the shale formation. The presence of hydroxyl (−OH) groups may be responsible for the good intercalation behavior of gly-DES. A larger number of hydroxyl ions are attracted to the surface cations and enter the space between the layers. In the case of a wet sample, it is seen that there is a varying result from the former one. XRD measurement of the interlayer spacing of the Na-bent wet sample is about 18.95 Å. After adding four types of DESs, this value was reduced drastically. This is due to the antiswelling

https://doi.org/10.1021/acsomega.2c03008
ACS Omega 2022, 7, 28723−28755

Table 13. XRD Analysis of Several DESs Used for Shale Stabilization

author	shale sample/ inhibitor	inhibitor conc.	interlayer space (Å) dry sample	interlayer space (Å) wet sample
Ma et al. (2021)	Na-bent	NA	12.11	18.95
Ma et al. (2021)	urea-DES	5 wt %	13.98	14.42
Ma et al. (2021)	gly-DES	5 wt %	14.71	14.26
Ma et al. (2021)	oxa-DES	5 wt %	13.88	14.42
Ma et al. (2021)	cit-DES	5 wt %	14.08	14.32
Jia et al. (2019b)	Na-bent	NA	12.87	19.08
Jia et al. (2019b)	CM-DES	0.05 w/v %	13.28	15.07
Jia et al. (2019b)	CM-DES	0.1 w/v %	14.43	15.25
Jia et al. (2019b)	CM-DES	0.2 w/v %	14.57	15.16
Jia et al. (2019b)	CM-DES	0.5 w/v %	14.65	14.92
Jia et al. (2019b)	CM-DES	1 w/v %	14.70	14.82
Jia et al. (2019b)	CM-DES	2 w/v %	14.74	14.89
Jia et al. (2019b)	Na-bent	NA	12.87	19.08
Jia et al. (2019b)	CP-DES	0.05 w/v %	13.70	14.71
Jia et al. (2019b)	CP-DES	0.1 w/v %	14.13	14.65
Jia et al. (2019b)	CP-DES	0.2 w/v %	14.15	14.41
Jia et al. (2019b)	CP-DES	0.5 w/v %	14.19	14.34
Jia et al. (2019b)	CP-DES	1 w/v %	14.21	14.27
Jia et al. (2019b)	CP-DES	2 w/v %	14.21	14.28
Jia et al. (2019b)	Na-bent	NA	12.87	19.08
Jia et al. (2019b)	CIM-DES	0.05 w/v %	13.95	15.09
Jia et al. (2019b)	CIM-DES	0.1 w/v %	14.14	14.53
Jia et al. (2019b)	CIM-DES	0.2 w/v %	14.22	14.50
Jia et al. (2019b)	CIM-DES	0.5 w/v %	14.24	14.48
Jia et al. (2019b)	CIM-DES	1 w/v %	14.25	14.47
Jia et al. (2019b)	CIM-DES	2 w/v %	14.25	14.46
Jia et al. (2019a)	Na-bent	NA	12.87	19.08
Jia et al. (2019a)	CU-DES	0.05 w/v %	14.36	18.46
Jia et al. (2019a)	CU-DES	0.1 w/v %	14.51	17.01
Jia et al. (2019a)	CU-DES	0.2 w/v %	14.52	16.08
Jia et al. (2019a)	CU-DES	0.5 w/v %	14.53	14.85
Jia et al. (2019a)	CU-DES	1 w/v %	14.52	14.69
Jia et al. (2019a)	CU-DES	2 w/v %	14.53	14.67

potential of these inhibitors. After analyzing the result, it is seen that gly-DES inhibited the growth of the spacing, which is only about 3.06% greater than the dry sample. The ability to reduce the interlayer spacing of the four DESs can be defined in the order of gly-DES > cit-DES > urea-DES > oxa-DES. This is due to the development of a hydrogen bond among the charges present in the clay surface and the hydroxyl groups of gly-DES. This hydrogen bond tightly bounded the layer together and repulsed the water molecules.

Jia et al.'s (2019b) study included three different types of DESs named CM-DES, CP-DES, and CIM-DES with varying concentration.[214] The interlayer spacing of a dry Na-bent sample is about 12.87 Å. After adding 0.05 w/v % of CM-DES, CP-DES, and CIM-DES, this spacing increased to 13.28 Å, 13.70 Å, and 13.95 Å, respectively. Among these three DESs, CIM-DES increases the interlayer spacing of the dry sample more, but this is not consistent with increasing concentration. At higher concentration, the adsorption ability is CM-DES > CIM-DES > CP-DES. For instance, at 2 w/v % the interlayer spacing of CM-DES, CP-DES, and CIM-DES is 14.70 Å, 14.21 Å, and 14.25 Å. So, it can be interpreted that at higher concentration the intercalation of CM-DES with clay particles increased. In the case of a wet sample, the antiswelling ability of these three DESs is clearly visualized. For example, at 0.05 w/v %, CM-DES reduced the interlayer spacing to 21.02% from the original wet sample's interlayer spacing. For CP-DES and CIM-DES, the reduction is about 22.90% and 20.91%, respectively. This is due to their antiswelling potential, which hinders the entrance of water molecules into the interlayer spacing of clay particles, thus helping to reduce hydration. At 1 w/v % they perform better at depressing the interlayer spacing of a wet NA-bent sample. Among three of the DESs, CP-DES performed as a more potential swelling inhibitor. The presence of a benzene ring, which is a strong hydrophobic material, and the long alkyl chain length of 3-phenylpropionic acid in CP-DES were responsible for good antiswelling potentiality.

Jia et al. (2019a) examined the XRD of CU-DES and found that the adsorption ability of CU-DES fluctuated between 14.36 Å and 14.53 Å for six different concentrations.[224] At higher concentration, the antiswelling ability of CU-DES increases. For example, adding 0.05 w/v % of CU-DES reduced the interlayer gaps of wet samples from 19.08 to 18.46 Å. Eventually, by adding 2 w/v % of CU-DES the interlayer spacing reduced to 14.67 Å, which is about 23.11% lower than the interlayer spacing of the original wet sample without any inhibitor. Among these several type of DESs, CU-DES which is comprised of choline chloride and urea shows the better inhibition performance. However, all the above experiments are done at different conditions. Temperature and pressure also have some effect on their inhibition and adsorption ability, so the potential of every individual inhibitor could not be fully compared.

4.8. FTIR Measurement of Different DESs. FTIR spectra reveal the composition of solids, liquids, and gases. FTIR is

https://doi.org/10.1021/acsomega.2c03008
ACS Omega 2022, 7, 28723−28755

used to investigate the structural information on materials. It detects the presence of specific chemical bonds, reflecting the chemical composition of materials. FTIR spectra have been utilized in various investigations to better understand the structure and potential interaction between DESs and shale formation.

Ma et al. (2021) used a Bruker FTIR spectrometer (Horiba, Germany) to record the FTIR of four DESs.[216] The experiment was done at room temperature. After the development of DESs, the distinguishing peaks of $-NH_2$ were red-shifted from 3430 to 3318 cm^{-1}, and the band was expanded, which indicates the establishment of hydrogen bonding. The hydrogen bond also affected the stretching vibration of C═O (wavenumber moves from 1675 to 1662 cm^{-1}), and the bending vibration of $-CH_2$ in ChCl was also red-shifted from 1481 to 1475 cm^{-1}. All of this shows that urea-DES can establish complicated hydrogen bond connections. The characteristic peaks of −OH and C═O in cit-DES show varying degrees of red-shift for other DESs, such as the hydroxyl group (OH) in oxa-DES, which indicates that phenomena of hydrogen bonding also exist.

Jia et al. (2019a) used FTIR to evaluate the presence of chemical bonds in the original Na-bent sample and improved the sample with CU-DES.[224] If the data from Table 14 are compared, then it is seen that the FTIR spectrum of the CU-DES-modified Na-bent has several new characteristic bands from the original Na-bent, which indicates the development of a hydrogen bond between CU-DES and the Na-bent sample. The stretching bands of O−H and Si−O, for example, changed to varying degrees.

Beg et al. (2021) used a PerkinElmer spectrometer to record the FTIR spectra of the DESs used for the study.[215] For diethylene glycol and diethanolamine the FTIR spectra were measured. The peak around 3000−3600 cm^{-1} resembled the existence of the stretching bond of −OH in all DESs. For diethanolamine-based DESs, a bending of roughly 1470 cm^{-1} was captured. The −NH bond is represented by this peak. The phosphonium (−PH) and ammonium (−NH) stretching expected in tetrabutyl ammonium bromide (TBAB) and methyltriphenyl phosphonium bromide (MTPPhBr) is likely overlapped by the −CH stretching, which is around 3000−2750 cm^{-1}. Except for a change in the −OH bond, the DES spectrum revealed no new bond formation. The −OH stretching of diethylene glycol shifted from 3338 cm^{-1} to lower wavenumbers of 3352 cm^{-1} and 3352 cm^{-1} for DES-II. This supported the creation of hydrogen bonds between the DESs and the shale formation. The diethanol amine-based DESs yielded similar results.

Rasool et al. (2021) used FTIR spectra, and the result reflects the same functional group of −OH in both glycerol and the formulated DES. However, for glycerol, the peak was around 3292 cm^{-1}, which was reduced to the wavelength of 3277 cm^{-1} for the DES.[36] So, this change in bond length corresponds to a change in electronegativity difference which reflects the new bond formation. The FIIR analysis also confirmed that glycerol (HBD) participated in hydrogen bond formation. At 1434 cm^{-1}, the presence of a carbonate ion in potassium carbonate is detected. In DES, the same ion occurred for the peak at 1454 cm^{-1}. This increased wavenumber means that the carbonate ion participated in hydrogen bonding with the −OH of glycerol. So, this result confirmed the formation of a hydrogen bond between potassium carbonate (HBA) and glycerol (HBD).

Table 14. FTIR Analysis of Different DESs Used for Shale Stabilization

author	studied inhibitor	peak (cm^{-1})	bond
Ma et al. (2021)	urea-DES	3430	$-NH_2$ (amino)
Ma et al. (2021)	NA	1675	C═O (carbonyl)
Ma et al. (2021)	NA	1481	$-CH_2$
Jia et al. (2019a)	NA	3623	stretching band of O−H
Jia et al. (2019a)	adsorbed water	1633	bending band of adsorbed water
Jia et al. (2019a)	adsorbed water	3420	stretching band of adsorbed water
Jia et al. (2019a)	Na-bent	1034	stretching band of Si−O
Jia et al. (2019a)	Na-bent	912	bending vibration of Al−Al−OH
Jia et al. (2019a)	Na-bent	879	bending vibration of Al−Fe−OH
Jia et al. (2019a)	Na-bent	797	bending vibration of quartz
Jia et al. (2019a)	altered Na-bent with CU-DES	between 3100 and 2800	C−H stretching vibration of alkyl group
Jia et al. (2019a)	altered Na-bent with CU-DES	1681	stretching vibration of C═O
Jia et al. (2019a)	altered Na-bent with CU-DES	1470	C−C
Jia et al. (2019a)	altered Na-bent with CU-DES	1400	C−N
Rasool et al. (2021)	glycerol	3292	−OH
Rasool et al. (2021)	DES	3277	−OH
Rasool et al. (2021)	K_2CO_3	1434	CO_3^{-2}
Rasool et al. (2021)	DES	1454	CO_3^{-2}
Beg et al. (2021)	DEG, DEA	3600 to 3000	−OH
Beg et al. (2021)	TBAB, MTPPhBr	1470	−NH

5. CONCLUDING REMARKS AND RECOMMENDATIONS

The efficacy of a newly developed shale inhibitor designated as a DES is explored in this research. When this chemical's inhibitory ability was compared to that of frequently used inhibitors, it provided a better result. For decades, the petroleum industry has shifted its attention toward the exploration of unconventional reservoirs in order to accommodate the burgeoning demand for natural gas, and it has already been proven that shale gas is one of the most anticipated natural gas resources to meet this rising demand. However, the limited permeability of shale is one of the biggest challenges in producing gas from shale deposits. Hydraulic fracturing is used to reduce this problem by increasing the permeability of shale reservoirs, resulting in increased gas output. WBDF as fracturing fluids are becoming more widespread as environmental legislation becomes more stringent, and the necessity to extract oil and gas deposits in more environmentally sustainable locations arises. Since shale is a highly swellable clay mineral, swelling happens at an unbearable rate while using a water−base fracturing fluid. In this regard, more effective swelling inhibitors to utilize with water-based drilling fluids that are also benign to the

https://doi.org/10.1021/acsomega.2c03008
ACS Omega 2022, 7, 28723−28755

environment (toxicity level is low and more biodegradable) are essential, especially where highly reactive clay formations are encountered. Various additives were mixed into water-based fluids to lower the rate of swelling during shale reservoir fracturing. KCl, ammonium chloride, and divalent brine with a high concentration were formerly employed widely. Unfortunately, KCl is detrimental to both the environment and all living creatures. Environmental problems have arisen as a result of the usage of KCl as a shale inhibitor. As a result, scientists are attempting to look for a replacement for KCl as a swelling inhibitor, as has been mentioned earlier.

In the research of the petroleum field, ILs have attracted a considerable amount of traction as shale inhibitors. Nevertheless, ILs were also disregarded as green solvents. Because of their toxicological properties, ILs are losing favor. ILs are poisonous solvents that are not biodegradable, which makes them unsuitable for the environment.

As a greener and less expensive inhibitor than other inhibitors, DESs are attracting attention. The materials and methods for preparing DESs are also simple. Furthermore, DESs are more efficient at lowering the rate of shale swelling. We assessed the inhibitory activation of different types of DESs. The study's final remarks on DESs as an inhibiting agent are emphasized below.

- With modest concentrations, DESs can effectively prevent shale swelling compared to other conventional inhibitors.
- Because of the significant electrostatic affinity between clay and the choline cations in DESs, the repulsive force is dramatically attenuated among them, impeding clay dispersion. Additionally, the hydrogen connections formed between the functional groups in DESs and the hydroxyl or oxygen atoms on the clay surface strongly connect the adjacent clay platelets and prevent water infiltration.
- DESs can help to weaken water infiltration by lessening the surface tension of water-based fracturing fluids.
- In shale cutting recovery experiments, DESs showed improved temperature resistance (more than 150 °C). They also exceeded the conventional inhibitor KCl in terms of stability.
- gly-DES is an effective shale inhibitor since it has a high inhibitory ability and has no effect on the basic rheological and filtration features of water-based drilling fluids.
- The benzene ring in CP-DES gave its aqueous phase a relatively high activity, resulting in a dense adsorption pattern of CP-DES on the clay surface and interlayer. As a result, they, notably CP-DES and CIM-DES, offer a lot of potential as strong shale inhibitors in water-based drilling fluids.
- Even when related cost is taken into account, DESs are found to be the best alternative as they surpass other inhibitors in terms of quantity and effectiveness.
- Inhibition potentiality of less expensive KCl also remains far behind DESs.

The following proposals are made to optimize and design commercially attractive and efficient DESs for mitigating shale swelling:

- The majority of the studies used deionized water to analyze the performance of DESs. However, testing DESs with drilling or fracturing fluids is suggested to see if they are compatible with other additives.
- Some research only used low levels of DESs in their testing medium. It is recommended that a variety of concentrations be used to avoid any errors in the results and to accurately evaluate the efficacy of DESs as a shale stabilizer.
- More research is required to completely understand the inhibitory mechanism of DESs on shale samples, incorporating analytical and experimental investigations as well as concentration, variation, stability, high temperature, adaptability, and finally simultaneous studies.
- The principle through which DESs hinder shale formation instability was not well-defined. Experiments and molecular dynamics research could have been used to precisely comprehend the inhibitory mechanisms of DESs.
- Since DESs are considered environmentally friendly solvents, as a result more study should be performed that considers biodegradability and toxicity. The ecological compatibility of DESs should be reviewed in association with performance monitoring.
- Moreover, when compared to other inhibitors, DESs work better at low concentrations. So, if it is to be used as a shale stabilizer, a thorough cost assessment is needed.

Due to their inhibitory performance, cost-effectiveness, and environmental friendliness, this analysis finds that DESs are better swelling inhibitors. This review also contains guidelines and recommendations for choosing and constructing DESs that will successfully reduce swelling.

AUTHOR INFORMATION

Corresponding Authors

Khairul Habib − *Department of Mechanical Engineering, Universiti Teknologi PETRONAS, 32610 Bandar Seri Iskandar, Perak Darul Ridzuan, Malaysia*; Phone: +60102442375; Email: khairul.habib@utp.edu.my

Md Tauhidur Rahman − *Department of Petroleum Engineering, Universiti Teknologi PETRONAS, 32610 Bandar Seri Iskandar, Perak Darul Ridzuan, Malaysia*; orcid.org/0000-0001-6865-4340; Phone: +8801704254234; Email: tauhidur.pme@gmail.com

Authors

Kakon Sultana − *Department of Petroleum and Mining Engineering, Chittagong University of Engineering and Technology, Chittagong, Bangladesh*

Likhan Das − *Department of Mechanical Engineering, Universiti Teknologi PETRONAS, 32610 Bandar Seri Iskandar, Perak Darul Ridzuan, Malaysia*

Complete contact information is available at: https://pubs.acs.org/10.1021/acsomega.2c03008

Notes

The authors declare no competing financial interest.

ACKNOWLEDGMENTS

The authors would like to express their gratitude to the International Collaborative Research Fund (ICRF) (Project

https://doi.org/10.1021/acsomega.2c03008
ACS Omega 2022, 7, 28723−28755

cost center: 015ME0-253) for the financial and technical support to accomplish this research.

NOMENCLATURE

API	American Petroleum Institute
AV	apparent viscosity
BMIM	1-butyl-3-methylimidazolium
BMIM(cl)	1-butyl-3-methylimidazolium chloride
CEC	cation exchange capacity
ChCl	choline chloride
CIM-DES	choline chloride-itaconic acid and 3-mercaptopropionic acid deep eutectic solvent
CM-DES	choline chloride-propanedioic acid deep eutectic solvent
CP-DES	choline chloride-3-phenyl propionic acid deep eutectic solvent
CU-DES	choline chloride-urea deep eutectic solvent
DEA	diethanolamine
DEG	diethylene glycol
DES	deep eutectic solvent
DES-I	tetrabutylammonium bromide-diethanolamine
DES-II	tetrabutylammonium bromide-diethylene glycol
DI water	deionized water
EF	edge-to-face
FF	face-to-face
GPa	gigapascal
HBA	hydrogen bond acceptor
HBD	hydrogen bond donor
HDES	hydrophobic deep eutectic solvents
ILs	ionic liquids
KCl	potassium chloride
mg/m^3	milligram per cubic meter
$mN\ m^{-1}$	millinewton per meter
MPa	megapascal
mPa.s	millipascal second
m/s	meter per second
MTPPhBr	methyl triphenyl phosphonium bromide
mV	millivolt
Na-bent	sodium-bentonite
OBDF	oil-based drilling fluid
Ohm-m	ohmmeter
Pa	pascal
PDA	polyether diamine
TBAB	tetrabutylammonium bromide
TOC	total organic carbon
UCS	uniaxial compressive strength
WBDF	water-based drilling fluid
wt %	percentage of weight
w/v %	percentage of weight per volume
XRD	X-ray diffraction
YP	yield point
μm	micrometer

REFERENCES

(1) Rahman, M. T.; Negash, B. M.; Moniruzzaman, M.; Quainoo, A. K.; Bavoh, C. B.; Padmanabhan, E. An overview on the potential application of ionic liquids in shale stabilization processes. *Journal of Natural Gas Science and Engineering* **2020**, *81*, 103480.

(2) Law, B. E.; Curtis, J. Introduction to unconventional petroleum systems. *AAPG bulletin* **2002**, *86* (11), 1851−1852.

(3) McGlade, C.; Speirs, J.; Sorrell, S. Unconventional gas−a review of regional and global resource estimates. *Energy* **2013**, *55*, 571−584.

(4) Holditch, S. A.; Madani, H. Global unconventional gas-it is there, but is it profitable? *Journal of petroleum Technology* **2010**, *62* (12), 42−48.

(5) Jin, X.; Wang, X.; Yan, W.; Meng, S.; Liu, X.; Jiao, H.; Su, L.; Zhu, R.; Liu, H.; Li, J. Exploration and casting of large scale microscopic pathways for shale using electrodeposition. *Applied Energy* **2019**, *247*, 32−39.

(6) Hurnaus, T.; Plank, J. Behavior of titania nanoparticles in cross-linking hydroxypropyl guar used in hydraulic fracturing fluids for oil recovery. *Energy Fuels* **2015**, *29* (6), 3601−3608.

(7) Danso, D. K.; Negash, B. M.; Ahmed, T. Y.; Yekeen, N.; Ganat, T. A. O. Recent advances in multifunctional proppant technology and increased well output with micro and nano proppants. *J. Pet. Sci. Eng.* **2021**, *196*, 108026.

(8) Vickers, N. J. Animal communication: when i'm calling you, will you answer too? *Current biology* **2017**, *27* (14), R713−R715.

(9) Li, Q.; Xing, H.; Liu, J.; Liu, X. A review on hydraulic fracturing of unconventional reservoir. *Petroleum* **2015**, *1* (1), 8−15.

(10) Lyu, Q.; Ranjith, P.; Long, X.; Kang, Y.; Huang, M. A review of shale swelling by water adsorption. *Journal of Natural Gas Science and Engineering* **2015**, *27*, 1421−1431.

(11) Li, A.; Ding, W.; He, J.; Dai, P.; Yin, S.; Xie, F. Investigation of pore structure and fractal characteristics of organic-rich shale reservoirs: A case study of Lower Cambrian Qiongzhusi formation in Malong block of eastern Yunnan Province, South China. *Marine and Petroleum Geology* **2016**, *70*, 46−57.

(12) Kumari, N.; Mohan, C. Basics of clay minerals and their characteristic properties. *Clay Clay Miner* **2021**, *24*, 1−29.

(13) Liu, D.; Yan, Y.; Bai, G.; Yuan, Y.; Zhu, T.; Zhang, F.; Shao, M.; Tian, X. Mechanisms for stabilizing and supporting shale fractures with nanoparticles in Pickering emulsion. *J. Pet. Sci. Eng.* **2018**, *164*, 103−109.

(14) Zhou, F.; Su, H.; Liang, X.; Meng, L.; Yuan, L.; Li, X.; Liang, T. Integrated hydraulic fracturing techniques to enhance oil recovery from tight rocks. *Petroleum Exploration and Development* **2019**, *46* (5), 1065−1072.

(15) Danso, D. K.; Negash, B. M.; Yekeen, N.; Khan, J. A.; Rahman, M. T.; Ibrahim, A. U. Potential valorization of granitic waste material as microproppant for induced unpropped microfractures in shale. *Journal of Natural Gas Science and Engineering* **2021**, *96*, 104281.

(16) Biswas, K.; Rahman, M.; Almulihi, A. H.; Alassery, F.; Al Askary, M.; Hasan, A.; Hai, T. B.; Kabir, S. S.; Khan, A. I.; Ahmed, R. Uncertainty handling in wellbore trajectory design: a modified cellular spotted hyena optimizer-based approach. *Journal of Petroleum Exploration and Production Technology* **2022**, 1−19.

(17) Rahman, M. T.; Negash, B. M.; Idris, A.; Miah, M. I.; Biswas, K. Experimental and COSMO-RS simulation studies on the effects of polyatomic anions on clay swelling. *ACS omega* **2021**, *6* (40), 26519−26532.

(18) Chatterjee, A.; Iwasaki, T.; Hayashi, H.; Ebina, T.; Torii, K. Electronic and structural properties of montmorillonite—a quantum chemical study. *J. Mol. Catal. A: Chem.* **1998**, *136* (2), 195−202.

(19) Liu, T.; Chen, Y.-Q. A molecular dynamics study of the swelling patterns of Na/Cs-montmorillonites and the hydration of interlayer cations. *Chinese Physics B* **2013**, *22* (2), 027103.

(20) Teich-McGoldrick, S. L.; Greathouse, J. A.; Jove-Colon, C. F.; Cygan, R. T. Swelling properties of montmorillonite and beidellite clay minerals from molecular simulation: comparison of temperature, interlayer cation, and charge location effects. *J. Phys. Chem. C* **2015**, *119* (36), 20880−20891.

(21) Steiger, R. P.; Leung, P. K. Quantitative determination of the mechanical properties of shales. *SPE drilling engineering* **1992**, *7* (03), 181−185.

(22) Guancheng, J.; Yourong, Q.; Yuxiu, A.; Xianbin, H.; Yanjun, R. Polyethyleneimine as shale inhibitor in drilling fluid. *Appl. Clay Sci.* **2016**, *127*, 70−77.

(23) Zhong, H.; Qiu, Z.; Zhang, D.; Tang, Z.; Huang, W.; Wang, W. Inhibiting shale hydration and dispersion with amine-terminated

https://doi.org/10.1021/acsomega.2c03008
ACS Omega 2022, 7, 28723−28755

polyamidoamine dendrimers. *Journal of Natural Gas Science and Engineering* **2016**, *28*, 52−60.
(24) Jain, R.; Mahto, V. Formulation of a water based drilling fluid system with synthesized graft copolymer for troublesome shale formations. *Journal of Natural Gas Science and Engineering* **2017**, *38*, 171−181.
(25) Zhao, X.; Qiu, Z.; Sun, B.; Liu, S.; Xing, X.; Wang, M. Formation damage mechanisms associated with drilling and completion fluids for deepwater reservoirs. *J. Pet. Sci. Eng.* **2019**, *173*, 112−121.
(26) Zhao, X.; Qiu, Z.; Zhao, C.; Xu, J.; Zhang, Y. Inhibitory effect of water-based drilling fluid on methane hydrate dissociation. *Chem. Eng. Sci.* **2019**, *199*, 113−122.
(27) Xu, J.-g.; Qiu, Z.-s.; Zhao, X.; Zhong, H.-y.; Li, G.-r.; Huang, W.-a. Synthesis and characterization of shale stabilizer based on polyethylene glycol grafted nano-silica composite in water-based drilling fluids. *J. Pet. Sci. Eng.* **2018**, *163*, 371−377.
(28) Biswas, K.; Vasant, P. M.; Vintaned, J. A. G.; Watada, J. A review of metaheuristic algorithms for optimizing 3D well-path designs. *Archives of Computational Methods in Engineering* **2021**, *28* (3), 1775−1793.
(29) Santos, H.; Diek, A.; Da Fontoura, S.; Roegiers, J. Shale reactivity test: a novel approach to evaluate shale-fluid interaction. *International Journal of Rock Mechanics and Mining Sciences* **1997**, *34* (3−4), 268. e1−268. e11.
(30) Patel, A.; Stamatakis, S.; Young, S.; Friedheim, J. In Advances in inhibitive water-based drilling fluids—can they replace oil-based muds? *International Symposium on Oilfield Chemistry*; OnePetro: 2007.
(31) Poudel, J.; Ohm, T.-I.; Oh, S. C. A study on torrefaction of food waste. *Fuel* **2015**, *140*, 275−281.
(32) Tiemeyer, C.; Plank, J. Synthesis, characterization, and working mechanism of a synthetic high temperature (200° C) fluid loss polymer for oil well cementing containing allyloxy-2-hydroxy propane sulfonic (AHPS) acid monomer. *J. Appl. Polym. Sci.* **2013**, *128* (1), 851−860.
(33) Gholizadeh-Doonechaly, N.; Tahmasbi, K.; Davani, E. In Development of high-performance water-based mud formulation based on amine derivatives. *SPE international symposium on oilfield chemistry*; OnePetro: 2009.
(34) Rahman, M. T.; Negash, B. M.; Danso, D. K.; Idris, A.; Elryes, A. A.; Umar, I. A. Effects of imidazolium-and ammonium-based ionic liquids on clay swelling: experimental and simulation approach. *Journal of Petroleum Exploration and Production Technology* **2021**, 1−13.
(35) Ahmed Khan, R.; Murtaza, M.; Abdulraheem, A.; Kamal, M. S.; Mahmoud, M. Imidazolium-based ionic liquids as clay swelling inhibitors: mechanism, performance evaluation, and effect of different anions. *ACS omega* **2020**, *5* (41), 26682−26696.
(36) Rasool, M. H.; Zamir, A.; Elraies, K. A.; Ahmad, M.; Ayoub, M.; Abbas, M. A. Potassium carbonate based deep eutectic solvent (DES) as a potential drilling fluid additive in deep water drilling applications. *Petroleum Science and Technology* **2021**, *39* (15−16), 612−631.
(37) Smith, E. L.; Abbott, A. P.; Ryder, K. S. Deep eutectic solvents (DESs) and their applications. *Chem. Rev.* **2014**, *114* (21), 11060−11082.
(38) Zhang, Q.; Vigier, K. D. O.; Royer, S.; Jérôme, F. Deep eutectic solvents: syntheses, properties and applications. *Chem. Soc. Rev.* **2012**, *41* (21), 7108−7146.
(39) Shahbaz, K.; Mjalli, F.; Hashim, M.; AlNashef, I. Prediction of the surface tension of deep eutectic solvents. *Fluid phase equilibria* **2012**, *319*, 48−54.
(40) Zhao, H.; Baker, G. A.; Holmes, S. New eutectic ionic liquids for lipase activation and enzymatic preparation of biodiesel. *Organic & biomolecular chemistry* **2011**, *9* (6), 1908−1916.
(41) Carriazo, D.; Serrano, M. C.; Gutiérrez, M. C.; Ferrer, M. L.; del Monte, F. Deep-eutectic solvents playing multiple roles in the synthesis of polymers and related materials. *Chem. Soc. Rev.* **2012**, *41* (14), 4996−5014.
(42) Kulkarni, P. S.; Branco, L. C.; Crespo, J. G.; Nunes, M. C.; Raymundo, A.; Afonso, C. A. Comparison of physicochemical properties of new ionic liquids based on imidazolium, quaternary ammonium, and guanidinium cations. *Chem. Eur. J.* **2007**, *13* (30), 8478−8488.
(43) Gore, S.; Baskaran, S.; Koenig, B. Efficient synthesis of 3, 4-dihydropyrimidin-2-ones in low melting tartaric acid−urea mixtures. *Green Chem.* **2011**, *13* (4), 1009−1013.
(44) Abo-Hamad, A.; Hayyan, M.; AlSaadi, M. A.; Hashim, M. A. Potential applications of deep eutectic solvents in nanotechnology. *Chem. Eng. J.* **2015**, *273*, 551−567.
(45) Aftab, A.; Ismail, A.; Ibupoto, Z. Enhancing the rheological properties and shale inhibition behavior of water-based mud using nanosilica, multi-walled carbon nanotube, and graphene nanoplatelet. *Egyptian journal of petroleum* **2017**, *26* (2), 291−299.
(46) Rahman, T.; Negash, B. M.; Moniruzzaman, M.; Padmanabhan, E.; Ato, Q. K. In Performance Evaluation of 1-Butyl-3-Methylimidazolium Chloride as Shale Swelling Inhibitor, *IOP Conference Series: Earth and Environmental Science*, IOP Publishing: 2022; p 012019.
(47) Murtaza, M.; Kamal, M. S.; Mahmoud, M. Application of a novel and sustainable silicate solution as an alternative to sodium silicate for clay swelling inhibition. *ACS omega* **2020**, *5* (28), 17405−17415.
(48) Murtaza, M.; Ahmed Khan, R.; Kamal, M. S.; Hussain, S. S.; Mahmoud, M. Poly (Oxyethylene)-amidoamine based gemini cationic surfactants with hydrophilic spacers as clay stabilizers. *Energy Fuels* **2020**, *34* (9), 10619−10630.
(49) Murtaza, M.; Kamal, M. S.; Hussain, S. S.; Mahmoud, M.; Syed, N. A. Quaternary ammonium gemini surfactants having different spacer length as clay swelling inhibitors: Mechanism and performance evaluation. *J. Mol. Liq.* **2020**, *308*, 113054.
(50) Ahmed, H. M.; Kamal, M. S.; Al-Harthi, M. Polymeric and low molecular weight shale inhibitors: A review. *Fuel* **2019**, *251*, 187−217.
(51) AlMubarak, T.; AlDajani, O.; AlMubarak, M. In A collective clay stabilizers review. *International Petroleum Technology Conference*; OnePetro: 2015.
(52) Barati, R.; Liang, J. T. A review of fracturing fluid systems used for hydraulic fracturing of oil and gas wells. *J. Appl. Polym. Sci.* **2014**, DOI: 10.1002/app.40735.
(53) Downs, J. D. In Drilling and completing difficult HP/HT wells with the aid of cesium formate brines-a performance review. *SPE/IADC Drilling Conference and Exhibition*, SPE: 2006; pp SPE-99068-MS.
(54) Gholami, R.; Elochukwu, H.; Fakhari, N.; Sarmadivaleh, M. A review on borehole instability in active shale formations: Interactions, mechanisms and inhibitors. *Earth-Science Reviews* **2018**, *177*, 2−13.
(55) Mair, R.; Bickle, M.; Goodman, D.; Koppelman, B.; Roberts, J.; Selley, R.; Shipton, Z.; Thomas, H.; Walker, A.; Woods, E. *Shale gas extraction in the UK: a review of hydraulic fracturing*; Royal Society and Royal Academy of Engineering: 2012.
(56) Thomas, L.; Tang, H.; Kalyon, D. M.; Aktas, S.; Arthur, J. D.; Blotevogel, J.; Carey, J. W.; Filshill, A.; Fu, P.; Hsuan, G.; et al. Toward better hydraulic fracturing fluids and their application in energy production: A review of sustainable technologies and reduction of potential environmental impacts. *J. Pet. Sci. Eng.* **2019**, *173*, 793−803.
(57) Rana, A.; Arfaj, M. K.; Saleh, T. A. Advanced developments in shale inhibitors for oil production with low environmental footprints−A review. *Fuel* **2019**, *247*, 237−249.
(58) Quainoo, A. K.; Negash, B. M.; Bavoh, C. B.; Ganat, T. O.; Tackie-Otoo, B. N. A perspective on the potential application of bio-inhibitors for shale stabilization during drilling and hydraulic fracturing processes. *Journal of Natural Gas Science and Engineering* **2020**, *79*, 103380.
(59) Abbas, M. A.; Zamir, A.; Elraies, K. A.; Mahmood, S. M.; Rasool, M. H. A critical parametric review of polymers as shale inhibitors in water-based drilling fluids. *J. Pet. Sci. Eng.* **2021**, *204*, 108745.

https://doi.org/10.1021/acsomega.2c03008
ACS Omega 2022, 7, 28723−28755

(60) Muhammed, N. S.; Olayiwola, T.; Elkatatny, S.; Haq, B.; Patil, S. Insights into the application of surfactants and nanomaterials as shale inhibitors for water-based drilling fluid: A review. *Journal of Natural Gas Science and Engineering* **2021**, *92*, 103987.
(61) Sivabalan, V.; Sahith, J. K.; Lal, B. In Deep Eutectic Solvents as the New Norm for Oil and Gas Industry: A Mini Review. *Third International Conference on Separation Technology 2020 (ICoST 2020)*; Atlantis Press: 2020; pp 119−124.
(62) Singh, M. B.; Kumar, V. S.; Chaudhary, M.; Singh, P. A mini review on synthesis, properties and applications of deep eutectic solvents. *Journal of the Indian Chemical Society* **2021**, *98* (11), 100210.
(63) Florindo, C.; Oliveira, F. S.; Rebelo, L. P. N.; Fernandes, A. M.; Marrucho, I. M. Insights into the synthesis and properties of deep eutectic solvents based on cholinium chloride and carboxylic acids. *ACS Sustainable Chem. Eng.* **2014**, *2* (10), 2416−2425.
(64) Boggs, S. *Principles of Sedimentology and Stratigraphy*; Prentice Hall: NJ, 1995; p 765.
(65) Taylor, G.; Attewell, P. B.; Farmer, I. W. Principles of Engineering Geology. *Geol. Mag* **1977**, *114* (1), 77−80.
(66) Hudson, J. A.; Dusseault, M. ;. Mc Graw-Hill International: New York, 1989; pp 14a.
(67) Liu, J.; Chen, Z.; Elsworth, D.; Qu, H.; Chen, D. Interactions of multiple processes during CBM extraction: a critical review. *International Journal of Coal Geology* **2011**, *87* (3−4), 175−189.
(68) Pan, Z.; Connell, L. D. Modelling permeability for coal reservoirs: a review of analytical models and testing data. *International Journal of Coal Geology* **2012**, *92*, 1−44.
(69) Behrang, A.; Mohammadmoradi, P.; Taheri, S.; Kantzas, A. A theoretical study on the permeability of tight media; effects of slippage and condensation. *Fuel* **2016**, *181*, 610−617.
(70) Nelson, R. *Geologic analysis of naturally fractured reservoirs*; Elsevier: 2001.
(71) Wu, J.; Yu, B.; Zhang, J.; Li, Y. Pore characteristics and controlling factors in the organic-rich shale of the Lower Silurian Longmaxi Formation revealed by samples from a well in southeastern Chongqing. *Earth Science Frontiers* **2013**, *20* (3), 260−269.
(72) Labani, M. M.; Rezaee, R.; Saeedi, A.; Al Hinai, A. Evaluation of pore size spectrum of gas shale reservoirs using low pressure nitrogen adsorption, gas expansion and mercury porosimetry: A case study from the Perth and Canning Basins, Western Australia. *J. Pet. Sci. Eng.* **2013**, *112*, 7−16.
(73) Yang, F.; Ning, Z.; Zhang, S.; Hu, C.; Du, L.; Liu, H. Characterization of pore structures in shales through nitrogen adsorption experiment. *Natural Gas Industry* **2013**, *33* (4), 135−140.
(74) Soeder, D. J. Porosity and permeability of eastern Devonian gas shale. *SPE formation evaluation* **1988**, *3* (01), 116−124.
(75) Loucks, R. G.; Reed, R. M.; Ruppel, S. C.; Jarvie, D. M. Morphology, genesis, and distribution of nanometer-scale pores in siliceous mudstones of the Mississippian Barnett Shale. *Journal of sedimentary research* **2009**, *79* (12), 848−861.
(76) Curtis, M. E.; Ambrose, R. J.; Sondergeld, C. H.; Rai, C. S. In Investigation of the relationship between organic porosity and thermal maturity in the Marcellus Shale. *North American unconventional gas conference and exhibition*; OnePetro: 2011.
(77) Mbia, E. N.; Fabricius, I. L.; Krogsbøll, A.; Frykman, P.; Dalhoff, F. Permeability, compressibility and porosity of Jurassic shale from the Norwegian−Danish Basin. *Petroleum Geoscience* **2014**, *20*, 257−281.
(78) Lu, S.; Huang, W.; Chen, W.; Li, J.; Wang, M.; Xue, H.; et al. Classification and evaluation criteria of shale oil and gas resources: Discussion and application. *Petroleum exploration and development* **2012**, *39* (2), 268−276.
(79) İnan, S.; Al Badairy, H.; İnan, T.; Al Zahrani, A. Formation and occurrence of organic matter-hosted porosity in shales. *International Journal of Coal Geology* **2018**, *199*, 39−51.
(80) Yaalon, D. Mineral composition of the average shale. *Clay Minerals Bull.*, v. 5. **1962**.531
(81) Pettijohn, F. Paleocurrents of Lake Superior Precambrian quartzites. *Geological Society of America Bulletin* **1957**, *68* (4), 469−480.
(82) Okeke, O.; Okogbue, C. Shales: A review of their classifications, properties and importance to the petroleum industry. *Global Journal of Geological Sciences* **2011**, *9* (1), 75−83.
(83) Anderson, R.; Ratcliffe, I.; Greenwell, H.; Williams, P.; Cliffe, S.; Coveney, P. Clay swelling—a challenge in the oilfield. *Earth-Science Reviews* **2010**, *98* (3−4), 201−216.
(84) Hill, D. G. In *Clay stabilization-criteria for best performance*, SPE Formation Damage Control Symposium, OnePetro: 1982.
(85) Berry, S. L.; Boles, J. L.; Brannon, H. D.; Beall, B. B. In *Performance evaluation of ionic liquids as a clay stabilizer and shale inhibitor*, SPE international symposium and exhibition on formation damage control, OnePetro: 2008.
(86) Cygan, R. T.; Romanov, V. N.; Myshakin, E. M. Molecular simulation of carbon dioxide capture by montmorillonite using an accurate and flexible force field. *J. Phys. Chem. C* **2012**, *116* (24), 13079−13091.
(87) Wilson, I. *Applied Clay Mineralogy. Occurrences, processing and application of kaolins, bentonite, palygorskite-sepiolite, and common clays*; Clay Minerals Society: 2007.
(88) Bailey, S. Structures of layer silicates. In *Crystal Structures of Clay Minerals and Their X-ray Identification*; Brindley, G. W., Brown, G., Eds.; Monograph: 1980; p 123.
(89) Brindley, G.; Brown, G. Crystal structure of clay minerals and their X-ray diffraction. *Mineralogical Society, London* **1980**, *46*.
(90) Pinnavaia, T. J. Intercalated clay catalysts. *Science* **1983**, *220* (4595), 365−371.
(91) Pohl, W. L. *Economic geology: principles and practice*; John Wiley & Sons: 2011.
(92) Grim, R. E. *Clay mineralogy*, 2nd ed.; McGraw-Hill Book Company: 1968.
(93) Varadwaj, G. B. B.; Parida, K. Montmorillonite supported metal nanoparticles: an update on syntheses and applications. *Rsc Advances* **2013**, *3* (33), 13583−13593.
(94) Pauling, L. The structure of the chlorites. *Proc. Natl. Acad. Sci. U.S.A.* **1930**, *16* (9), 578.
(95) Brigatti, M. F.; Galan, E.; Theng, B. Structure and mineralogy of clay minerals. In *Developments in clay science*; Elsevier: 2013; Vol. *5*, pp 21−81.
(96) Kumari, N.; Mohan, C. Basics of clay minerals and their characteristic properties. *Clay and Clay Minerals* **2021**, 1−29.
(97) Bibi, I.; Icenhower, J.; Niazi, N. K.; Naz, T.; Shahid, M.; Bashir, S. Clay minerals: Structure, chemistry, and significance in contaminated environments and geological CO2 sequestration. *Environmental materials and waste* **2016**, 543−567.
(98) Hu, C.; Gu, L.; Luan, Z.; Song, J.; Zhu, K. Effects of montmorillonite−zinc oxide hybrid on performance, diarrhea, intestinal permeability and morphology of weanling pigs. *Animal Feed Science and Technology* **2012**, *177* (1−2), 108−115.
(99) Duman, O.; Tunç, S. Electrokinetic and rheological properties of Na-bentonite in some electrolyte solutions. *Microporous Mesoporous Mater.* **2009**, *117* (1−2), 331−338.
(100) Garg, N.; Skibsted, J. Thermal activation of a pure montmorillonite clay and its reactivity in cementitious systems. *J. Phys. Chem. C* **2014**, *118* (21), 11464−11477.
(101) Ismadji, S.; Soetaredjo, F. E.; Ayucitra, A. *Clay materials for environmental remediation*; Springer: 2015.
(102) Murray, H. H. Structure and composition of the clay minerals and their physical and chemical properties. *Developments in clay science* **2006**, *2*, 7−31.
(103) Gualtieri, A. F.; Ferrari, S.; Leoni, M.; Grathoff, G.; Hugo, R.; Shatnawi, M.; Paglia, G.; Billinge, S. Structural characterization of the clay mineral Illite-1M. *J. Appl. Crystallogr.* **2008**, *41* (2), 402−415.
(104) Douglas, L. A. Vermiculites. *Minerals in soil environments* **1989**, *1*, 635−674.
(105) Brady, N. C. Soil Colloids: Their Nature and Practical Significance. *Nature and Properties of Soils* **1990**, 177−212.

https://doi.org/10.1021/acsomega.2c03008
ACS Omega 2022, 7, 28723−28755

(106) Deer, W. A. *Rock-forming minerals: Sheet silicates*; Longmans: 1962; Vol. 3.
(107) Burrafato, G.; Miano, F. Determination of the cation exchange capacity of clays by surface tension measurements. *Clay minerals* **1993**, *28* (3), 475−481.
(108) Abdullatif, A.; Al-Hulail, I. A.; Al-Mutawa, E. In Robust clay stabilizer to control swelling in a rich swellable clay formation: A laboratory study. *International Petroleum Technology Conference*; OnePetro: 2020.
(109) Low, P. F.; Anderson, D. M. Osmotic pressure equations for determining thermodynamic properties of soil water. *Soil Science* **1958**, *86* (5), 251−253.
(110) Amorim, C.; Lopes, R.; Barroso, R.; Queiroz, J.; Alves, D.; Perez, C.; Schelin, H. Effect of clay−water interactions on clay swelling by X-ray diffraction. *Nuclear Instruments and Methods in Physics Research Section A: Accelerators, Spectrometers, Detectors and Associated Equipment* **2007**, *580* (1), 768−770.
(111) Wilson, M.; Wilson, L. Clay mineralogy and shale instability: an alternative conceptual analysis. *Clay Minerals* **2014**, *49* (2), 127−145.
(112) Yuan, W.; Li, X.; Pan, Z.; Connell, L. D.; Li, S.; He, J. Experimental investigation of interactions between water and a lower Silurian Chinese shale. *Energy Fuels* **2014**, *28* (8), 4925−4933.
(113) Wang, L.; Bornert, M.; Héripré, E.; Chanchole, S.; Pouya, A.; Halphen, B. Microscale insight into the influence of humidity on the mechanical behavior of mudstones. *Journal of Geophysical Research: Solid Earth* **2015**, *120* (5), 3173−3186.
(114) Madsen, F. T.; Müller-Vonmoos, M. The swelling behaviour of clays. *Appl. Clay Sci.* **1989**, *4* (2), 143−156.
(115) Worden, R. H.; Morad, S. Clay minerals in sandstones: controls on formation, distribution and evolution. *Clay mineral cements in sandstones* **1999**, 1−41.
(116) Kraehenbuehl, F.; Stoeckli, H. F.; Brunner, F.; Kahr, G.; Müller-Vonmoos, M. Study of the water-bentonite system by vapour adsorption, immersion calorimetry and X-ray techniques: I. Micropore volumes and internal surface areas, following Dubinin's theory. *Clay Minerals* **1987**, *22* (1), 1−9.
(117) Abbott, A. P.; Boothby, D.; Capper, G.; Davies, D. L.; Rasheed, R. K. Deep eutectic solvents formed between choline chloride and carboxylic acids: versatile alternatives to ionic liquids. *J. Am. Chem. Soc.* **2004**, *126* (29), 9142−9147.
(118) El Achkar, T.; Greige-Gerges, H.; Fourmentin, S. Basics and properties of deep eutectic solvents: a review. *Environmental Chemistry Letters* **2021**, *19* (4), 3397−3408.
(119) Zeng, Q.; Wang, Y.; Huang, Y.; Ding, X.; Chen, J.; Xu, K. Deep eutectic solvents as novel extraction media for protein partitioning. *Analyst* **2014**, *139* (10), 2565−2573.
(120) Tang, W.; An, Y.; Row, K. H. Emerging applications of (micro) extraction phase from hydrophilic to hydrophobic deep eutectic solvents: opportunities and trends. *TrAC Trends in Analytical Chemistry* **2021**, *136*, 116187.
(121) Shahbaz, K.; Mjalli, F.; Hashim, M.; AlNashef, I. Using deep eutectic solvents based on methyl triphenyl phosphunium bromide for the removal of glycerol from palm-oil-based biodiesel. *Energy Fuels* **2011**, *25* (6), 2671−2678.
(122) Gutiérrez, M. C.; Ferrer, M. L.; Mateo, C. R.; del Monte, F. Freeze-drying of aqueous solutions of deep eutectic solvents: a suitable approach to deep eutectic suspensions of self-assembled structures. *Langmuir* **2009**, *25* (10), 5509−5515.
(123) Dai, Y.; van Spronsen, J.; Witkamp, G.-J.; Verpoorte, R.; Choi, Y. H. Natural deep eutectic solvents as new potential media for green technology. *Analytica chimica acta* **2013**, *766*, 61−68.
(124) Santana, A. P.; Mora-Vargas, J. A.; Guimaraes, T. G.; Amaral, C. D.; Oliveira, A.; Gonzalez, M. H. Sustainable synthesis of natural deep eutectic solvents (NADES) by different methods. *J. Mol. Liq.* **2019**, *293*, 111452.
(125) Kaur, S.; Kumari, M.; Kashyap, H. K. Microstructure of deep eutectic solvents: Current understanding and challenges. *J. Phys. Chem. B* **2020**, *124* (47), 10601−10616.
(126) Kareem, M. A.; Mjalli, F. S.; Hashim, M. A.; AlNashef, I. M. Phosphonium-based ionic liquids analogues and their physical properties. *Journal of Chemical & Engineering Data* **2010**, *55* (11), 4632−4637.
(127) DL, A. A. C. G. D.; Munro, H. L.; Rasheed, R. K.; Tambyrajah, V. *Chem. Commun.* **2010**.
(128) Sitze, M. S.; Schreiter, E. R.; Patterson, E. V.; Freeman, R. G. Ionic liquids based on FeCl3 and FeCl2. Raman scattering and ab initio calculations. *Inorg. Chem.* **2001**, *40* (10), 2298−2304.
(129) Moura, L.; Moufawad, T.; Ferreira, M.; Bricout, H.; Tilloy, S.; Monflier, E.; Costa Gomes, M. F.; Landy, D.; Fourmentin, S. Deep eutectic solvents as green absorbents of volatile organic pollutants. *Environmental Chemistry Letters* **2017**, *15* (4), 747−753.
(130) Garcia, M. T.; Gathergood, N.; Scammells, P. J. Biodegradable ionic liquids Part II. Effect of the anion and toxicology. *Green Chem.* **2005**, *7* (1), 9−14.
(131) Gathergood, N.; Scammells, P. J. Design and preparation of room-temperature ionic liquids containing biodegradable side chains. *Aust. J. Chem.* **2002**, *55* (9), 557−560.
(132) Gathergood, N.; Garcia, M. T.; Scammells, P. J. Biodegradable ionic liquids: Part I. Concept, preliminary targets and evaluation. *Green Chem.* **2004**, *6* (3), 166−175.
(133) Gathergood, N.; Scammells, P. J.; Garcia, M. T. Biodegradable ionic liquids Part III. The first readily biodegradable ionic liquids. *Green Chem.* **2006**, *8* (2), 156−160.
(134) Zhao, B.-Y.; Xu, P.; Yang, F.-X.; Wu, H.; Zong, M.-H.; Lou, W.-Y. Biocompatible deep eutectic solvents based on choline chloride: characterization and application to the extraction of rutin from Sophora japonica. *ACS Sustainable Chem. Eng.* **2015**, *3* (11), 2746−2755.
(135) Kohli, R., Applications of ionic liquids in removal of surface contaminants. In *Developments in surface contamination and cleaning: applications of cleaning techniques*; Elsevier: 2019; pp 619−680.
(136) Abbott, A. P.; Capper, G.; Davies, D. L.; Rasheed, R. K.; Tambyrajah, V. Novel solvent properties of choline chloride/urea mixtures. *Chem. Commun.* **2003**, No. 1, 70−71.
(137) Abbott, A. P.; Capper, G.; Davies, D.; Rasheed, R.; Tambyrajah, V. Novel solvent properties of choline chloride/urea mixtures. *Chem. Commun.* **2003**, *10*, 70−71.
(138) Abbott, A. P.; Capper, G.; Davies, D. L.; McKenzie, K. J.; Obi, S. U. Solubility of metal oxides in deep eutectic solvents based on choline chloride. *Journal of Chemical & Engineering Data* **2006**, *51* (4), 1280−1282.
(139) Martins, M. A.; Pinho, S. P.; Coutinho, J. A. Insights into the nature of eutectic and deep eutectic mixtures. *J. Solution Chem.* **2019**, *48* (7), 962−982.
(140) Alonso, D. A.; Baeza, A.; Chinchilla, R.; Guillena, G.; Pastor, I. M.; Ramón, D. J. Deep eutectic solvents: the organic reaction medium of the century. *Eur. J. Org. Chem.* **2016**. DOI: 10.1002/ejoc.201501197
(141) Tang, B.; Row, K. H. Recent developments in deep eutectic solvents in chemical sciences. *Monatshefte für Chemie-Chemical Monthly* **2013**, *144* (10), 1427−1454.
(142) Florindo, C.; Branco, L. C.; Marrucho, I. M. Quest for green-solvent design: from hydrophilic to hydrophobic (deep) eutectic solvents. *ChemSusChem* **2019**, *12* (8), 1549−1559.
(143) Shahbaz, K.; Baroutian, S.; Mjalli, F.; Hashim, M.; AlNashef, I. Densities of ammonium and phosphonium based deep eutectic solvents: Prediction using artificial intelligence and group contribution techniques. *Thermochim. Acta* **2012**, *527*, 59−66.
(144) Abbott, A. P.; Barron, J. C.; Ryder, K. S.; Wilson, D. Eutectic-based ionic liquids with metal-containing anions and cations. *Chemistry−A European Journal* **2007**, *13* (22), 6495−6501.
(145) Shahbaz, K.; Mjalli, F.; Hashim, M.; AlNashef, I. Prediction of deep eutectic solvents densities at different temperatures. *Thermochimica acta* **2011**, *515* (1−2), 67−72.
(146) Delgado-Mellado, N.; Larriba, M.; Navarro, P.; Rigual, V.; Ayuso, M.; García, J.; Rodríguez, F. Thermal stability of choline

https://doi.org/10.1021/acsomega.2c03008
ACS Omega 2022, 7, 28723−28755

chloride deep eutectic solvents by TGA/FTIR-ATR analysis. *J. Mol. Liq.* **2018**, *260*, 37−43.
(147) Geiculescu, O.; DesMarteau, D.; Creager, S.; Haik, O.; Hirshberg, D.; Shilina, Y.; Zinigrad, E.; Levi, M.; Aurbach, D.; Halalay, I. Novel binary deep eutectic electrolytes for rechargeable Li-ion batteries based on mixtures of alkyl sulfonamides and lithium perfluoroalkylsulfonimide salts. *J. Power Sources* **2016**, *307*, 519−525.
(148) Millia, L.; Dall'Asta, V.; Ferrara, C.; Berbenni, V.; Quartarone, E.; Perna, F. M.; Capriati, V.; Mustarelli, P. Bio-inspired choline chloride-based deep eutectic solvents as electrolytes for lithium-ion batteries. *Solid State Ionics* **2018**, *323*, 44−48.
(149) Tripathy, S. N.; Wojnarowska, Z.; Knapik, J.; Shirota, H.; Biswas, R.; Paluch, M. Glass transition dynamics and conductivity scaling in ionic deep eutectic solvents: The case of (acetamide+ lithium nitrate/sodium thiocyanate) melts. *J. Chem. Phys.* **2015**, *142* (18), 184504.
(150) Nunes, R. J.; Saramago, B.; Marrucho, I. M. Surface tension of dl-menthol: octanoic acid eutectic mixtures. *Journal of Chemical & Engineering Data* **2019**, *64* (11), 4915−4923.
(151) AlOmar, M. K.; Hayyan, M.; Alsaadi, M. A.; Akib, S.; Hayyan, A.; Hashim, M. A. Glycerol-based deep eutectic solvents: physical properties. *J. Mol. Liq.* **2016**, *215*, 98−103.
(152) Abbott, A. P.; Barron, J. C.; Frisch, G.; Gurman, S.; Ryder, K. S.; Silva, A. F.; et al. Double layer effects on metal nucleation in deep eutectic solvents. *Phys. Chem. Chem. Phys.* **2011**, *13* (21), 10224−10231.
(153) Chen, W.; Bai, X.; Xue, Z.; Mou, H.; Chen, J.; Liu, Z.; Mu, T. The formation and physicochemical properties of PEGylated deep eutectic solvents. *New J. Chem.* **2019**, *43* (22), 8804−8810.
(154) Abbott, A. P.; Harris, R. C.; Ryder, K. S.; D'Agostino, C.; Gladden, L. F.; Mantle, M. D. Glycerol eutectics as sustainable solvent systems. *Green Chem.* **2011**, *13* (1), 82−90.
(155) García, G.; Aparicio, S.; Ullah, R.; Atilhan, M. Deep eutectic solvents: physicochemical properties and gas separation applications. *Energy Fuels* **2015**, *29* (4), 2616−2644.
(156) Hayyan, A.; Mjalli, F. S.; AlNashef, I. M.; Al-Wahaibi, T.; Al-Wahaibi, Y. M.; Hashim, M. A. Fruit sugar-based deep eutectic solvents and their physical properties. *Thermochim. Acta* **2012**, *541*, 70−75.
(157) Reichardt, C. Solvatochromic dyes as solvent polarity indicators. *Chem. Rev.* **1994**, *94* (8), 2319−2358.
(158) Pandey, A.; Rai, R.; Pal, M.; Pandey, S. How polar are choline chloride-based deep eutectic solvents? *Phys. Chem. Chem. Phys.* **2014**, *16* (4), 1559−1568.
(159) Pandey, A.; Pandey, S. Solvatochromic probe behavior within choline chloride-based deep eutectic solvents: effect of temperature and water. *J. Phys. Chem. B* **2014**, *118* (50), 14652−14661.
(160) Ma, Y.; Wang, Q.; Zhu, T. Comparison of hydrophilic and hydrophobic deep eutectic solvents for pretreatment determination of sulfonamides from aqueous environments. *Analytical Methods* **2019**, *11* (46), 5901−5909.
(161) Shahbaz, K.; Mjalli, F. S.; Vakili-Nezhaad, G.; AlNashef, I. M.; Asadov, A.; Farid, M. M. Thermogravimetric measurement of deep eutectic solvents vapor pressure. *J. Mol. Liq.* **2016**, *222*, 61−66.
(162) Wu, S.-H.; Caparanga, A. R.; Leron, R. B.; Li, M.-H. Vapor pressure of aqueous choline chloride-based deep eutectic solvents (ethaline, glyceline, maline and reline) at 30−70 C. *Thermochimica acta* **2012**, *544*, 1−5.
(163) Dwamena, A. K. Recent advances in hydrophobic deep eutectic solvents for extraction. *Separations* **2019**, *6* (1), 9.
(164) Passos, H.; Tavares, D. J.; Ferreira, A. M.; Freire, M. G.; Coutinho, J. A. Are aqueous biphasic systems composed of deep eutectic solvents ternary or quaternary systems? *ACS Sustainable Chem. Eng.* **2016**, *4* (5), 2881−2886.
(165) Florindo, C.; Branco, L.; Marrucho, I. Development of hydrophobic deep eutectic solvents for extraction of pesticides from aqueous environments. *Fluid Phase Equilib.* **2017**, *448*, 135−142.
(166) Ghareh Bagh, F. S.; Mjalli, F. S.; Hashim, M. A.; Hadj-Kali, M. K. O.; AlNashef, I. M. Solubility of sodium salts in ammonium-based deep eutectic solvents. *Journal of Chemical & Engineering Data* **2013**, *58* (8), 2154−2162.
(167) van Osch, D. J.; Zubeir, L. F.; van den Bruinhorst, A.; Rocha, M. A.; Kroon, M. C. Hydrophobic deep eutectic solvents as water-immiscible extractants. *Green Chem.* **2015**, *17* (9), 4518−4521.
(168) Li, X.; Row, K. H. Development of deep eutectic solvents applied in extraction and separation. *J. Sep. Sci.* **2016**, *39* (18), 3505−3520.
(169) Nakhle, L.; Kfoury, M.; Mallard, I.; Landy, D.; Greige-Gerges, H. Methods for extraction of bioactive compounds from plant and animal matter using deep eutectic solvents. In *Deep eutectic solvents for medicine, gas solubilization and extraction of natural substances*; Springer: 2021; pp 183−240.
(170) Sang, J.; Li, B.; Huang, Y.-y.; Ma, Q.; Liu, K.; Li, C.-q. Deep eutectic solvent-based extraction coupled with green two-dimensional HPLC-DAD-ESI-MS/MS for the determination of anthocyanins from Lycium ruthenicum Murr. fruit. *Analytical Methods* **2018**, *10* (10), 1247−1257.
(171) Lima, F.; Gouvenaux, J.; Branco, L. C.; Silvestre, A. J.; Marrucho, I. M. Towards a sulfur clean fuel: Deep extraction of thiophene and dibenzothiophene using polyethylene glycol-based deep eutectic solvents. *Fuel* **2018**, *234*, 414−421.
(172) Warrag, S. E.; Fetisov, E. O.; Van Osch, D. J.; Harwood, D. B.; Kroon, M. C.; Siepmann, J. I.; Peters, C. J. Mercury capture from petroleum using deep eutectic solvents. *Ind. Eng. Chem. Res.* **2018**, *57* (28), 9222−9230.
(173) Li, G.; Jiang, Y.; Liu, X.; Deng, D. New levulinic acid-based deep eutectic solvents: synthesis and physicochemical property determination. *J. Mol. Liq.* **2016**, *222*, 201−207.
(174) Ji, X.; Xie, Y.; Zhang, Y.; Lu, X. In CO2 capture/separation using choline chloride-based ionic liquids. *International Conference on Properties and Phase Equilibria for Process and Product Design*; 26/05/2013−30/05/2013, 2013.
(175) Warrag, S. E.; Peters, C. J.; Kroon, M. C. Deep eutectic solvents for highly efficient separations in oil and gas industries. *Current Opinion in Green and Sustainable Chemistry* **2017**, *5*, 55−60.
(176) Mohsenzadeh, A.; Al-Wahaibi, Y.; Al-Hajri, R.; Jibril, B.; Mosavat, N. Sequential deep eutectic solvent and steam injection for enhanced heavy oil recovery and in-situ upgrading. *Fuel* **2017**, *187*, 417−428.
(177) Khan, M. S.; Lal, B.; Partoon, B.; Keong, L. K.; Bustam, A. B.; Mellon, N. B. Experimental evaluation of a novel thermodynamic inhibitor for CH4 and CO2 hydrates. *Procedia engineering* **2016**, *148*, 932−940.
(178) Nguyen, C.-H.; Augis, L.; Fourmentin, S.; Barratt, G.; Legrand, F.-X. Deep eutectic solvents for innovative pharmaceutical formulations. In *Deep eutectic solvents for medicine, gas solubilization and extraction of natural substances*; Springer: 2021; pp 41−102.
(179) Ramesh, S.; Shanti, R.; Morris, E. Studies on the plasticization efficiency of deep eutectic solvent in suppressing the crystallinity of corn starch based polymer electrolytes. *Carbohydr. Polym.* **2012**, *87* (1), 701−706.
(180) Abbott, A. P.; Bell, T. J.; Handa, S.; Stoddart, B. Cationic functionalisation of cellulose using a choline based ionic liquid analogue. *Green Chem.* **2006**, *8* (9), 784−786.
(181) Alrazzouk, A. H. *Acids and Deep Eutectic Solvents as Novel Catalysts for the Processing of Low Grade Palm Oil for Biofuel Production*; Jabatan Kejuruteraan Kimia, Fakulti Kejuruteraan, Universiti Malaya, 2015.
(182) Cruz, H.; Jordão, N.; Branco, L. C. Deep eutectic solvents (DESs) as low-cost and green electrolytes for electrochromic devices. *Green Chem.* **2017**, *19* (7), 1653−1658.
(183) Xu, P.; Zheng, G.-W.; Zong, M.-H.; Li, N.; Lou, W.-Y. Recent progress on deep eutectic solvents in biocatalysis. *Bioresources and bioprocessing* **2017**, *4* (1), 1−18.
(184) Abbott, A. P.; Cullis, P. M.; Gibson, M. J.; Harris, R. C.; Raven, E. Extraction of glycerol from biodiesel into a eutectic based ionic liquid. *Green Chem.* **2007**, *9* (8), 868−872.

https://doi.org/10.1021/acsomega.2c03008
ACS Omega 2022, 7, 28723−28755

(185) Hayyan, M.; Mbous, Y. P.; Looi, C. Y.; Wong, W. F.; Hayyan, A.; Salleh, Z.; Mohd-Ali, O. Natural deep eutectic solvents: cytotoxic profile. *SpringerPlus* **2016**, *5* (1), 1−12.
(186) Juneidi, I.; Hayyan, M.; Hashim, M. Evaluation of toxicity and biodegradability for cholinium-based deep eutectic solvents. *Rsc Adv.* **2015**, *5*, 83636−83647.
(187) Radošević, K.; Bubalo, M. C.; Srček, V. G.; Grgas, D.; Dragičević, T. L.; Redovniković, I. R. Evaluation of toxicity and biodegradability of choline chloride based deep eutectic solvents. *Ecotoxicology and environmental safety* **2015**, *112*, 46−53.
(188) Juneidi, I.; Hayyan, M.; Hashim, M. A. Evaluation of toxicity and biodegradability for cholinium-based deep eutectic solvents. *RSC Adv.* **2015**, *5* (102), 83636−83647.
(189) Hayyan, M.; Hashim, M. A.; Al-Saadi, M. A.; Hayyan, A.; AlNashef, I. M.; Mirghani, M. E. Assessment of cytotoxicity and toxicity for phosphonium-based deep eutectic solvents. *Chemosphere* **2013**, *93* (2), 455−459.
(190) Wen, Q.; Chen, J.-X.; Tang, Y.-L.; Wang, J.; Yang, Z. Assessing the toxicity and biodegradability of deep eutectic solvents. *Chemosphere* **2015**, *132*, 63−69.
(191) Modica-Napolitano, J. S.; Aprille, J. R. Delocalized lipophilic cations selectively target the mitochondria of carcinoma cells. *Advanced drug delivery reviews* **2001**, *49* (1−2), 63−70.
(192) Gu, T.; Zhang, M.; Tan, T.; Chen, J.; Li, Z.; Zhang, Q.; Qiu, H. Deep eutectic solvents as novel extraction media for phenolic compounds from model oil. *Chem. Commun.* **2014**, *50* (79), 11749−11752.
(193) Oliveira, F. S.; Pereiro, A. B.; Rebelo, L. P.; Marrucho, I. M. Deep eutectic solvents as extraction media for azeotropic mixtures. *Green Chem.* **2013**, *15* (5), 1326−1330.
(194) Ruesgas-Ramón, M.; Figueroa-Espinoza, M. C.; Durand, E. Application of deep eutectic solvents (DES) for phenolic compounds extraction: Overview, challenges, and opportunities. *J. Agric. Food Chem.* **2017**, *65* (18), 3591−3601.
(195) Maugeri, Z.; de María, P. D. Novel choline-chloride-based deep-eutectic-solvents with renewable hydrogen bond donors: levulinic acid and sugar-based polyols. *Rsc Advances* **2012**, *2* (2), 421−425.
(196) Adhikari, L.; Larm, N. E.; Baker, G. A. Argentous deep eutectic solvent approach for scaling up the production of colloidal silver nanocrystals. *ACS Sustainable Chem. Eng.* **2019**, *7* (13), 11036−11043.
(197) Shishov, A.; Bulatov, A.; Locatelli, M.; Carradori, S.; Andruch, V. Application of deep eutectic solvents in analytical chemistry. A review. *Microchemical journal* **2017**, *135*, 33−38.
(198) Jaumaux, P.; Liu, Q.; Zhou, D.; Xu, X.; Wang, T.; Wang, Y.; Kang, F.; Li, B.; Wang, G. Deep-eutectic-solvent-based self-healing polymer electrolyte for safe and long-life lithium-metal batteries. *Angew. Chem., Int. Ed.* **2020**, *59* (23), 9134−9142.
(199) Gutiérrez, A.; Atilhan, M.; Aparicio, S. Theoretical study on deep eutectic solvents as vehicles for the delivery of anesthetics. *J. Phys. Chem. B* **2020**, *124* (9), 1794−1805.
(200) Makoś, P.; Słupek, E.; Gębicki, J. Hydrophobic deep eutectic solvents in microextraction techniques−A review. *Microchemical journal* **2020**, *152*, 104384.
(201) Sarmad, S.; Mikkola, J. P.; Ji, X. Carbon dioxide capture with ionic liquids and deep eutectic solvents: a new generation of sorbents. *ChemSusChem* **2017**, *10* (2), 324−352.
(202) Chen, Y.; Han, X.; Liu, Z.; Yu, D.; Guo, W.; Mu, T. Capture of toxic gases by deep eutectic solvents. *ACS Sustainable Chem. Eng.* **2020**, *8* (14), 5410−5430.
(203) Perna, F. M.; Vitale, P.; Capriati, V. Deep eutectic solvents and their applications as green solvents. *Current Opinion in Green and Sustainable Chemistry* **2020**, *21*, 27−33.
(204) Chandran, D.; Khalid, M.; Walvekar, R.; Mubarak, N. M.; Dharaskar, S.; Wong, W. Y.; Gupta, T. C. S. M. Deep eutectic solvents for extraction-desulphurization: A review. *J. Mol. Liq.* **2019**, *275*, 312−322.
(205) Cai, T.; Qiu, H. Application of deep eutectic solvents in chromatography: A review. *TrAC Trends in Analytical Chemistry* **2019**, *120*, 115623.
(206) Wagle, D. V.; Zhao, H.; Baker, G. A. Deep eutectic solvents: sustainable media for nanoscale and functional materials. *Accounts of chemical research* **2014**, *47* (8), 2299−2308.
(207) Macário, I.; Oliveira, H.; Menezes, A.; Ventura, S.; Pereira, J.; Gonçalves, A.; Coutinho, J.; Gonçalves, F. Cytotoxicity profiling of deep eutectic solvents to human skin cells. *Sci. Rep.* **2019**, *9* (1), 1−9.
(208) Hayyan, M.; Hashim, M. A.; Hayyan, A.; Al-Saadi, M. A.; AlNashef, I. M.; Mirghani, M. E.; Saheed, O. K. Are deep eutectic solvents benign or toxic? *Chemosphere* **2013**, *90* (7), 2193−2195.
(209) Kudłak, B.; Owczarek, K.; Namieśnik, J. Selected issues related to the toxicity of ionic liquids and deep eutectic solvents—a review. *Environmental Science and Pollution Research* **2015**, *22* (16), 11975−11992.
(210) Earle, M. J.; Esperança, J. M.; Gilea, M. A.; Canongia Lopes, J. N.; Rebelo, L. P.; Magee, J. W.; Seddon, K. R.; Widegren, J. A. The distillation and volatility of ionic liquids. *Nature* **2006**, *439* (7078), 831−834.
(211) Leitch, A. C.; Abdelghany, T. M.; Probert, P. M.; Dunn, M. P.; Meyer, S. K.; Palmer, J. M.; Cooke, M. P.; Blake, L. I.; Morse, K.; Rosenmai, A. K.; et al. The toxicity of the methylimidazolium ionic liquids, with a focus on M8OI and hepatic effects. *Food Chem. Toxicol.* **2020**, *136*, 111069.
(212) e Silva, F. A.; Coutinho, J. A.; Ventura, S. P. *Aquatic Toxicology of Ionic Liquids (ILs)*; Springer Singapore: Singapore, 2019; pp 1−18.
(213) Jia, H.; Huang, P.; Han, Y.; Wang, Q.; Jia, K.; Sun, T.; Zhang, F.; Yan, H.; Lv, K. Investigation for the novel use of a typical deep eutectic solvent as a potential shale inhibitor. *Energy Sources, Part A: Recovery, Utilization, and Environmental Effects* **2022**, *44* (1), 1402−1415.
(214) Jia, H.; Huang, P.; Wang, Q.; Han, Y.; Wang, S.; Zhang, F.; Pan, W.; Lv, K. Investigation of inhibition mechanism of three deep eutectic solvents as potential shale inhibitors in water-based drilling fluids. *Fuel* **2019**, *244*, 403−411.
(215) Beg, M.; Haider, M. B.; Thakur, N. K.; Husein, M.; Sharma, S.; Kumar, R. Clay-water interaction inhibition using amine and glycol-based deep eutectic solvents for efficient drilling of shale formations. *J. Mol. Liq.* **2021**, *340*, 117134.
(216) Ma, J.; Pang, S.; Zhou, W.; Xia, B.; An, Y. Novel deep eutectic solvents for stabilizing clay and inhibiting shale hydration. *Energy Fuels* **2021**, *35* (9), 7833−7843.
(217) Florindo, C.; Lima, F.; Ribeiro, B. D.; Marrucho, I. M. Deep eutectic solvents: Overcoming 21st century challenges. *Current Opinion in Green and Sustainable Chemistry* **2019**, *18*, 31−36.
(218) Palmelund, H.; Rantanen, J.; Löbmann, K. Deliquescence behavior of deep eutectic solvents. *Applied Sciences* **2021**, *11* (4), 1601.
(219) Dai, Y.; Witkamp, G.-J.; Verpoorte, R.; Choi, Y. H. Tailoring properties of natural deep eutectic solvents with water to facilitate their applications. *Food chemistry* **2015**, *187*, 14−19.
(220) Lu, C.; Cao, J.; Wang, N.; Su, E. Significantly improving the solubility of non-steroidal anti-inflammatory drugs in deep eutectic solvents for potential non-aqueous liquid administration. *MedChemComm* **2016**, *7* (5), 955−959.
(221) Shah, D.; Mjalli, F. S. Effect of water on the thermo-physical properties of Reline: An experimental and molecular simulation based approach. *Phys. Chem. Chem. Phys.* **2014**, *16* (43), 23900−23907.
(222) Rathore, A. S. Roadmap for implementation of quality by design (QbD) for biotechnology products. *Trends Biotechnol.* **2009**, *27* (9), 546−553.
(223) Quainoo, A. K.; Negash, B. M.; Bavoh, C. B.; Idris, A. Natural amino acids as potential swelling and dispersion inhibitors for montmorillonite-rich shale formations. *J. Pet. Sci. Eng.* **2021**, *196*, 107664.
(224) Jia, H.; Huang, P.; Han, Y.; Wang, Q.; Jia, K.; Sun, T.; Zhang, F.; Yan, H.; Lv, K. Investigation for the novel use of a typical deep

https://doi.org/10.1021/acsomega.2c03008
ACS Omega 2022, 7, 28723−28755

eutectic solvent as a potential shale inhibitor. *Energy Sources, Part A: Recovery, Utilization, and Environmental Effects* **2019**, 1−14.
(225) Heidug, W.; Wong, S. W. Hydration swelling of water-absorbing rocks: a constitutive model. *International journal for numerical and analytical methods in geomechanics* **1996**, *20* (6), 403−430.
(226) Alemdar, A.; Güngör, N.; Ece, O.; Atici, O. The rheological properties and characterization of bentonite dispersions in the presence of non-ionic polymer PEG. *J. Mater. Sci.* **2005**, *40* (1), 171−177.
(227) Okoro, E. E.; Igwilo, K. C.; Mamudu, A. O.; Ekeinde, E. B.; Dosunmu, A. Data on shale-water based drilling fluid interaction for drilling operation. *Data in brief* **2018**, *19*, 1620−1626.
(228) Ritter, A.; Geraut, R. In New optimization drilling fluid programs for reactive shale formations. *SPE annual technical conference and exhibition*, OnePetro: 1985.
(229) Zhong, H.; Qiu, Z.; Tang, Z.; Zhang, X.; Xu, J.; Huang, W. Study of 4, 4′-methylenebis-cyclohexanamine as a high temperature-resistant shale inhibitor. *J. Mater. Sci.* **2016**, *51* (16), 7585−7597.

https://doi.org/10.1021/acsomega.2c03008
ACS Omega 2022, 7, 28723−28755